Guiding synthetic dynamic soft materials to grow like living organisms

Dissertation

zur Erlangung des Grades

des Doktors der Naturwissenschaften

der Naturwissenschaftlich-Technischen Fakultät

der Universität des Saarlandes

von

Lulu Xue

Saarbrücken

2020

Tag des Kolloquiums:	12. November 2020
Dekan:	Prof. Dr. Jörn Eric Walter
Berichterstatter:	Prof. Dr. Aránzazu del Campo Bécares Prof. Dr.-Ing. Markus Gallei
Akad. Mitglied:	Dr. Lola Gonzales-Garcia
Vorsitz:	Prof. Dr. Guido Kickelbick

Guiding synthetic dynamic soft materials to grow like living organisms

Lulu Xue

geb. in Dongying, China

DISSERTATION

INM-Leibniz Institut für neue Materialien, Saarbrücken

Logic will get you from A to B. Imagination will take you everywhere.

-----Albert Einstein

博学使人谦逊，无知使人骄傲。

Knowledge makes people humble, while ignorance makes people proud.

Acknowledgements

Without proper feeding and careful care, small saplings cannot grow into towering trees. A similar case, without the kind help from many people, scientific and infrastructure support from INM-Leibniz Institute for New Materials and Saarland University and financial support by China Scholarship Council (CSC), it would have been impossible to carry out my doctoral study. All of them are like the rising stars in the night sky, illuminating the way forward me in the last four years. Therefore, it is a great pleasure to convey my deepest and sincerest gratitude to them all here.

Above all, Jiaxi (Dr. Jiaxi Cui), I would like to thank you for providing me the opportunity to conduct and complete my PhD in your group. In the past four years, thank you for bringing me to the “magic” world of dynamic soft materials. I still remember the first time we talked on the phone that we could have the opportunity to work in an institution located in Germany, and maybe more challenging projects compared with previous research topics. You have led me to new fundamental research about self-growing polymeric materials, teaching me a lot on both investigations and experimental skills, and guiding me carefully whenever I need step by step, which has definitely benefited me a lot. I am so happy to work in a multi-disciplinary group (Switchable Microfluidics, INM) with friendly and enthusiastic colleagues from different countries, which has made working here with a pretty enjoyable memory and experience. Of course, you also show me how to balance life and work, which will benefit me throughout my lifetime. Thanks a lot Jiaxi.

Prof. Dr. Aránzazu del Campo Bécares, thank you so much for being my first supervisor and supporting my work. Thank you a lot for giving me the authority to conduct and finish part of my PhD thesis in your labs. I cannot forget how our conversations influenced me and my research, which will carry with me in my future

career.

Dr. Baiju Pazhamkalathil Krishnan, you are always friendly, helpful, and patient collaborator when I have questions to ask you, when I have encountered problems, and when we discussed. I'd like to convey my great gratitude to you for sharing your organic synthesis skills with me, encouraging me whenever I lost, and helping me whenever I cannot figure out the problems. It was an unforgettable memory to work, share free time, and cook with you. You have brought me very traditional and delicious India food. I hope you can enjoy life with your family in India, and believe you can have a successful scientific research career in India.

Dr. Jingnan Zhang, you are one of the most exciting and helpful friends after I joined INM. Without you, my life in Saarland would lose the gorgeous color. Thank you for sharing me with lots of impressive menus, making happiness time from Monday to Sunday, and having fun together to see many beautiful sceneries. I hope you can start a new family soon and get a satisfying position shortly.

Prof. Dr. Qianqiang Pei, thank you so much for helping me assimilate into the new life in Germany. You have helped me a lot both in life and work. I give my highest appreciation for your kind attention when my wife delivered the baby, your professional knowledge in nanoindentation, and your unique personality. I hope you usually operate your new lab soon and get great scientific achievements in the future.

Prof. Dr. Lu Han, many thanks for your kindness to my family and professional help in material science. I have learned a lot from you on hydrogels. I hope you open a new chapter in Ocean University of China. You have everything for a great and successful research career.

Dr. Bin Li, thank you for helping me when I just started experiments in INM, sharing encouraging time with me, and taking care of my baby. I hope and believe you have a great success in Munich and also China soon.

Prof. Dr. Huaixia Zhao, many thanks for your help to me. I enjoyed the time for working in the same office with you. I have learned a lot from you for thinking of life and investigating of research. I hope you have a prosperous and joyful scientific future in Nanjing Tech University (China).

Dr. Johanna Blass, many thanks for your help when I encountered some problems. You always tirelessly help me to figure out the issues generated by Germany language. I hope your baby grows up fast and healthy, and a successful scientific career.

Dr. Jun Feng, thank you a lot for your kindness to help me start the new life in Saarbrücken. Without your delicious Chinese food, I could not adjust to the new life soon. I hope you get a satisfying position in the future.

Ms. Qiyang Jiang, thanks a lot for being the godmother of my baby. Your patience, attention and love to my baby mean a lot to my wife and me.

Many thanks to Stefan for your kind help. Whenever I got problems in the labs, you are always the first person who can offer the best solution. I respect you so much for your professional and responsible attitude as a research scientist and lab manager.

I would like to say thank Dr. Terriac, Emmanuel so much for training me with microscope techniques. I hope you enjoy the “romantic” work in France.

I would like to show gratitude to Sabine Müller for your kind help in work and life, especially your assistance to prolong my visa. I would also thank Dr. Gosia, Christina for your training patience in the rheology test. Many thanks to Mr. Haoran Ma for your help in life and working in the same office.

Many thanks to Fatih Puza, Dr. Sheng Wang, Xiaozhuang Zhou, Zeyu Fu and Dr. Prieto López, Lizbeth Ofelia. To work with you in the same group is a great and unforgettable memory.

I give special thanks to Prof. Dr. Tobias Kraus for being my scientific advisor.

It is my honor to thank the INM, Saarland University, China Scholarship Council to give

me the opportunity to do my research work. Without their support, it is impossible to finish my PhD here.

Many thanks to other colleagues in the group of Dynamic Biomaterials and all other Chinese people for your kindness and help.

Xinhong Xiong, I appreciate everything to my wife for what you did for me. Without your continuous accompany and support to me, it is impossible for me to start and complete my PhD thesis in Germany. You always back me for my decision and pursuing my dream. Your love gives me the courage, endows me with limitless power to finish my PhD. Thousands of words can't express my gratitude to you. Thank you, my wife!

Ziyu Xue, now you are two years old. Whenever I felt tired, whenever I felt frustrated, and whenever I wanted to give up, as long as saw your picture and smile, I would be full of energy to work. Thank you for your birth to me and your mother, which brings brightness to my PhD thesis.

My fantastic family members Yunchao Xue, Xinlan Wang, Bisheng Xiong and Rong Li, thanks a lot for supporting me all the time. Every time we talk, you will always encourage me to keep going and complete my PhD work. Undoubtedly, you are still the most enormous support and motivation to drive me forward.

Lulu Xue

20. 04. 2020, in Saarbrücken

Abstract

Living organisms share the ability to grow that allows them to absorb, transport, and integrate nutrient to continually increase in size, change in shape and modulate in strength. In contrast, synthetic polymers are constructed in fundamentally different ways. Bioinspired by this, this thesis presents various approaches to guide synthetic soft materials to grow and to mimic this fundamental growing capability. The first part presented a photoactivation approach to probe the growth of bulky soft materials. Based on the growth concept, bulk elastomer could be grown with controllable size, strength and compositions. This approach is envisioned as a way to regulate the bulk wettability of materials, by introducing organic and aqueous based nutrients *via* the growth cycle. In part 2 a light-induced site-specific self-growth strategy for making microstructures from the surface a dynamic soft substrate with fine modulation in size, composition, and mechanical properties, for the creation of rough surface and restoration of large-scale surface damage was demonstrated. In the last part, self-growth and self-strengthening of interlocked poly(disulfide)s based polycatenanes elastomers with unique intermolecular interlocking topologies is achieved. These results contribute to the topic of polymer network chain topologies, providing useful information for the future both in chemistry and materials.

Zusammenfassung

Lebende Organismen teilen die Fähigkeit zu wachsen. Ihr Aufbau ermöglicht es ihnen, Nährstoffe zu absorbieren, zu transportieren und zu integrieren, um kontinuierlich an Größe zuzunehmen, ihre Form zu ändern und ihre Stärke zu modulieren. Synthetische Polymere sind dagegen grundsätzlich unterschiedlich aufgebaut. Von der Natur inspiriert, präsentiert diese Arbeit verschiedene Ansätze, um synthetische weiche Materialien wachsen zu lassen und die grundlegende Wachstumsfähigkeit nachzuahmen. Im ersten Teil wird die Photoaktivierung vorgestellt, um das Wachstum voluminöser weicher Materialien zu beeinflussen. Basierend auf diesem Wachstumskonzept wurde ein Elastomer mit kontrollierbarer Größe, Festigkeit und Zusammensetzung hergestellt. Dieser Ansatz kann zur Regulierung der Benetzbarkeit durch Zufuhr von Nährstoffen auf organischer und wässriger Basis während des Polymerwachstums ins Auge gefasst werden. Im zweiten Teil wird ein lichtinduziertes und ortsspezifisches Selbstwachstum von Mikrostrukturen auf der Oberfläche eines dynamischen weichen Substrats demonstriert. Die erzielte feine Modulation von Größe, Zusammensetzung und mechanischen Eigenschaften führt zur Erzeugung einer rauen Oberfläche und zur Wiederherstellung großflächiger Oberflächenschäden. Im letzten Teil wird das Selbstwachstum und die Selbstverstärkung von ineinandergreifenden Polycatenanelastomeren auf Poly (disulfid)-Basis mit einzigartigen intermolekularen ineinandergreifenden Topologien erreicht. Die Ergebnisse tragen zum Thema von neuen Topologien von Polymer¬netzwerk¬ketten bei und liefern nützliche Informationen für die Zukunft seitens ihrer Chemie als seitens neuer Materialien.

List of Abbreviations

AIBN	2,2'-Azobisisobutyronitrile
ATR-FTIR	Attenuated total reflection-Fourier transform infrared
ATRP	Atom transfer radical polymerization
BA	Butyl acrylate
BMI	Bismaleimide
BZSA	Benzensulfonic acid
$CDCl_3$	Chloroform-$_d$
CDs	Cyclodextrins
$CHCl_3$	Chloroform
CL	Cross-linkers
CPADB	4-Cyano-4-(phenylcarbonothioylthio)pentanoic acid
Cs_2CO_3	Cesium carbonate
CTAB	Cetyltrimethylammonium bromide
D1173	2-Hydroxy-2-methylpropiophenone
DA reaction	Diels-Alder reaction
DB24C8	Dibenzo 24 crown 8
DBCO	Dibenzocyclooctyne
DBTDL	Dibutyltin dilaurate
DCBs	Dynamic covalent bonds
DCM	Dichloromethane
DHB	2,5-Dihydroxybenzoic acid
DMAP	4-(Dimethylamino)pyridine

DMF	*N*,*N*-Dimethylformamid
DMSO	Dimethyl sulfoxide
DMSO-$_{d6}$	Dimethyl sulfoxide-$_{d6}$
DN	Double network
DPD	Dissipative particle dynamics
DSC	Differential scanning calorimetry
EDC·HCl	1-(3-Dimethylaminopropyl)-3-ethylcarbodiimid Hydrochlorid
e.u.	Entropy units
ESR	Electron spin resonance
H_2SO_4	Sulfuric acid
HB acetate	4-Hydroxybutyl acetate
HBA	4-hydroxybutyl acrylate
HDDA	1,6-Hexanediol diacrylate
HEA	2-Hydroxylethyl acrylate
I-819	Irgacure 819
Irgacure 2959	2-hydroxy-4'-(2-hydroxyethoxy)-2-methylpropiophenone
K_2CO_3	Potassium carbonate
KI	Potassium iodide
LC-MS	Liquid chromatography–mass spectrometry
M	Monomers
MALDI-TOF	Matrix assisted laser desorption ionization-time of flight
MeCN	acetonitrile
MeOH	Methanol

Mn	Number-average molecular weight
Mw	Weight-average molecular weight
Na_2CO_3	Sodium carbonate
Na_2SO_4	Sodium sulfate
$NaBH_4$	Sodium borohydride
NaCl	Sodium chloride
$NaHCO_3$	Sodium bicarbonate
NBA	*o*-nitrobenzyl acrylate
NIPAAm	*N*-Isopropylacrylamide
NMP	*N*-Methyl-2-pyrrolidon
NMR	Nuclear magnetic resonance
PDIDA	Bis-*N*,*N*'-6-hydroxyhexanol perylenetetracarboxylic diimide-acrylate
PDMS	Polydimethylsiloxane
PDT	Propane dithioctic
PEG	Polyethylene glycol
PEGA	Poly(ethylene glycol) methyl ether acrylate
PRCG	Photoredox catalyzed growth
PS	Polystyrene
PSFB	Furan-containing polymer
PTFE	Polytetrafluorethylen
PTH	10-Phenylphenothiazine
PVA	Poly(vinyl alcohol)

RAFT	Reversible addition fragmentation chain transfer
rDA reaction	retro-Diels-Alder reaction
SDS	Sodium dodecyl sulfate
SPAAC	Strain promoted copper free Click chemistry
STEM	Structurally tailored and engineered macromolecular
TAD	1,2,4-triazoline-3,5-dione
TE	Transesterification
TEA	Triethylamine
TEG	DL-Thioctic ethylene glycol
THE	DL-Thioctic hydroxyethyl
THF	Tetrahydrofuran
TTC	Trithiocarbonate(s)
UV	Ultroviolet
UV-Vis	Ultraviolet-visible
WCA	Water contact angle
3D	Three-dimensional
4D	Four-dimensional

Whenever it is not stated here, all other abbreviations have their usual default meaning.

Contents

Motivation and scope of this thesis

Growing is the natural property of all living organisms under suitable conditions, which makes them adaptable to the environment in size, shape, and strength. In this process, nutrients are transported, adsorbed, and integrated into the body. Non-living materials do not show this property, though it could be highly beneficial in many applications. For example, implanted medical devices with self-growing possibility would be highly beneficial for children. They would avoid successive surgical interventions during the growing period of the child to exchange the device by larger ones. Thus, designing engineered materials to confer growing property is of paramount relevance. Herein several approaches to guide synthetic dynamic materials to grow like living organisms have been investigated and explored.

Self-growing polymeric material should have these characters (Scheme 1): (1) swelling ability to monomers and crosslinkers (termed as nutrient solution), (2) a mechanism for *in situ* polymerization to extend the network, and (3) chain-exchange reaction to homogenize the original and newly formed network. Self-growing materials in previous reports possess the swelling capability when soaked in their good solvents (elastomers in organic solvents and hydrogels in water). Besides, most studies in the field have focused on incorporating new molecules into as-prepared polymer networks to vary the material properties post-synthesis. This approach restructures the material to a limited extent, and is not suitable to modify bulk properties. The integration of original and newly formed networks in the material has been less explored. This strategy can lead to materials with multiple growing abilities. In this context, this PhD thesis presents various approaches to the design and synthesis of elastomers based on self-growing polymeric materials with tunable size, shape, and mechanical properties. Light-induced self-growth of bulky materials can be obtained *via* growth

cycle. This approach can be used for regulating the bulk wettability by introducing organic and aqueous based nutrients. Furthermore, a light-regulated methodology was established to control the site-specific self-growth of microstructures from the surface of dynamic soft poly(4-hydroxylbutyl acrylate-*co*-*o*-nitrobenzyl acrylate) [poly(HBA-*co*-NBA)] elastomers. Such light-regulated growth is spatially controllable and dose-dependent, and allows fine modulation of the size, composition, and mechanical properties of the grown structures. These model platforms were used to structure the material surface and restore large-scale surface damage. In addition, an evaporation-induced entropy replenishment approach was developed to fabricate fully interlocked soft poly(disulfide)s based elastomers with unique interlocking network topologies, and being applied to self-grow and self-strengthen the interlocked bulky material. These engineered approaches were used to study how the incorporation and integration of small molecules to make the growth of material, and the modulation in size, shape and strength of grown substrates under stimuli.

This thesis work is presented as follows:

1) **Chapter 1** elaborates on the general state-of-art within this field, in which it separately introduces the research status of dynamic soft materials, and different investigation levels like dynamic linkages, matter transfer, and intermolecular matter conversion and/or integration within materials so far.
2) In **Chapter 2,** I evaluate a photo-induced activation strategy to continually incorporate nutrient (monomer and crosslinker), to expand bulky elastomers with controllable mechanical properties and compositions. Then, multiply growth cycle treatment of the bulky material by insertion and integration of nutrients enables bulk elastomers to multi-time grow with a variety of size and strength. By changing different types of nutrient solutions, heterogeneous growth of bulky materials is achieved. Finally, its potential application was envisioned for regulating the bulk

wettability by introducing organic and aqueous based nutrients *via* the growth cycle.

3) **Chapter 3** describes a photo-induced strategy for regulating the localized self-growth of microstructures from the surface of a swollen dynamic substrate, by coupling photolysis, photopolymerization, and transesterification together. Specifically, the design and preparation of poly(HBA-*co*-NBA) elastomer model is elaborated first, followed by the exploration of the mechanism of self-growth involved evaluating the role of NBA as a promoter, integrating of polymer networks by transesterification and certificating their grown structures. Then, the tuning of light-induced growth with temporal and spatial modulation of the size, shape, and mechanical properties of the grown structures was quantified. Finally, the potential applications of light-regulated self-growth in structuring material surface and restoring large-scale surface damage were demonstrated.

4) In **Chapter 4**, a novel methodology of evaporation-induced entropy replenishment was further developed to fabricate fully interlocked poly(disulfide)s based elastomer. The supply of increased entropy energy by evaporation can compensate for the entropy loss of cyclization of rings within the precursor was investigated. In addition, certification of this unique interlocking network topology was then studied. Furthermore, dynamic functions of fully interlocked elastomers based on disulfide exchanging were deeply investigated. At last, self-growing and self-strengthening of interlocked material owing to the facile evaporation approach were evaluated.

5) Finally, a conclusion about self-growing soft materials based on engineered approaches and platforms and a brief outlook for further development of material-based models to novel dynamic soft materials are expounded in **Chapter 5**.

The concept and design of self-growing polymeric materials in this thesis are demonstrated in Scheme 1.

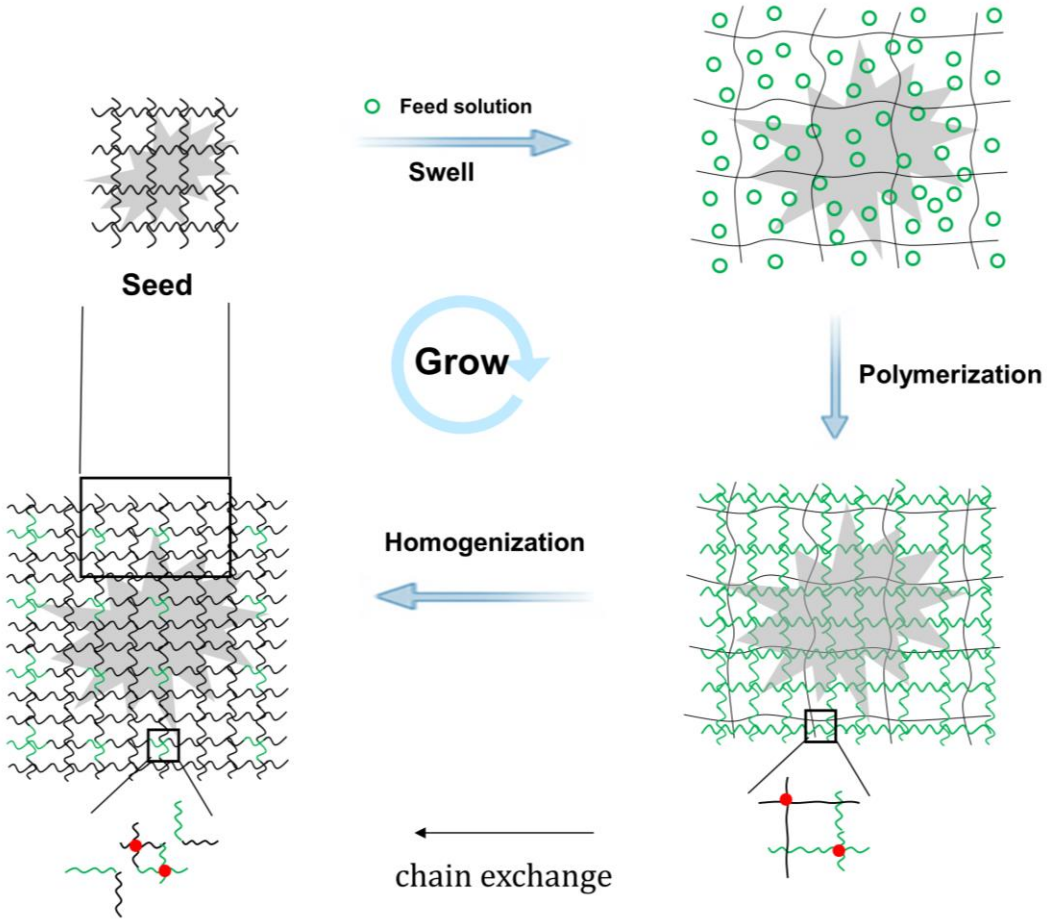

Scheme 1. Schematic process of fabrication of self-growing polymeric materials, which involved several characters, (a) swelling ability, (b) robust *in situ* repolymerization, and (c) chain exchange reaction for homogenization. Feed solution usually composed by monomer, crosslinker, initiator, and/or catalyst.

Chapter 1

1. Introduction

1.1. Dynamic soft materials

Classical soft materials are expected to be chemically inert and possess fixed molecular structure formed by covalent bonds, and intermediate mechanical properties between a crystallized solid and a liquid that makes them deformable under external forces.[1-3] Dynamic soft materials developed in the last decades, contain other types of molecular interactions beyond covalent bonds, which allow them to adapt and respond to their environment.[4-6] These materials can respond to varieties of stimuli, ranging from physicochemical (light, pH, temperature, magnetic, force, and electric field) to biochemical (introducing biomolecules) inputs.[7-8] Therefore, dynamic soft materials broaden material properties and application ranges for soft materials and derived devices, including stimuli-responsive materials, robotic actuation, controlled drug release, and self-healing materials.[9-13]

Among dynamic soft materials, elastomers[14-15] and hydrogels[12-13] are widely used and investigated in our daily life. Different aspects of dynamic soft materials are a matter of current research, such as probing the dynamic linkages within the materials,[4-6] observing molecules transportation within the swollen dynamic substrates,[16-17] and exploring the conversion and integration of molecules within the dynamic soft materials to develop growing materials.[18-20] Most research focuses on investigating the dynamic behaviors of soft materials based on the bonding and debonding of dynamic crosslinks. Meanwhile, great attention has been paid to understand the motion of molecules entrapped in the matrix when applied with external stimuli. However, only a few of them follow closely with cognizing the effects between the adsorbed small molecules and gel materials. Importantly, understanding the

underlying interactions between entrapped components and the formed networks will inspire people to design novel soft materials to meet their desires. For example, guiding synthetic materials to “grow” with coded manner to mimic the self-growth property of living organisms. Therefore, it is desired to fabricate novel dynamic soft materials to study the theory behind and overcome highlighted restrictions.

In this introductory chapter, dynamic linkages used in dynamic soft materials are introduced. Then, matter transfer among the functionalized dynamic soft gels is summarized. At last, the fabrication and applications of growing materials are introduced.

1.1.1 Dynamic linkages

Dynamic crosslinks can break and reform reversibly either autonomously or in response to stimuli, which has been used in organic synthesis, material science, and biomedical applications.[4, 7, 12] In general, several kinds of bonds are categorized as dynamic crosslinks, including dynamic covalent bonds, and noncovalent interactions.

1.1.1.1 Dynamic covalent bonds

Dynamic covalent bonds (DCBs) have facilitated the development of new classes and understanding of polymer materials.[4-6] DCBs are normally stable at ambient conditions, but dynamic under stimuli, e.g. light, temperature, pH, and electricity.[4-6] Going beyond the breaking and reforming of the covalent bonds, soft polymeric materials with DCBs are both robust and adaptable. Typically, the exchange of DCBs occurs through associative or dissociative pathways (Figure 1a and 1b).[5] In an associative pathway, chemical bonds are activated by breaking and reforming simultaneously during the exchange process (Figure 1a). Meanwhile, the macromolecular structure has dramatic responsiveness due to the decreased number of linkages. In a dissociative pathway (Figure 1b), the dynamic linkages dissociate firstly and then new linkages form after

some time. The change in the macromolecular structure is minimized during the exchange process, resulting from the approximately constant bond density in the activated state.

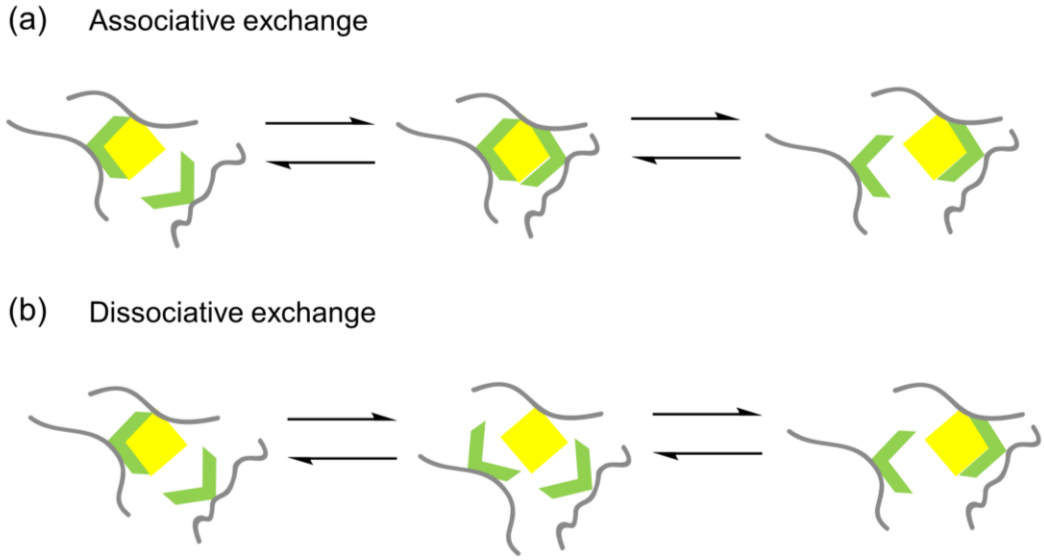

Figure 1. (a) Associative exchange and (b) dissociative exchange of DCBs. Reproduced with permission.[5] Copyright 2018, Wiely-VCH.

Various kinds of DCBs have been used to develop dynamic soft materials:

- **Sulfur related chemistry.** Sulfur chemistry has been an indispensable member in materials science and engineering with the development of rubber vulcanization.[4, 21] With the increased demand for rubber recycling in both industrial and societal applications, the evolution of disulfide bond is of great research value. Tobolsky et al. firstly reported the stress relaxation within poly(disulfide)s rubber attributing to the rapid disulfide exchange.[22] During the bond exchanging process, disulfide bonds can be dissociated into thiols and return to their disulfide state through heating, catalyst, light and external radicals (Figure 2a),[8, 23] which favored valuable applications in designing self-healing and recyclable networks.[24-25] For instance, Rowan and co-workers reported a rapidly photo-healable poly(disulfide)s system according to the rearrangement of the

disulfide bonds.[25] In the presence of mechanical force and light, the macroscopic cracks could be easily reconfigured, which was enhanced by faster thiol-disulfide exchange chemistry. Besides, other sulfur derivatives also brought excellent potential applications, such as allyl sulfide-based addition-fragmentation process (Figure 2b),[26] chain shuffling of iniferters (Figure 2c and 2d),[27-28] and thiol–thioester exchange reactions (Figure 2e).[29-30] Sulfur related chemistry was also extended by combing selenium and disulfide to design dynamic soft materials recently (Figure 2f).[31]

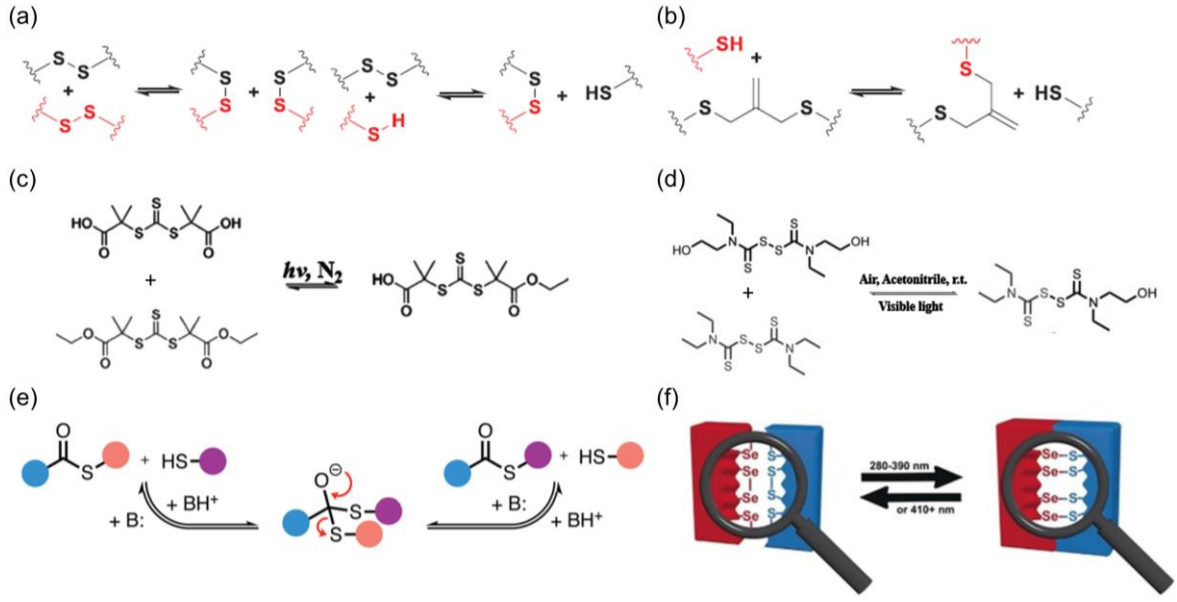

Figure 2. Sulfur based dynamic soft materials. (a) Poly(disulfide)s and thiol-disulfide exchange within soft materials. Stimuli can be temperature, pH and light. (b) Addition–fragmentation chain transfer for developing dynamic soft gels. (c) (d) Example of typical chain shuffling iniferter of photoresponsive materials. (e) Dynamic thiol and thiol-ester exchange catalyzed by a base. (f) Wavelength selective exchange between disulfides and diselenides based materials. Reproduced with permission.[8, 26-29, 31] Copyright 2005, AAAS. Copyrights 2011, 2012, 2018, 2020 Wiely-VCH. Copyright 2018, The Royal Society of Chemistry.

- **Diels-Alder chemistry.** Diels-Alder (DA) reaction usually occurs between an electron-rich diene and an electron-poor dienophile to produce a cyclohexene

adduct *via* [4+2] cycloadditions by Diels and Alder in 1928, which can be reversed at elevated temperature *via* a dissociative retro-Diels-Alder (rDA) reaction.[32] The excellent thermal reversibility has made DA chemistry an ideal possibility to construct dynamic soft materials. Wudl and co-workers firstly proposed the self-healing soft materials based on thermoreversible DA reaction (Figure 3a).[33] The materials were prepared by using DA reaction between tetrafunctional furan and trifunctional maleimide monomers, which showed approximately 50% mending efficiency after being heated at 150 ^{o}C for 2h by the dynamic DA linkages. Inspired by this, more researches based on remendable DA interaction have emerged and broadened its scope to polyamides,[34] poly(lactic acid),[35] polycaprolactone,[36] polyurethanes,[37] epoxy resins,[38] polyketones[39,] and ethylene/propylene/diene rubbers.[40] Although these encouraging progress, the elevated reaction time and required high temperatures limit their real applications. Recently, Du Prez and co-workers demonstrated novel DA chemistry involving 1,2,4-triazoline-3,5-dione (TAD) as an alternative dienophile to achieve more quickly reaction at room temperature (Figure 3b).[41] They also found that after replacing the diene with indole in a PU system with TAD, the soft materials showed good reversibility under temperature.

- **Transesterification**. A classic dynamic transesterification (TE) reaction happens between an alcohol and an ester to create a new pair of ester and alcohol until the equilibrium achieves (Figure 3c).[42] Normally, it requires high temperatures and catalysts like Lewis acids, strong Brønsted bases, inorganic salts, and Brønsted acid to trigger the exchangeable reaction.[43] Although TE is widely used in recycling and reprocessing epoxy networks by the efficient bond exchange characteristics, there is still a requirement in dynamic soft materials. Reversible crosslinked polydimethylsiloxane (PDMS) network could be obtained

via TE reaction under high temperature, broadening the practical application area of recycling silicon elastomers.[44] In addition, introducing TE reaction into soft material can also programmable stiffen polymer substrate by deeply guide the transesterification degree.[45] However, the required catalyst or high temperature for TE reaction restricts their attempts of designing dynamic gel fields in some extent.

- **Imine chemistry.** Well-known imine chemistry occurs by a condensation reaction between an aldehyde and a primary amine to produce an imine and water.[46-47] In general, imine can hydrolyze back to its starting material reversibly in a dissociable pathway (Figure 3d).[46] When another amine molecules are introduced, transamination would happen with or without adding the catalyst through an associable pathway in the absence of water (Figure 3d).[46] Furthermore, imine metathesis would occur by dynamic exchanging of imines in the presence of catalysts (Figure 3d).[46] Owing to the reversible formation and dissociation of imine bonds, imine chemistry has been adequately utilized in dynamic soft materials.[48-49] Wei et al. reported multi-stimuli-responsive dynamic soft hydrogels by integrating dynamic imine condensation, showing responsiveness drug delivery and self-healing capabilities.[48] However, imine chemistry still has some drawbacks, such as its hydrolytic instability. In order to eliminate the hydrolysis susceptibility, more stable acylhydrazones and oximes are developed. In fact, acylhydrazones and oximes form by reacting an aldehyde with hydrazide and hydroxylamine, respectively, the reversibility of which is generated under mild conditions and activated by pH value. Deng et al. reported the pH-responsiveness of crosslinked polyacylhydrazone gels with self-healing abilities.[50] When pH <4, gels turn into sol, but the gel state can be restored when pH >4.

- **Olefin Metathesis.** Polymer materials composed by reversible carbon-carbon bonds may provide the capability to develop stronger self-healing materials than dynamic polymers involving heteroatoms. Guan and co-workers incorporated olefin metathesis of shuffling carbon-carbon double bonds into crosslinked polybutadiene networks to achieve malleability and self-healing capability catalyzed by Grubb catalyst (Figure 3e).[51-52] In this study, the catalyst swelled into the dynamic networks and cleaved the polymer chains partially, not only leading to a reduction in crosslinking density and mechanical property, but also resulting in good malleability at room temperature with fast relaxation.

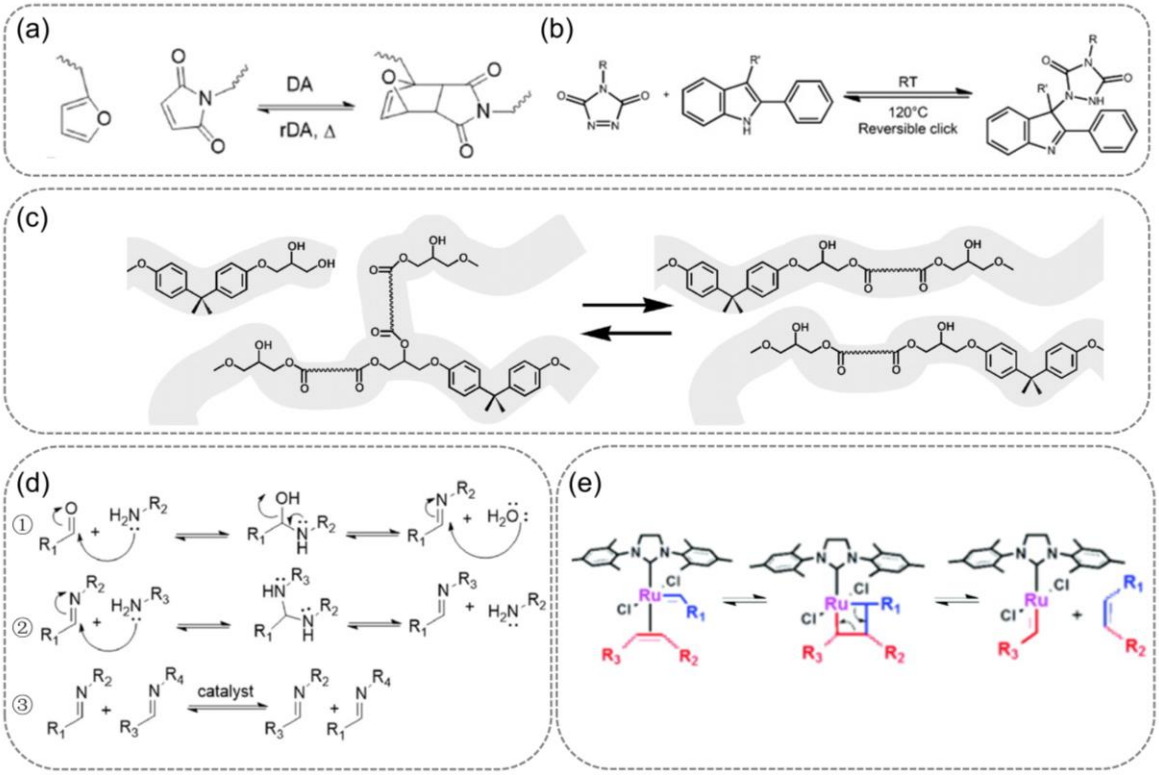

Figure 3. Examples of dynamic covalent linkages within soft materials. (a) (b) Diels-Alder chemistry for applying in dynamic materials. (c) Topographical rearrangement triggered by β-hydroxyl ester-based transesterification. (d) Mechanism of reversible imine chemistry when meeting dynamic materials. (e) Dynamic exchange between carbon–carbon double bonds within olefin metathesis. Reproduced with permission.[33, 41-42, 46, 52] Copyrights 2015, Wiely-VCH. Copyright 2002, 2011, AAAS. Copyright 2012, American Chemical Society. Copyright 2015, The Royal Society of Chemistry.

- **Boronic esters and boronates.** The esterification between a boronic acid with a diol can generate a boronic ester with reversibility under ambient conditions.[53] If the pH is above the pK_a of the boronic acid, the equilibrium prefers boronate ester state while it transforms to boronic acid and diol below this pK_a (Figure 4a). This rapid dynamic exchanging behavior at mild conditions has attracted great attention and been proposed in degrading and architecture-transformable materials. For instance, Sumerlin and co-workers described the influence of pH (acidic or neutral) to self-heal the boronate ester crosslinked soft hydrogels, and highlighted its application in biomedical materials.[54] Boroxines are cyclic trimers, which can be produced by reversible dehydration of boronic acids. In this process, equilibrium can be ruptured by addition or removal of water, this kind of reaction has been used for developing dynamic assemblies and covalent organic frameworks.[55]
- **Si-O exchange in siloxanes and silyl ethers.** Siloxanes exchanges is another dynamic equilibrium in a PDMS elastomer for stress relaxation discovered by Osthoff in 1954, which always needs an anionic initiator or a basic catalyst to activate the nucleophilic Si-O exchange (Figure 4b).[56] McCarthy et al. used this chemistry in developing self-healing PDMS networks with living characters, as the reactive silanolate end group can further initiate nucleophilic exchange of Si-O bonds between the siloxane moieties.[57] In this kind of dynamic networks, the dynamic performances can be finely tuned by regulating the concentration of anionic initiator and crosslink density.[58] In addition, Si-O bond exchange is extended in developing silyl ether-based dynamic materials. Guan and co-workers reported thermally stable materials by introducing silyl ether linkages, where Si-O exchange can be altered by adding neighboring amino groups (Figure 4c).[59]

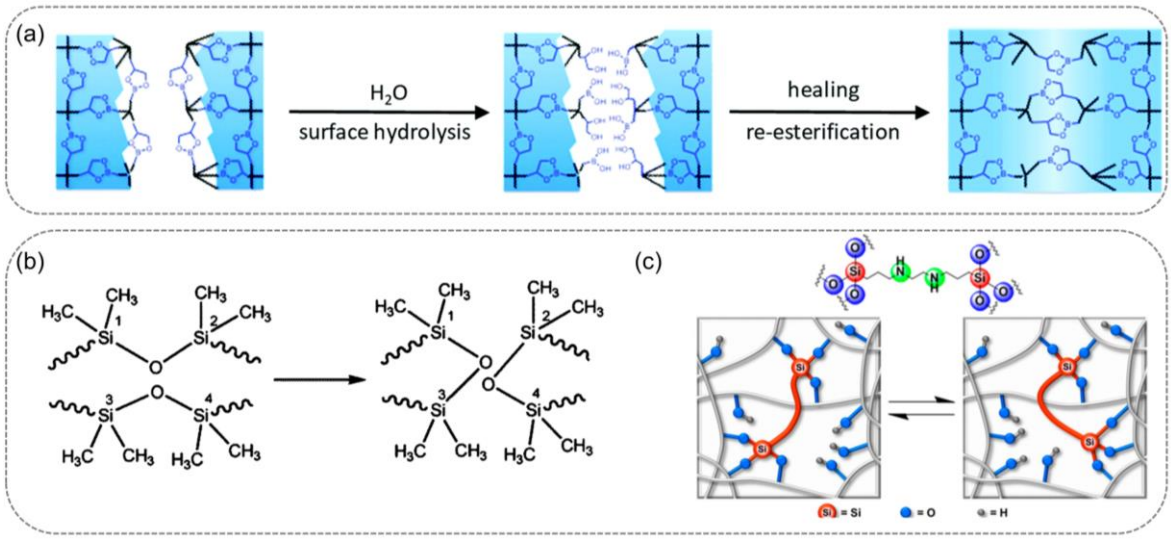

Figure 4. Other dynamic covalent chemistries in soft materials. (a) Mechanism of dynamic boronic esters exchange in a hydrogel system. (b) (c) Dynamic Si-O exchange in siloxanes and silyl ethers based materials. Reproduced with permission.[55-56, 59] Copyright 1954, 2017, American Chemical Society. Copyright 2020, The Royal Society of Chemistry.

1.1.1.2 Noncovalent interactions

Contrary to the dynamic covalent bonds, noncovalent interactions usually happen between a protein and a drug, or a catalyst and its substrate, or within self-assembled nanomaterials, or in some chemical reactions or dynamic materials to form molecular clusters, which is of importance in regulating the secondary and tertiary structures of natural macromolecular (e.g., peptides, nucleotides, and saccharides).[60] Noncovalent interactions were firstly developed by J. D. van der Waals, and have achieved valuable progress in chemistry, physics, and bio-disciplines over the previous two decades.[61-63] In essence, noncovalent interactions are considerably weaker (1 or 2 orders of magnitude) than covalent interactions, possessing stabilization energy between 1 and 20 kcal/mol. These properties make noncovalent interactions to spring up like mushrooms in stretchable hydrogels, flexible bioelectronics, self-healing conductors and switchable adhesives.[64-67] To date, amounts of noncovalent interactions have been developed.

- **Hydrogen bonding.** As one of the most used noncovalent interactions, hydrogen bonding is a physical interaction occurred between a given hydrogen atom and a highly electronegative atom (e.g., O, N, or F). In this reversible bonding, hydrogens act as hydrogen donors while electronegative atoms behave as hydrogen acceptors (Figure 5a).[60, 68] With the development of hydrogen bonding based chemistry, single hydrogen bonding system, double hydrogen bonding system, triple hydrogen-bonding system and quadruple hydrogen bonding system are incorporated into dynamic soft materials. The simplest hydrogen bonding polymeric networks belong to the single hydrogen bonding system. Self-healable poly(vinyl alcohol) (PVA) hydrogels were fabricated by hydrogen bonding between the hydroxyl group of adjacent chains.[69] When two separated PVA hydrogels contacted, polymer chains diffuse across the interface of the cut samples could autonomously reform the hydrogen bonding. Thus the interface of bulky hydrogels was disappeared after 12h contacting at room temperature.
- **Ionic bonding.** The reversible electrostatic interactions of oppositely charged ions form the ionic bonded hydrogel composites, which involve positively charged polymer chains crosslinked with other negative charged polymers chains or with ions (Figure 5b).[70-71] It is also noted that these oppositely charged ions may become deprotonated and lead to electrostatic repulsion depending on the pH conditions. By combing polyelectrolytes and/or counterions in aqueous media will generate three-dimensional (3D) hydrogel material *via* ionic bonding. Gong and co-workers reported tough hydrogel networks by ionic bonding between polymers hanging randomly dispersed cationic and anionic repeat groups.[71] The strong bonds act as permanent crosslinks to impart elasticity, whereas weak bonds serve as sacrifice crosslinks with reversible breaking and

reformation to dissipate energy. Additionally, the mechanical property of the obtained physical hydrogels can be finely tuned by using diverse ionic combinations.

- **Hydrophobic bonding.** Hydrophobic interactions occur by the interaction of hydrophobic molecular interfaces in aqueous solutions to form hydrophobic aggregates that can quickly re-form when suffered a destruction.[72-74] To apply this approach to dynamic soft materials (i.e., hydrogels), micelle copolymerization is usually introduced to form stable hydrophobic domains without disrupting this hydrophilic nature (Figure 5c).[73] This typical method includes the concurrent polymerization of hydrophilic monomers with small amount of hydrophobic monomers to form micelles. Micelles could be stably formed by association between the hydrophobic monomers and the surfactant. When sodium dodecyl sulfate (SDS) was solely used as the surfactant, the obtained hydrogel with reversible hydrophobic bonding showed self-healing abilities to some extent.[75] This self-healing efficiency depends on the dissociation and re-association of the micelles, thus improving the hydrophobe solubility that can enhance the self-healing performance. The addition of sodium chloride (NaCl) could lead to the growth of wormlike micelles and increase the hydrophobe's inclusion within the hydrophobic hydrogels.[76] Alternatively, the combination of oppositely charged surfactant is another approach. By mixing of anionic surfactant SDS and cationic surfactant cetyltrimethylammonium bromide (CTAB) could also induce the micelle growth to enhance the mechanical property of self-healable soft gels.[77]
- **Physical entanglements.** Physically entanglement of polymer chains is a universal phenomenon of polymers in static and solution states, which cross each other arbitrarily to restrict the molecular motion, representing a weak and

dynamic intermolecular interaction but has been proven to be too weak to build 3D polymer networks.[78] With the development of microgel or nanogel technologies, however, Cui and co-workers created a highly crosslinked nanogel system to form entanglement cluster, thus physically crosslinking the hydrogel recently (Figure 5d).[79] Polymer chains with high molecular weight passed through and slide on the nanogel cluster, demonstrating multiple entanglement force to retain the elastic state of dynamic soft hydrogels.

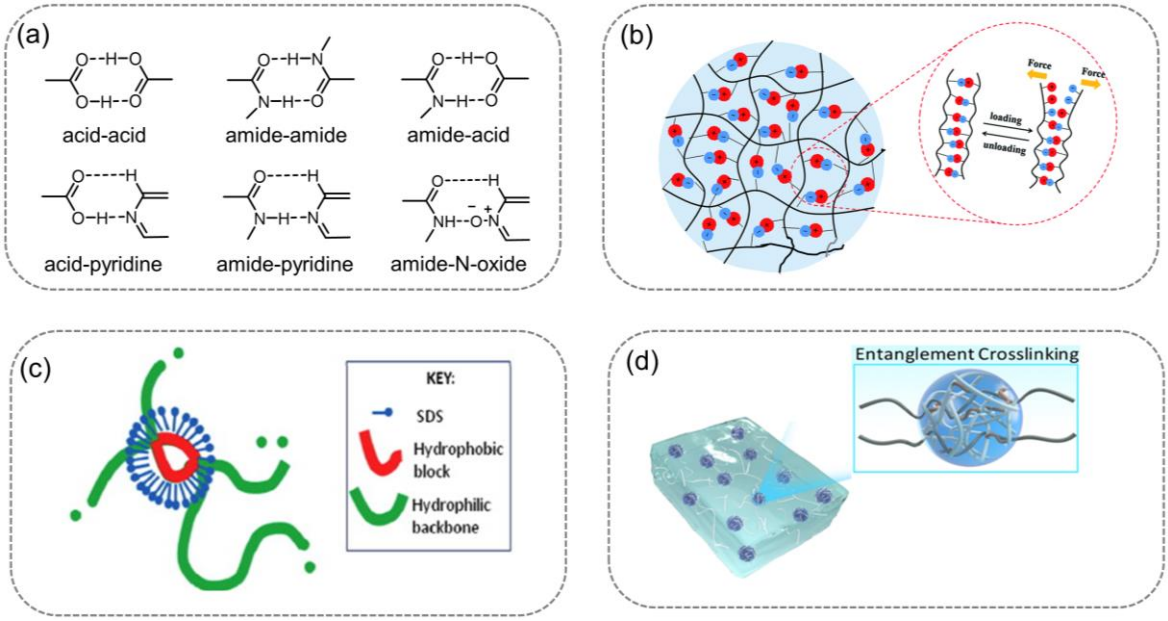

Figure 5. Noncovalent interactions used in dynamic soft materials. (a) Examples of some common hydrogen bonds of compounds. (b) Dynamic ionic bonding to prepare self-healing hydrogels. (c) A typical structure of hydrophobic interaction within soft hydrogels. (d) Physical entanglement crosslinking of hydrogel system. Reproduced with permission.[68, 71, 74, 79] Copyright 2015, BRNSS Publication Hub. Copyright 2012, Elsevier B.V. Copyrights 2013, Nature Publishing Group. Copyright 2020, The Royal Society of Chemistry

- **Inclusion complexations.** Inclusion complexation is one of the special noncovalent interactions which involve two or more chemical species. In this reaction, one chemical entity (the “host”) forms a cavity where the other chemical entity (the “guest”) is then located; thus inclusion complexation usually

mentioned as host-guest interactions.[80-81] Due to the cavity structures, macrocycles are the widely used potentials as the great “host”. With huge developments, varieties of macrocycles have been discovered, for instance, cavitands (including cyclodextrins (CDs), calixarenes and cucuibit[n]urils), crown ether, catenanes, cyclophanes, pillararene, cryptophanes, and porphyrins.[82] These macrocycles possess specific properties such that they can combine with the guest molecules and generate inclusion complexes in the solvent or material matrix. Benefiting from the reversible deformation and reformation behavior of dynamic host-guest interactions (Figure 6a), inclusion complexations have been widely applied in self-healing hydrogels, stimuli-responsive soft materials, and drug delivery system.[83] Among the most used macrocycles for inclusion complexations, cavitands are served as ideal choices, in which CDs have strong host-guest interactions with different functional groups and biocompatible and biodegradable properties. In recent decades, CDs was first introduced into the supramolecular soft hydrogels by Kamachi and co-workers, in which they described sol-gel transitions resulted from inclusion complexation between α-CD and poly(ethylene glycol) in aqueous media.[84]

- **Metal coordination interactions.** In dynamic soft materials areas, metal coordination interactions have been developed in recent years and used as crosslinking junctions which involve metal ions to a ligand (e.g., atoms, molecules, or ions that donate electrons) to form coordinated complexes (Figure 6b).[85-86] Typically, coordination is a special chemical bond where one atom offers electrons, which is different from traditional covalent bonds where each atom offers electrons. Moreover, metal coordination interactions resulting from Lewis acid-base interactions can be stronger than most of the noncovalent bonding but weaker than covalent bonding.[60] Coordinated bonds are capable of reforming

after rupture and functionalized as sacrificial bonds to work in self-healing hydrogels, redox-responsive materials, adhesives, and stretchable soft elastomers.[85-88] Suo and co-workers reported one of the typical hydrogel systems by combing polyvalent metal ions and polysaccharide (alginate).[89] In general, anionic alginate can form hydrogels by incorporating the carboxylate groups with metal cations (Fe^{3+}, Ca^{2+}, Sr^{2+}, Ba^{2+}). The guluronic acid blocks in different alginate chains could generate dynamic crosslinks through metal coordination, resulting in metal-alginate hydrogel.

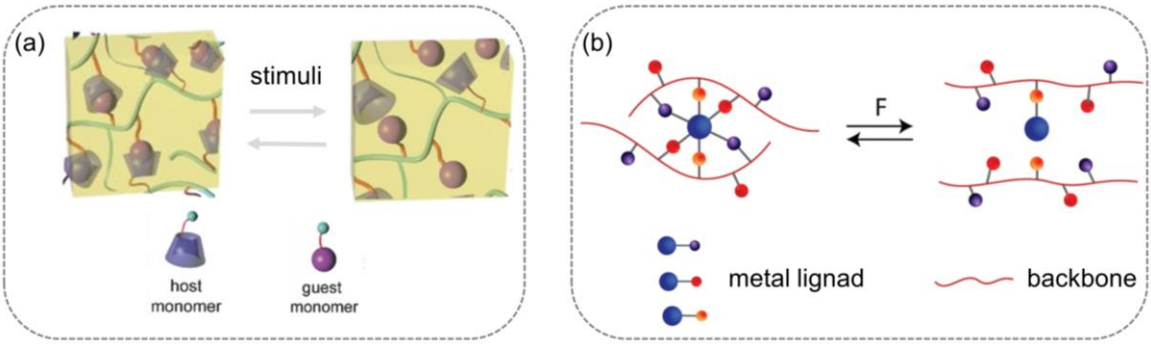

Figure 6. Other types of noncovalent interactions used in dynamic soft materials. (a) Dynamic behavior of host-guest interaction-based hydrogel under stimuli. (b) Reaction mechanism of metal coordination interactions under force within soft gels. Reproduced with permission.[83, 86] Copyrights 2014, 2019, Wiely-VCH.

1.1.2 Matter transfer

The understanding of the behavior of soluble molecules within a dynamic matrix is relevant for the design of new materials with bio-inspired functions. Living organisms in nature possess the ability to be adaptable to environmental changes through autonomously packaging, transporting, and secreting fluids and liquids by a delicate code.[90] Matter transfer within soft materials has received increasing attention. This idea was observed in a layered film of azobenzene-containing polymers by Rochon and co-workers in earlier studies, who suggested a corrugation whose amplitude could

be up to fifty percent of the initial thickness.[91] Therefore, dynamic wrinkled surfaces have been obtained by modulating the stress or strain distribution in the system through external stimuli. Diels-Alder (DA) reaction between furan and maleimide was also introduced to fabricate wrinkle topology that can be reversibly erased and tuned by DA reaction *via* regulating the temperature of the system.[92-93] However, these studies only demonstrated the mass transport or motion of polymer chains, not the molecules within the soft materials. Currently, Jiang and co-workers developed a simple strategy for fabricating 3D reconfigurable wrinkles on material surfaces, in which a DA reaction in the top soft layer, consisting of reversible crosslinked polymer networks composed of furan-containing copolymers and bismaleimide (Figure 7).[16] In this study, bismaleimide can undergo a spatial and controllable photodimerization. When a photomask was used during UV irradiation, selective photodimerization of the maleimide generated a difference in the concentrations of bismaleimide between the exposed and unexposed regions, leading to the diffusion of bismaleimide to form the relief pattern. The diffusion of bismaleimide resulted in an increased thickness of the exposed region while that of unexposed regions decreased. Orthogonal wrinkles were sequentially generated or erased by mass transport in both irradiated and unirradiated regions of the soft material layers through temperature-responsive dynamic DA reactions.

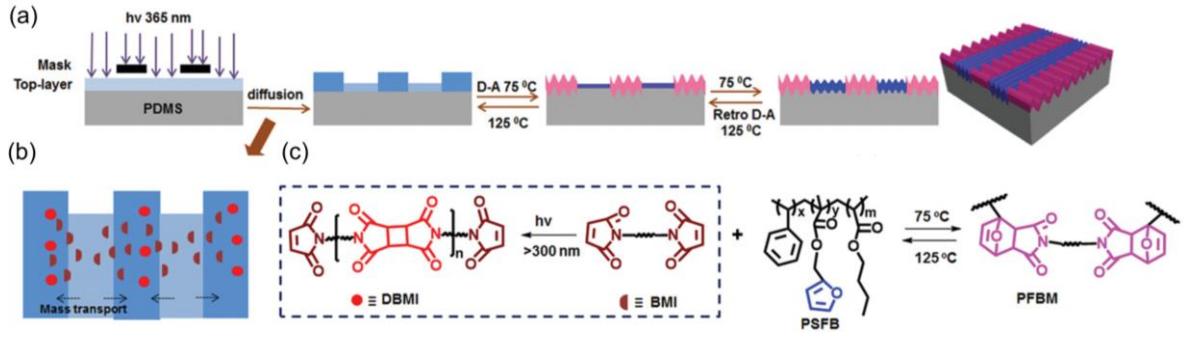

Figure 7. 3D hierarchical patterns with dynamic wrinkles. (a) Schematic process of hierarchical pattern with dynamic wrinkles through DA reaction. (b) Diffusion of bismaleinide (BMI) under light. (c) Chemical

structures of BMI and furan-containing polymer (PSFB) and the mechanism of photocontrolled DA reaction. Reproduced with permission.[16] Copyrights 2020, Wiely-VCH.

The self-secretion of fluid or liquids onto material surfaces is still essential and indispensable in our daily life, for example, human body secret sweat on the skin as a response to heat and emotional stress. Cui and co-workers firstly reported a self-secretion system involving liquid-storage compartments in a supramolecular gel with a thin liquid layer on the top (Figure 8).[17] By disturbing or removing the top layer, the disjoining pressure resulting from the continuous and dynamic liquid exchange between the droplets, matrix, and surface will drive the liquid to restore the original thickness and self-report their liquid content. In this system, $\gamma_{ga} - (\gamma_{la} + \gamma_{gl}) > 0$, where γ_{ga}, γ_{la} and γ_{gl} are the gel-air, liquid-air, and gel-liquids interfacial tensions, respectively, thus the surface of supramolecular polymer-gel matrix will always be coated by a liquid overlayer. Meanwhile, when droplets shrinks, the matrix will reversibly reconfigure through bond disassemble and re-assemble. During the removal and restoring cycles, liquid droplets will continuously shrink and transport to the surface, leading to progressive transparency of the gels. Based on this, the localization of liquid droplets embedded into a dynamic solid matrix could also be controlled by evaporative lithography.[94] When the solvent evaporated selectively under a mask, the homogeneous liquid and polymer compounds were redistributed. The polymer responsible for the resulting crosslinked matrix moved to the region of hindered evaporation while the excess nonvolatile liquid concentrated in the region with faster evaporation, resulting in the phase separation to localized create liquid droplets. Regarding this, droplet-containing and droplet-free regions displayed distinct properties, such as transparency and fouling resistance. Moreover, the secretion of liquids could also be realized by mechano-stimuli.[95] Zhao and co-workers created textured liquid releasing coatings, which exhibited site-specifically releasing under

friction. The released liquid could be stabilized within the textured surfaces to form lubricate layers to reduce friction. With the development of self-secretion dynamic systems, lots of interesting soft materials are prepared for self-replenishing slippery surface, sponge-like coatings and programmable droplet-guiding reactors.[96-99]

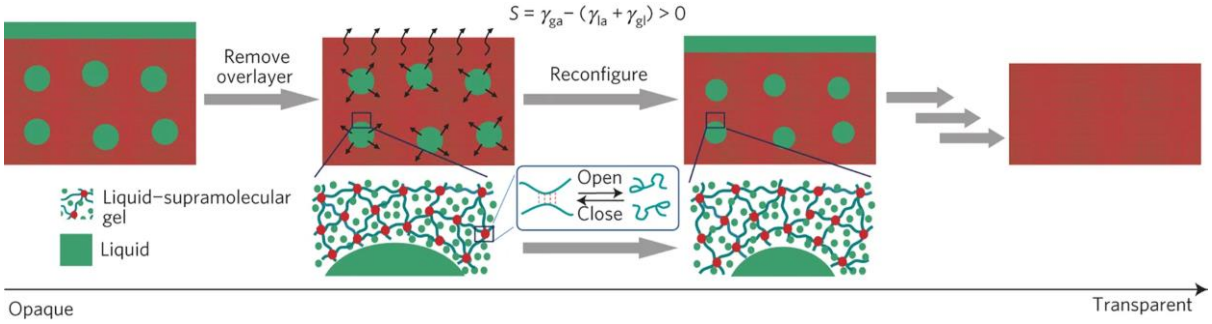

Figure 8. Schematic process of self-regulated secretion system. Secreted liquid is stored as shell-less droplets inside the gel matrix with the ongoing liquid exchange between droplet, matrix and surface. Reproduced with permission.[17] Copyrights 2015, Nature Publishing Group.

1.2 Growing materials

Living organisms, including cell, tissue, and organ, autonomously grow and remodel themselves to adapt to their surrounding environment through metabolic processes. For example, skeletal muscles can hypertrophy and strengthen due to repeated exercise.[100] Once the collagen fibril structure is damaged, the supply of procollagen building blocks grows new muscle. However, typical synthetic materials are static and closed systems, lacking a mechanism to extend and reconstruct and undergo substance exchange with surroundings. Bioinspired from nature, research effort is nowadays focused towards the implementation of growth concepts into synthetic materials to achieve extension of network chains, self-strengthening and post-regulation of mechanical properties.[18-20, 101] Growing materials are emerging as a new kind of dynamic soft materials, in which monomers are incorporated into the matrix. In 2013, Johnson and co-workers developed a photo-controlled system based on the reversible trithiocarbonates linkages.[101] In this system, the linkages allow for insertion

of new monomer into as-prepared gels under light irradiation. This extending process represents a novel strategy in material science. A “growing” strategy has been implied in this research although the concept is not been proposed at that time. With this basic knowledge, lots of researches have been focused on the fabrication and applications of growing materials.

1.2.1. Strategies to develop growing materials

1.2.1.1. Light-based approaches

Comparing with other external stimuli for materials modification,[9, 11, 102] such as electric, temperature, moisture, strength, and pH, light is environmentally friendly, noncontact, and spatiotemporally controllable and therefore, is widely used for photo-motility,[103] photo-degradation,[104] photo-functionalization,[105] photo-induced plasticity,[26] and photo-induced self-healing[28] of soft materials. More importantly, light activation provides opportunity to reaction pathways that are difficult to reach through classical thermo activation. Numerous examples of photo-activable components for polymerization technologies have been developed with success, including photo-initiator, photo-catalyst, and iniferter.

Iniferters were introduced by Otsu and co-workers, which serving as an initiator, chain transfer agent, and terminator in controlled free radical polymerization.[106] When the photo-responsive iniferters are exposed to light, they dissociate into two fragments: a carbon-centered radical that can initiate polymerization and an iniferter-based radical that can reversibly terminate growing chains. In this regard, monomer molecules are inserted into the iniferer bond, generating polymers with two iniferter fragments at the chain ends. Iniferters also have a high activity that can “live” rather than “die” when they are reused in a polymerization system.[107] Taking these characteristics into mind, Johnson and co-workers firstly reported the photo-activation polymeric materials by

preparation of bis-norbornene trithiocarbonate (TTC) telechelic *N*-isopropylacrylamide (NIPAAm) polymers crosslinked by tris-tetrazine *via* DA reaction (Figure 9a).[101] The obtained photo-responsive gels still have the “living” possibility to undergo re-polymerization under UV irradiation. Photo-activation mediated insertion of new NIPAAm monomers directly into the network chains of original gels led to grown materials with a larger molecular weight between junctions, and a correspondingly increasing of swelling ratios. Coincidentally, Kloxin and co-workers reported a similar research of light-triggered modulus enhancement by using UV-activable dithiocarbamate iniferters entrapped in the polymer network backbone. Under UV irradiation, the dithiocarbamate bond homolytically cleaves and generates a radical that can initiate free radical polymerization of dimethacrylate monomers then directly incorporated into the network.[108] However, the surface of photo-activation polymer networks can adsorb most of the UV light and undergo uncontrolled polymerization/decomposition, impossibly achieving uniform and living growth of the entire gel material. In addition, the iniferter radical is usually unstable, leading to irreversible termination in the UV-photolysis approach. To address this, Johnson and co-workers demonstrated a proof-of-concept study of transforming of “parent” gels into functionalized “daughter” gels through a living additive manufacturing strategy, which using polymer gels embedded with trithiocarbonate iniferters that could be activated by photoredox catalyzed growth (PRCG) (Figure 9b).[18] The parent gel bears end-linked trithiocarbonate iniferters within the network strands, then which is swelled in a solution containing monomers, crosslinkers and photocatalyst to achieve swelling equilibrium. Irradiation with blue light excites photocatalyst in solution and incorporates the living insertion of monomers and crosslinkers from solution into the networks to produce diverse daughter materials with homogeneously altered size, strength and compositions. They also used dissipative particle dynamics (DPD) to model the photo-

activation growth of a gel matrix when a significant portion of the material is severed.[109] Under this theory, gels formed two distinctly and spatially separated layers with low trithiocarbonate concentrations, while gels formed incompatible components displayed well-intermixed structures at high trithiocarbonate concentrations.[110] This strategy was further used to in a nanonetwork or tailor bulky property of soft materials.[111]

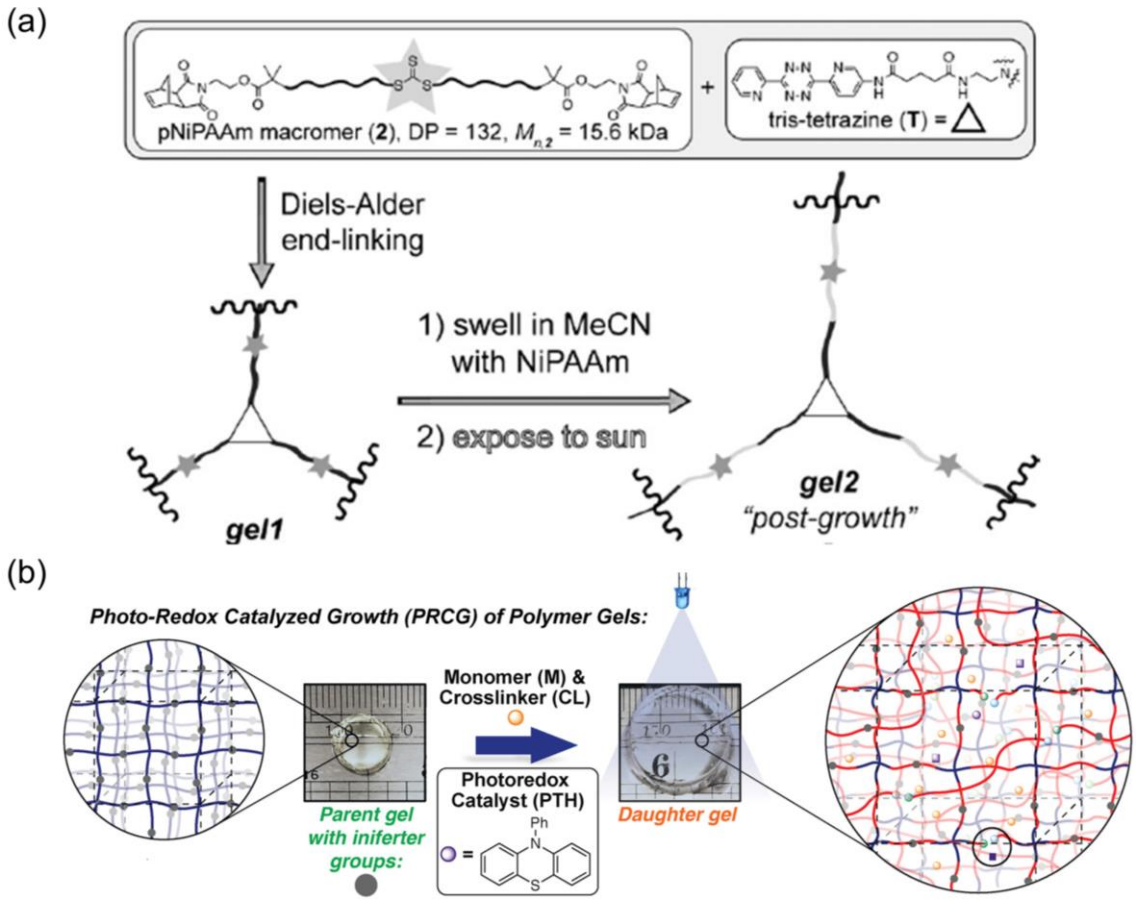

Figure 9. Introducing light to guide matter conversion and integration within dynamic soft gels. (a) End-linking pNIPAAm with a tris-tetrazine to form gel networks. After swelling in acetonitrile (MeCN) with NIPAAm and exposure to sun light, the photoresponsive gel can grow. (b) General strategy for regulating polymer network structures by photoredox catalyzed growth (PRCG). Monomers and cross-linkers can be directly incorporated into the as-prepared networks through photoredox catalyzed process. Reproduced with permission.[18, 101] Copyrights 2012, Wiely-VCH. Copyright 2017, American Chemical Society.

1.2.1.2. Mechanical force-based approaches

Mechanochemical phenomena which ubiquitously existed in a rubbery state of polymers is attributed to the reduction in the molecular weight of polymers under mastication, where the constituent macromolecules are mechanically ruptured.[112] In this reaction, covalent bonds undergo homolytic cleavage, generating radicals within the stressed polymers. The formation of free radicals within polymers at low temperatures (e.g. 77 K) under strong mechanical forces has been realized based on Electron Spin Resonance (ESR) experiments.[113] In the absence of oxygen and other terminating compounds, these radicals initiate the polymerization of monomer incorporated in the polymers. Based on this, several attempts have been reported by integrating mechanochemistry in soft materials to handle their functions by mechanical stimuli, such as regulating the rheological property of rubbers, polymerizing through vigorous milling and grinding, and creating polymeric sponges for reactions.[114] However, these researches mainly relied on the mechanochemical crosslinking reactions, which only remodel the polymer architectures, not the bulky solid materials. To date, Kloxin and co-workers introduced a powerful approach towards force-induced polymerization with a trithiocarbonate group as the mechanochemical linker.[115] Under sonication, the scission of weak carbon-sulfur bond on polymer chains generates radicals to trigger polymerization with external diacrylate based crosslinkers in the surroundings. The covalent incorporation of secondary polymerizable functional groups leads to solid-state polymeric material healing under mechanical force. Moreover, Gong and co-workers developed self-growing hydrogels that can respond to repetitive mechanical force *via* effective mechanochemical transduction to remodel bulk solid-state materials and enhance their mechanical properties (Figure 10).[20] For a double network hydrogel system fed 2 M monomers, the monomer conversion could reach 90% for the stretched gel in an argon atmosphere. Such mechano-radical

polymerization results in the force-induced formation of new networks within double network hydrogel to exhibit self-growing performances.

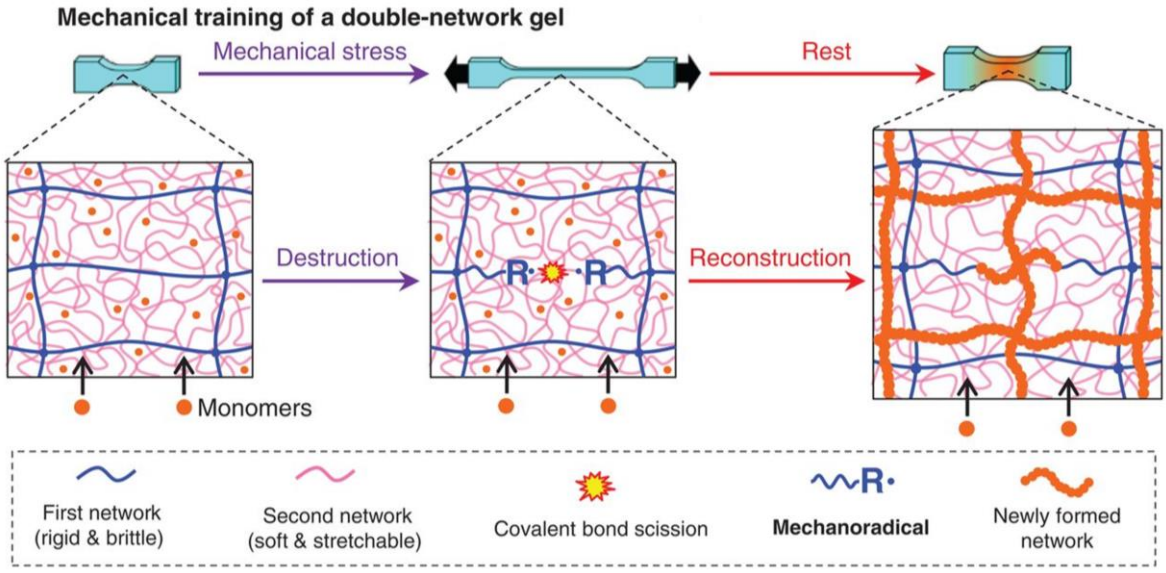

Figure 10. Self-growing hydrogels under mechanical training. Mechanical force leads to rupture of the brittle network (blue), while the highly stretchable network (pink) maintains the entirety of the DN gel. The mechanoradicals generated at the broken network strands further initiate polymerization of monomers entrapped in the DN gel to form a new polymer network (orange). Reproduced with permission.[20] Copyright 2019, AAAS.

1.2.2. Applications of growing materials

1.2.2.1. Self-strengthening of materials

Introducing more crosslinker fraction or newly formed crosslinked polymers within a given polymer network could enhance the mechanical properties of materials, which could satisfy the practical application on-demand.

Kloxin and co-workers found that a polymer network's modulus can be over two orders of magnitude stiffer after UV irradiation by incorporating photoactive monomer molecules containing dithiocarbamate iniferters with dimethacrylate crosslinkers. This photo-triggerable dynamic soft material can not only simultaneously strengthen and

heal after damage using iniferters linkages, but also spatially control the shape of materials on demand.[108] In addition to these useful applications, they developed other dynamic systems relying on mechanochemical treatment. The introducing of trithiocarbonate iniferters into functional polymer chains enable cleavage in response to external force (i.e., sonication), which further generate radical to initiate diacrylate monomers crosslinked into the network on the polymer chains strands.[115] Polymer solutions containing the higher molecular weight of trithiocarbonate based polymers and tetraethylene glycol diacrylate can be triggered gel formation within 10 min sonication, demonstrating the bulk material strengthening under mechanical forcing.

Not only soft polymeric materials bearing mechanophore in their network backbone possess the potential to self-strengthen the networks under external stimuli, typical crosslinked materials also can enhance themselves. Gong and co-workers developed the self-strengthening double network (DN) hydrogels with typical polymer chains that can be stretched to generate radicals, which could further integrate with monomers in the surroundings.[20] By repetitive loading-unloading of double network hydrogels in the feed solution of monomer and crosslinkers, the size and strength of the gels are visually grown. In a closed system of repetitive lifting of a double network gel which connects to weight in an environment surrounding of monomer solutions, the weight could not be successfully lifted in the first cycle but lifted to higher levels with several lifting cycles training as the gel changes from soft to stiffen (Figure 11). The modulus of gel fed with monomers and crosslinkers after stretching is over 20-folds than its virgin state.

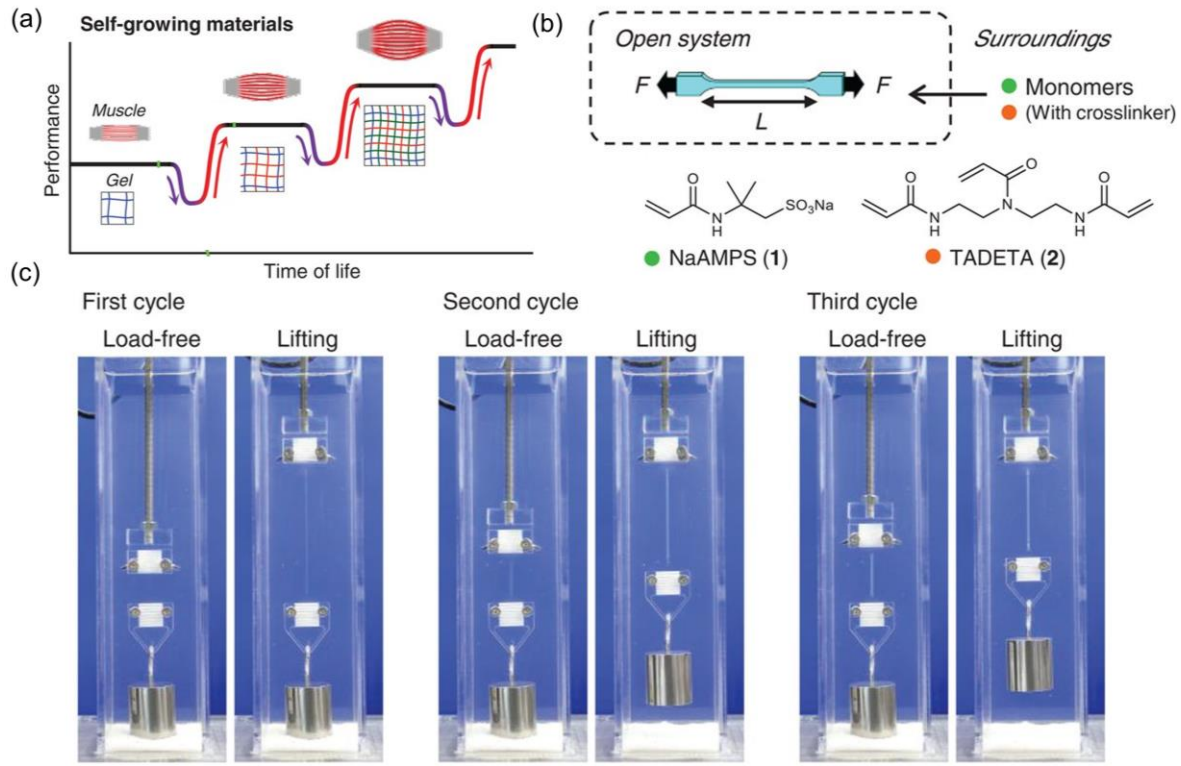

Figure 11. Self-strength of hydrogels. (a) Under mechanical stimuli, a tissue is initially weakened or destroyed (purple arrows) but then recovers or further strengthened (red arrows). (b) Demonstration of stretching a double network gel with continuously supply of monomers from surrounding solutions containing monomer and crosslinkers, acting as an open system. (c) Optical images of self-growing DN gel caused by repetitive mechanical training. Reproduced with permission.[20] Copyright 2019, AAAS.

1.2.2.2. Network expansion of growing materials

Many of the soft materials formed by nonliving, free radical polymerization technologies that render the materials “dead” towards the further insertion of monomers, in which the polymer chains cannot be activated under stimuli. To broaden the field of dynamic soft materials, “living additive manufacturing” is a novel approach to endow materials with living fashion which could be subsequently reactivated to continuously introduce new monomers and/or functionality.[18] Johnson and co-workers firstly proposed this strategy by introducing photocontrolled living radical polymerization to spatially and temporally feed monomers and/or crosslinkers into

original “parent” gel materials to generate a new “daughter” gel networks with tuned shape, composition, and properties. By involving only monomers (e.g., NIPAAm) in the designed “parent” hydrogels and controlling the conversion of monomers, the obtained “daughter” hydrogel showed different swelling ability in pure water. Higher conversion of monomers would generate softer “daughter” gels with more increased swelling capability. Meanwhile, the designed “parent” networks can functionalize with different compositions by entrapping various kinds of monomer within polymer backbones, such as hydrophobic n-butyl acrylate monomer and hydrophilic poly(ethylene glycol) methyl ether acrylate monomer. Due to the dynamic character of trithiocarbonate iniferters involved in the polymer chain strands under light, the “daughter” gels showed great healing and welding manner. If the damaged “parent” gel was treated in a surrounding solution containing monomer, crosslinker, and photocatalyst, followed by exposing to blue light, a healed “daughter” gel was then obtained. In addition, it is possible to weld different “parent” and/or “daughter” gels to create new complex gel materials with variable compositions and functions by photoredox catalyst growth. This is the first and essential step for the development of living additive manufacturing.

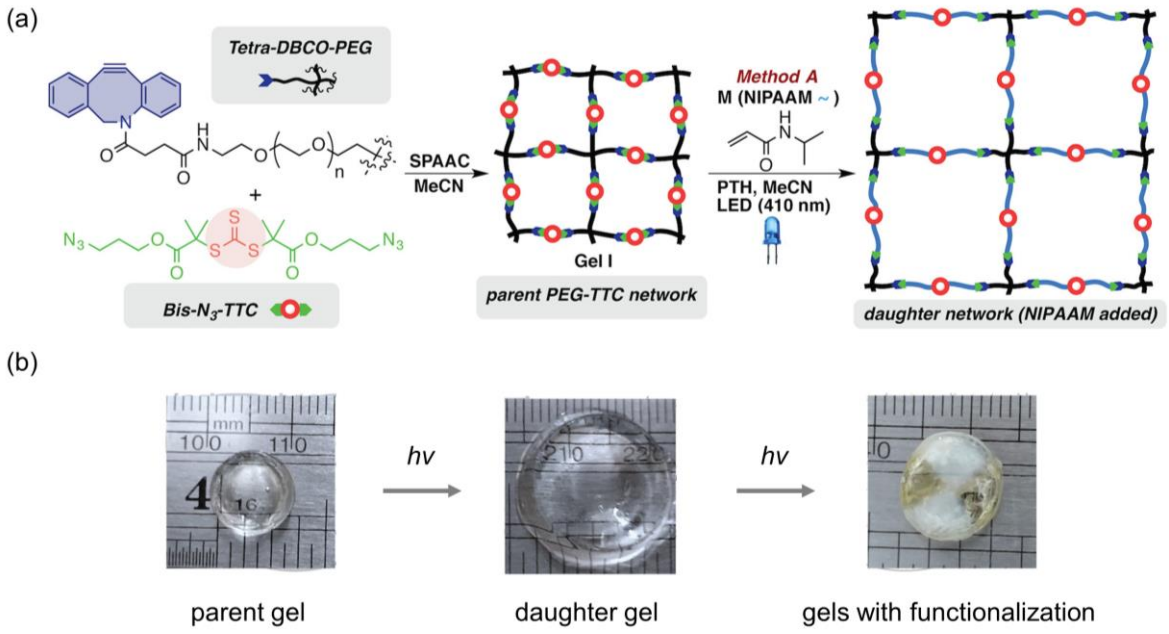

Figure 12. Network expansion *via* PRCG insertion of NIPAAM into as-prepared gel network. (a) After "parent" gel forms, PRCG is activated in the presence of inserted monomer and catalyst under blue light irradiation. (b) Optical images from parent gel to daughter gel and its functionalization. The size of the daughter gel is bigger than the corresponding parent gel. Reproduced with permission.[18] Copyright 2017, American Chemical Society.

1.2.2.3. Post-modulation of growing materials

Unlike the living materials in organisms, synthetic polymeric materials usually lack the ability to diversified and post-regulate their bulky properties, which limits their application in advanced functional materials. Inspired by natural stem cells, structurally tailored and engineered macromolecular (STEM) soft polymer gels emerge as a new kind of polymeric materials (Figure 13).[19] These gels involved a two-step synthetic procedures. In the first step, STEM gels are fabricated to be "undifferentiated" templates containing latent active sites. Then in the second step, STEM gels can be post-modified to introduce new functionality to the original gel materials. By the "graft-from" approach of the active sites, numerous potential modifications, such as grafting polymer side chains, functionalization with natural biomolecules, and spatially differentiated properties, are introduced within the primary gel networks. This smart STEM strategy was first developed by Matyjaszewski and co-workers, photo-active STEM gels were synthesized by free radical polymerization of different monomers, crosslinkers, and a photo-active element based on the photoinitiator of 2-hydroxy-4'-(2-hydroxyethoxy)-2-methylpropiophenone (Irgacure 2959). A crosslinker solution could be infiltrated and incorporated into the as-prepared gel to reinforce the network under UV irradiation.[116] However, the polymer architecture cannot be precisely controlled by free radical polymerization. Therefore they further exploited more homogeneously tailoring and tuning STEM gels (i.e., control of mesh size and composition of networks) by controlled radical polymerization method. In the beginning,

atom transfer radical polymerization (ATRP) technology was introduced into the STEM gel system. An ATRP initiator was incorporated into the original hydrophobic STEM-0 gel network, followed by swelling in a hydrophilic monomer solutions.[117-118] When polymerization was triggered, side chains grafted from the latent active sites, thus the hydrophobic STEM-0 gel can be finely transformed into amphiphilic STEM-1 gels. The obtained single-piece amphiphilic gels can be significantly spatial and temporal control to form hard/soft materials. In addition, temperature or pH stimulus, as well as raising or lowering of Tg, can be introduced by this approach. Besides, they also proposed a novel metal-free approach based on the reversible addition-fragmentation chain transfer (RAFT) polymerization to prepare the STEM gel.[119] This approach relies on spatially activating the fragmentation of trithiocarbonate iniferter under visible light photolysis. The generated gels are compositionally and mechanically differentiated from their pristine network, ranging from becoming stiffer or softer with different responsiveness, to tunable polarity (hydrophilicity/hydrophobicity).To broaden this applicable RAFT technology, Boyer and co-worker reported a 3D printable hydrogel relying on the usage of iniferters. After obtaining the printed hydrogels, the reinitiation of dormant RAFT agents on the surface of the printed hydrophilic network allows for a robust chain extension with hydrophobic monomers to post-functionalize the surface hydrophobicity.[120]

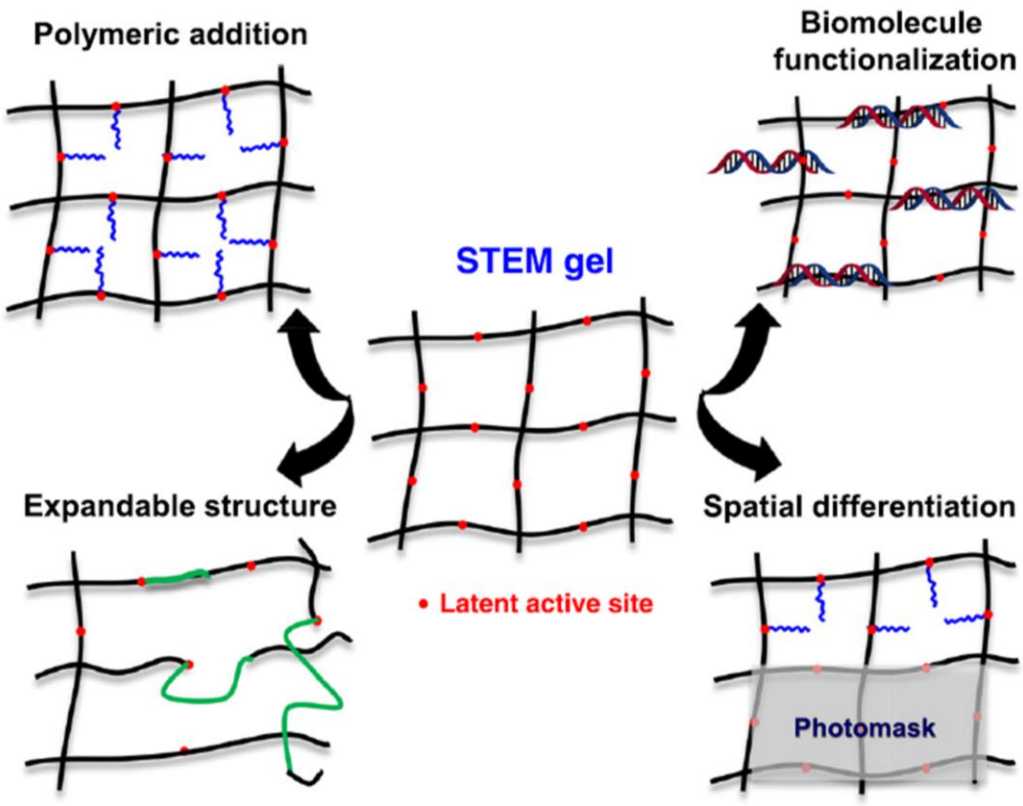

Figure 13. Post modulation of structurally tailored and engineered macromolecular (STEM) gel concept. The gel was composed with a primary material (black) and perform post-synthesis modification from latent active sites (red), including grafting polymer side chains, expanding network segments, functionalizing of biomolecules and spatially controlling with a photomask. Reproduced with permission.[19] Copyrights 2020, Elsevier Inc.

Chapter 2

2 Probing the growth of bulky materials with on-demand size, strength, and composition

Herein a photo-induced activation strategy to continuously incorporate nutrient (monomer and crosslinker), to expand bulky elastomers with controllable mechanical properties and compositions, was reported. Multiply growth cycle treatment of the bulky material by insertion and integration of nutrients enables bulk elastomers to multi-time grow with a variety of size and strength. By changing different types of nutrient solutions, heterogeneous growth of bulky materials is achieved. I also envision its potential application in regulating the bulk wettability by introducing organic and aqueous based nutrients *via* the growth cycle.

2.1. Introduction

Living organisms are endowed with the ability to grow that allows them to absorb and integrate nutrients to continuously increase in size, strength, and change in shape.[90, 121] Typically, growth is an extremely complicated process involving extremely complex ongoing mass transport, exchange, and multi-step biochemical transformations, which are precisely directed by various intrinsic codes stored in the gene but also response to environmental stimuli.[122-123] In contrast, artificial materials are fabricated through completely different strategies like molding, assembling, printing, tailoring, etc.[124-127] which generally result in fixed structure and could not be reconstructed. Although

various methods have been developed to smart materials with tunable size,[18, 128-129] shape,[130-134] structures,[135-136] and property,[137-142] none of them commonly possesses the capability to continuously integrate external mass without compromising the integrity of bulk materials.

To endow materials with the ability to grow on-demand in a designed manner would allow for mimicking and capitalizing on the remarkable capabilities of living organisms. Recently, applying the concept of self-growth into dynamic polymer systems has become a powerful strategy to post-tailor and rebuild functions of freestanding bulk materials. For instance, Gong et al. reported self-growing hydrogels that respond to mechanical stress through mechanochemical transduction.[20] The prepared double network hydrogels can absorb and integrate external monomers under the polymerization by mechano-generated radicals to grow and self-strengthen them. The newly formed network is extended directly on the original polymer backbone. However, there still lacks a mechanism to continuously incorporate separated polymers (homogenization) within a growable matrix. Inspired by this, in this chapter a new growth mode of synthetic polymer materials that can integrate continually nutrient, i.e., monomer and crosslinker, to grow in a controllable manner, which includes processes of swelling, polymerization, and homogenization (Figure 1), was designed. After polymer network seeds (made in a piece of elastomer) in which monomer molecules can be continually absorbed and incorporated are prepared,[143-144] the nutrient solution (the mixture of monomer, crosslinker, photoinitiator, and transesterification catalyst) is added to the elastomer (which was termed as original seed), causing it to swell to form a gel and grow in size. Then the polymerizable units can now readily be UV-triggered to form new networks. At last chain-exchange reactions between the original and newborn networks can be achieved *via* heating induced efficient transesterification to relieve the stretching tension during the swelling process. By varying the incubation

time between original network and nutrient, the composition in the nutrient, the homogenization degree of chain exchange reaction, I achieve exquisite control over growing polymer materials into a variety of sizes, tuning their compositions, modulating their mechanical properties, and availability for multiply growth from the desired object. The regulation of bulk wettability from elastomer to grow into organogel and hydrogel is also demonstrated.

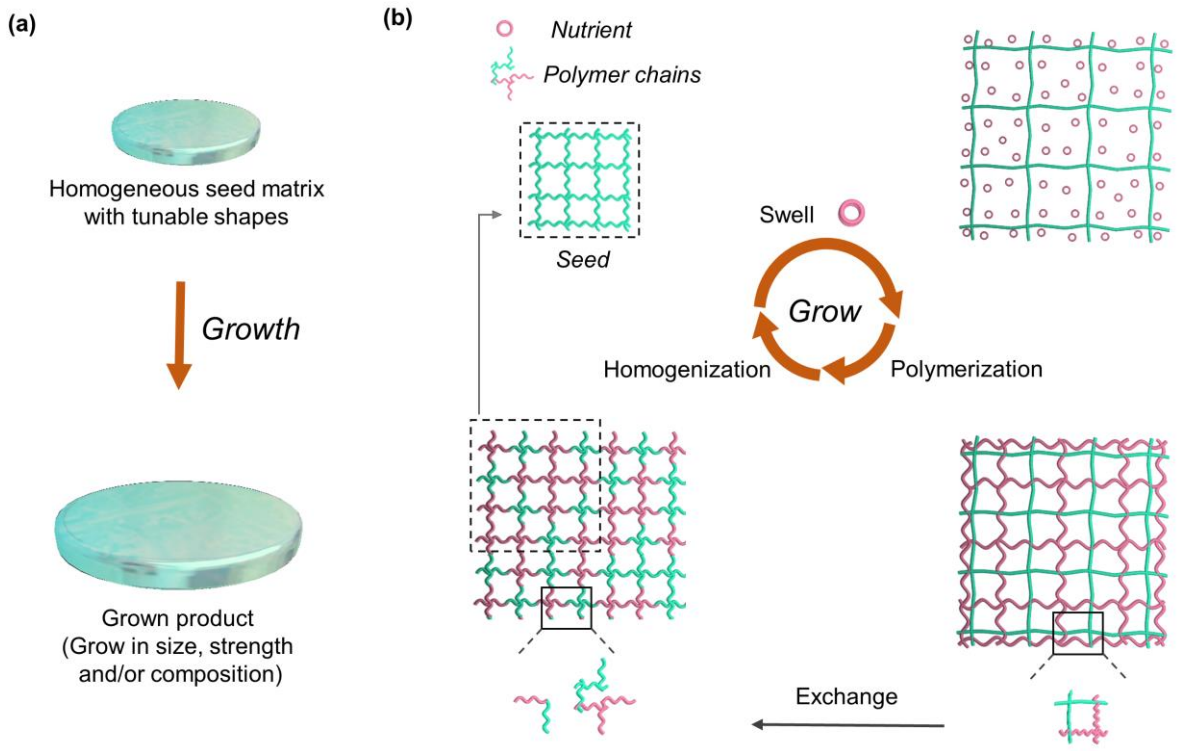

Figure 1. Concept of self-growing materials. (a) Homogeneous seed matrix with tunable shapes can be grown into a product with controllable size, strength and composition *via* growth cycle. (b) Growth mode for self-growing materials. In a growth cycle, a seed can swell and absorb the nutrient to obtain the swollen seed, then which undergo polymerization to form new-born network. The original network can incorporate with the newly formed network through a chain exchange reaction to get the growth materials. The initial network shown in green and the new-born networks are indicated in red.

2.2. Results

2.2.1. Proof of light-triggered growth of bulky elastomer

Within this general design, creating a material to grow requires a polymer system with the ability to induce both post-polymerization and ongoing chain-exchange reactions. Figure 2a (left) shows the solid images of cylinder seed samples before and after growth treatment. To demonstrate this concept, a material system of 4-hydroxybutyl acrylate (HBA) and 1,6-hexanediol diacrylate (HDDA, 1 wt%) was selected (Figure 2a, right). HBA is a commercially available precursor for preparing polymer networks with good monomer swelling ability, while HDDA has an ester linkage that undergoes a transesterification reaction with the hydroxyl group of HBA. PolyHBA networks were fabricated *via* photopolymerization under UV light (365 nm, 10 mW/cm^2) in the presence of 2-hydroxy-2-methylpropiophenone (D1173, photoinitiator). As-prepared seeds can be swelled when brought in contact with the mixture of their parent monomer, crosslinker, photoinitiator, and an external transesterification catalyst (nutrient solution). During swelling, HBA, HDDA, D1173 and transesterification catalyst dibutyltin dilaurate (DBTDL) are homogeneously absorbed by the seeds.

I first describe in detail the behavior of the light-triggered growth cycle of bulky elastomers. The original seeds showed excellent swelling ability in its nutrient solutions. The weight continually increases up to 290 wt% over the swelling process (Figure 2b). After polymerization and washed by ethanol to remove the unpolymerized components, the weight of grown samples retained 275 wt% comparing with the original seed (100 wt%). I attribute this further increase in weight to the incorporation of the nutrient reagents into the seed through the growth cycle. For comparison, a swollen seed without photopolymerization was used as a control, which completely shrinks back after the adsorbed liquids are removed by washing.

The stretching tension was generated during this swelling process, which hinders the further uptake of nutrients. Therefore, I used transesterification technology to homogenize and integrate polymer chains with different time scales for growth due to its simplicity, robustness, and versatility.[145-147] To show the essentials of transesterification, I detected the swelling ability of samples with and without chain exchange reaction. The sample with transesterification still can swell the nutrient solution, which reached its equilibrium with a swelling ratio of 160 % (Figure 2c). In contract, the sample without transesterification can hardly swell again. The transesterification was further proven by the significantly higher modulus of the control samples (Figure 2d). Without a chain exchange reaction, a double-network structure formed to stiffen the grown structure (650 ± 60 KPa), while chain exchange reaction-induced homogenization reduced this stiffening effect (420 ± 40 KPa). A growth process was proposed as follows: in this growth cycle, after polyHBA based original seeds swell in the nutrient solution containing HBA, HDDA, D1173 and DBTDL, HBA components entrapped in the original seed chains undergo photopolymerization upon UV irradiation, then short-time heating at 150 ^{o}C triggers mild dynamic transesterification reactions to homogenize the original and newly formed networks to get a homogeneous growth of material.

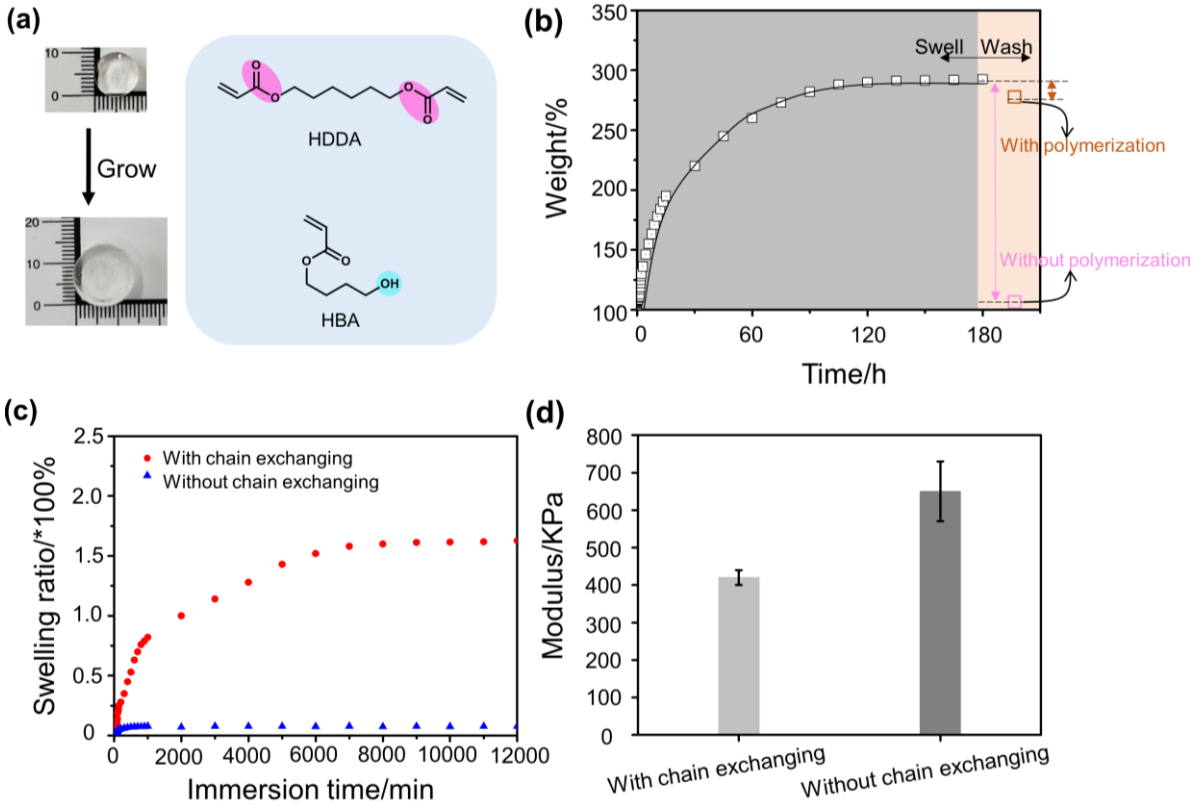

Figure 2. HBA-based growth materials. (a) Left: Seed samples before and after 1st growth cycle. Right: Monomer and crosslinker used to demonstrate the growth behavior. (b) Time-dependent weight change of seeds immersed in the nutrient solution. Ethanol was used to wash out the nutrient solution. The sample without polymerization was used as control. (c) The swelling ratio of grown samples with and without chain exchange reaction. (d) Young's modulus of grown samples with and without chain exchange reaction. Error bars are s.e.m.

2.2.2. Control of light-triggered growth of bulky elastomer

Different parameters have been studied to modulate the bulky growth of elastomers. The composition of the grown samples can be tuned by the composition of the nutrient solution and swelling time, paving ways to regulate the sample's mechanical properties (Figure 3a). Growth in the nutrient solution with lower crosslinker fraction (0.1 wt% HDDA) leads to a reduction in Young's modulus: 420 ± 40 KPa (seed) *vs* 330 ± 35 KPa. I attribute it to the reduction in the overall cross-linking density of the grown

sample after the growth cycle. On the other hand, increasing crosslinker fraction in the nutrient solution stiffens the grown samples. The Young's modulus was even up to 1.4 MPa when a crosslinker concentration of 10 wt% was used in the nutrient solution. (Figure 3a) I also found that the incubation time of the original seed network had nearly no influence on the mechanical property of the grown seed sample (made from 1 wt% crosslinker, 440 ± 120 KPa), which also proved the homogeneous swelling and absorption of nutrients in the seed.

In addition to the variation in mechanical property of grown materials, the growing degree of the samples, defined as growth index (W_{grown}/W_{seed}), can be well controlled. In a single growth cycle, controlling the incubation time of the original seed sample in nutrient solutions is a facile and simple approach to control the size of swollen seed (Figure 3c). With increasing the incubation time, the size of swollen seed also increased, thus resulting in an increased growth index of grown seed after growth. For instance, when the incubation time was only 5 hours, the growth index was restricted to 1.32. But this value would increase to 2.75 when increasing the incubation time to 120 hours.

Crosslinking degree is another essential factor in controlling the swelling ability of the original seed sample in nutrient solutions. A lower cross-linking density of seed material features higher swelling capability in the nutrient solution and vice versa. When more crosslinkers are introduced into the network, the number of polymer chains between linkages strands becomes less, making the material more rigid. Thus less nutrient solution can diffuse into the sample during the swelling process. Higher swelling ability of original seed samples indicates a bigger growth index of grown seed material. For example, when the fraction of crosslinkers in the original seed samples increased from 0.1 wt% to 5 wt%, the grown index of 1st grown seed decreased from 3.96 to 1.78 (Figure 3d).

Besides, the grown index can also be controlled by nonequilibrium transesterification.[145] High temperature could activate the transesterification process thereby leading to deep cross-linking.[45, 145] As transesterification catalyst-DBTDL could be embedded into the seed sample during its preparation process, annealing at a higher temperature, such as 150 ^{o}C, can further trigger deep transesterification to deeper cross-linking of the material, which results in the decreased swelling ability of initial seeds in nutrient solutions and finally weakens grown index. When the seed sample was fixed at 150 ^{o}C for 2 hours, the grown index sharply decreased to 1.31 (Figure 3e).

The sequential growth of bulky material was also possible. To better show this multiply growth capability, a cube (Length: 10 mm) with a round hole (Diameter: 4 mm) in the middle was used for modeling this behavior. Figure 3f described that the Length (*L*) of cube and Diameter (*D*) of round hole increased linearly even after three times growth cycle, which mainly depended on (1) the original and grown seed samples have the nearly same composition and (2) mild dynamic transesterification to endow original and grown seeds with similar mechanical properties. For instance, *L* linearly increased from 10 mm to 28 mm, while *D* increased from 4 mm to 12 mm after three-time growth. In the meantime, the grown index increased from 4.25 to 19.8, which showed huge growth. Up to now, this is the most excellent growth in the size of soft material after treatment compared with other studies.[18, 20, 116-118]

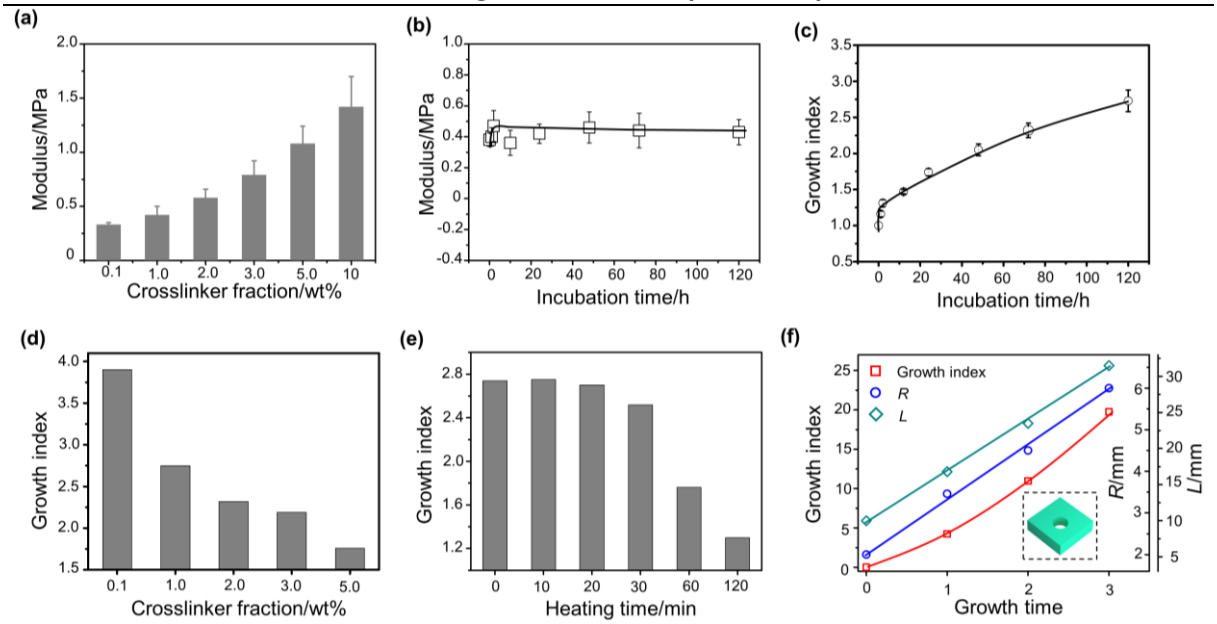

Figure 3. Control of growth. (a) Modulation of Young's modulus of grown samples by changing the crosslinker fraction in the nutrient solution. (b) Young's modulus of grown samples when changing the incubation time. (c)The relation between grown index and incubation time. (d) The influence of crosslinker fraction of initial seed sample to grown index. (e) The influence between the heating time at 150 ^{o}C for seed samples and grown index. (f) Grown index of the different growth cycles of a cube sample with a round hole in the middle. Inset cartoon image shows the appearance of sample. Error bars are s.e.m.

2.2.3. Light-triggered heterogeneous growth of materials

Hetero-grown samples can be easily obtained by varying different kinds of nutrient solution, providing ways to modulate the sample's intrinsic properties. I designed heterogeneous growth materials shown in Figure 4a. The initial seed can be swelled in nutrient solution containing a second monomer, after growth cycle, the obtained grown sample possesses the heterogeneous structures of both the initial and second molecules, then which could also be soaked in the third solution, finally I can get grown sample bearing these three different polymer structures. The obtained heterogeneous grown sample still features the growing ability *via* transesterification induced chain exchange reaction.

By this way, I immerse the original seed sample (PHBA based) in different nutrient solutions to change its identity. Different hydrophilic monomer (2-hydroxylethyl acrylate, HEA; Hydroxypropyl acrylate, HPA; hydroxypropyl methacrylate, HPMA), hydrophobic monomer (n-butyl acrylate, BA) and higher viscous monomer liquids (poly(ethylene glycol) methacrylate, EOMA) can be used as nutrient components to vary the material composition and then properties. As shown in Figure 4b, the grown index is up to 4.1 after soaking in HEA based hydrophilic nutrient solution, but it is only 1.19 in BA based hydrophobic nutrient solution. It can be explained by the compatibility of original seed networks and nutrient solutions.[135] PHBA based seed samples could not swell in higher viscous liquids (EOMA), thus no growth for this sample. To better show the modulation in composition, I measured the water contact angle (WCA) of the original seed network and grown sample in HEA and BA based nutrients. The PHBA based original seed has a WCA of 87^{o}, which switches to 62^{o} and 109^{o} after grown into PHBA-PHEA and PHBA-PBA material, respectively. Matyjaszewski and Boyer also showed a hydrophilic-hydrophobic transition after light-induced activation of networks, but they have relied on the grafting of polymer brushes,[116-118, 120] which need more rigorous condition and procedures. Here, I have shown an identity composition change of seed materials by photo-regulated growth, which could become more hydrophilic or hydrophobic by introducing further hydrophilic or hydrophobic monomers into the growth cycle.

Multiply heterogeneous growth of bulky materials could also be realized by a multi-time growth model. After I got the PHEA based seed sample, I can continuously treat this sample in HEA, HBA, HPA, HPMA, and mixture of NIPAM aqueous and HEA based nutrient solutions. A BEPP* based heterogeneous grown samples was then obtained with a growth index of 10.3 (Figure 4c). Interestingly, the prepared PHBA-PHEA grown seed sample switched the hydrophobic property of PHBA to hydrophilic,

which could immerse in *N*-isopropylacrylamide (NIPAM) aqueous and HEA based solution to get the swollen sample. After the growth cycle, the PHBA based elastomer material can be grown into an elastomer-hydrogel hybrid material, the growth index of which can achieve 12.2 (Figure 4c).

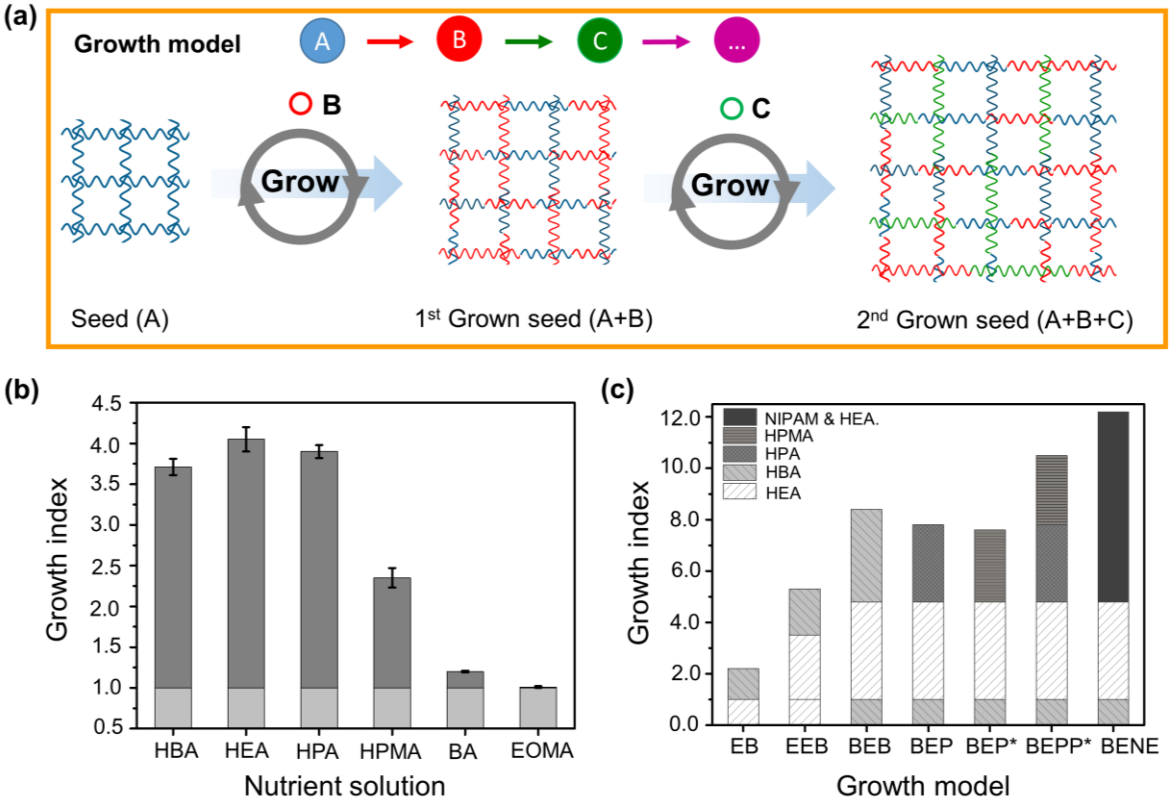

Figure 4. Heterogeneous growth of seed samples. (a) Schematic process of the heterogeneous growth model. Seed fabricated by A can be soaked and integrated by B to obtain grown seed containing both A and B, which while can be further soaked and integrated by C to obtain 2nd grown seed features properties of A, B and C. (b) Growth index of heterogeneous grown seed samples when incubated PHBA based initial seed samples in various nutrient solutions. (C) Growth index of heterogeneous grown samples treated by different growth models. The abbreviation of E, B, P, P*, and NE represent HEA, HBA, HPA, HPMA, and mixture of NIPAM aqueous and HEA, respectively. EB means PHEA based initial seed sample soaked and integrated into HBA based nutrient solutions.

2.2.4. Demonstration of light-triggered growth of materials

In addition to the tunable size, mechanical properties, and compositions, the growth also brings about other appealing capabilities. Due to the multiply growth capability and good compatibility of nutrient solutions, an elastomer seed material can be grown into organogel or hydrogel. As shown in Figure 5a, after the elastomer seed (PHEA seed) was incubated into an organic nutrient (butyl acrylate/dodecyl acrylate/THF/silicon oil) using D1173 and benzenesulfonic acid as the photoinitiator and transesterification catalyst, respectively, it can be grown into an organogel after growth cycle. To better distinguish the original and grown samples, I dyed the organogel by Sudan Red. Transparent PHEA seed transferred to opaque organogel due to the phase separation between the grown organogel matrix and the silicon oil, while the non-slippery elastomer surface becomes an oil-infused slippery organogel surface. Comparing with the seed sample, water droplet (30 μL) can be easily slid on the tilted (30 ^{o}) organogel surface. The embedded THF and silicon oil within the grown organogel could be washed away, and then it was incubated into an aqueous nutrient (HEA/NIPAM aqueous), which could be further grown into a hydrogel (Figure 5a). I also dyed the hydrogel by a green food dye. The surface wettability of the hydrogel can be easily tuned by regulating temperature. The thermoresponsive grown hydrogel sample exhibits a noticeable lower critical solution temperature (LCST) behavior in water. The water contact angle of the grown hydrogel was 67^{o} at room temperature, while which changed to 95^{o} after baking it at 50 ^{o}C.

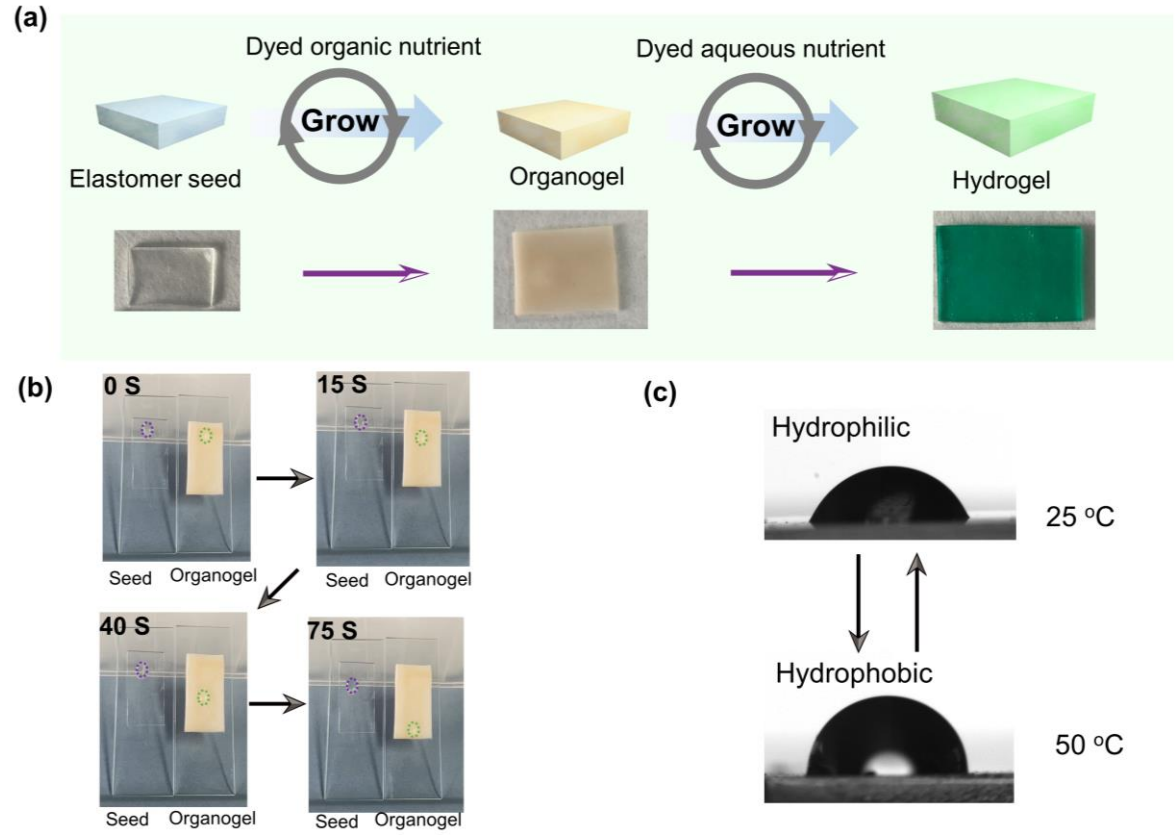

Figure 5. Demonstration of the capability of regulating bulk wettability of light-triggered self-growing materials. (a) Schematic process of changing the wettability of bulky materials *via* growth cycle. An elastomer seed (PHEA) can be soaked in an organic nutrient (butyl acrylate/dodecyl acrylate/THF/silicon oil) using D1173 and benzenesulfonic acid as the photoinitiator and transesterification catalyst, respectively, to obtain organogel. The unpolymerized solution can be washed by THF, then which can be further immersed in an aqueous nutrient (HEA/NIPAM aqueous) to prepare grown hydrogel. The organogel was dyed by Sudan Red, while hydrogel was dyed by a green food dye. Bottom images show the physical pictures of the original seed and grown samples. (b) Slippery performance of original seed and grown organogel surface. 30 μL water droplet was added on the material surface with a tilted angle of 30 °. (c) The water contact angle of grown hydrogel under different temperatures.

2.3. Discussion

Although previous studies of Johnson, Kloxin and Matyjaszewski had showed the awesome photo-activation systems involved photoresponsive iniferters,[18, 101, 108, 116-118] there were still some disadvantages for them. Firstly, the synthesis of functional iniferters is difficult, which always needs several steps with low yielding. Secondly, these systems usually need an oxygen-free atmosphere or complicated devices. Thirdly, the conversion of iniferters based polymerization is relatively as low as 60%.

Here I described a facile and simple approach to probe the bulky growth of soft materials. There is no extra synthesis procedures for molecules, and this system is oxygen tolerant, as well as possesses high conversion of monomers (over 85%). My approach consists of several processes, swelling, polymerization and integration, which are very simple procedures for both performing and large-scale fabrication. I used this facile method to regulate the growth of elastomers in controlled size, which can be easily mapped by incubation time, crosslinking fraction and heating time. This is not the first attempt to prepare self-growth soft material, but my method is one of the most robust. In addition, I explore the multiply growth ability of the seed sample, as well as their modulation of strength and compositions. The facile modulation of the grown samples in size, strength and composition provides strong attempts to probe the growth of materials on demand. There are still some drawbacks need to be dissolved, such as, this fundamental approach is based on an organic polymer system which could not be used for bio-applications directly. In the near future, I hope that I can develop suitable hydrogel system for practical biomaterials.

2.4. Conclusion

In summary, I have developed a facile approach of the swelling-polymerization-

homogenization approach to probe the bulky growth of dynamic soft materials by photo-activation. Photopolymerization was used to cross-link the newly polymers, while heating trigger transesterification was used to reconfigure newly formed and original polymers. The size of grown seed samples can be easily regulated by incubation time, cross-linking fraction, and heating time. The mechanical properties of the grown samples can be easily maintained to their original strength or be stiffened by introducing more crosslinker fraction. By varying nutrient solutions, the composition of grown material can be well-modulated. Besides, the multiply homogeneous and heterogeneous growth of bulk materials are easily achieved. I also demonstrate its potential application in regulating the bulk hydrophobicity of materials through growth cycle treatment without any preprogramming.

2.5. Materials and methods

2.5.1. Chemicals and materials

4-Hydroxybutyl acrylate (HBA) (TCI Deutschland GmbH), butyl acrylate (BA) (99%, Sigma-Aldrich), hydroxypropyl acrylate (HPA) (Sigma-Aldrich), hydroxypropyl methacrylate (HPMA) (Sigma-Aldrich), poly(ethylene glycol) methacrylate (EOMA) (Sigma-Aldrich), *N*-isopropylacrylamide (NIPAM) (97%, Sigma-Aldrich), dodecyl acrylate (DA) (90%, Sigma-Aldrich), benzenesulfonic acid (BZSA) and 2-hydroxyethyl acrylate (HEA) (Sigma-Aldrich) were purified by passing through a column of neutral alumina to remove the inhibitors before being used. 1,6-Hexanediol diacrylate (HDDA) (99%, Alfa Aesar), 2-hydroxy-2-methylpropiophenone (D1173) (97%, Sigma-Aldrich) and dibutyltin dilaurate (DBTDL) (95%, Sigma-Aldrich), were used as received.

2.5.2. Instruments

UV 365 nm LED light (Olympus BX & 1X, 1700 mA) was provided by THORLABS, of which intensity was set as 10 mW/cm2 during the experiments. Optical images of seed samples before and after growth were recorded by NIKON camera. Water contact angles of materials were collected by an OCA 20 instrument. Elastic moduli of seed samples were measured on a universal testing machine (ZWICK 1446, Germany) with a load cell of 200 N, and crosshead velocity of 10 mm min−1 and values were calculated in the linear elastic region of the stress-strain curves from 1 to 5%. Every measurement was conducted three times.

2.5.3. Fabrication of seed sample

Taking original HBA based seed sample as an example: HDDA (crosslinker, 1 wt%) and D1173 (photoinitiator, 1 wt%) were added to HBA solution (98 wt%) to obtain the precursor. The precursor solution was coated on Teflon substrates and cured under UV light (intensity: 10 mW/cm^2) for 30 min to afford the original HBA based seed sample.

During this fabrication process, the fraction of HDDA can be changed to 0.1 wt%, or 2 wt%, or 3 wt%, or 5 wt% to obtain HBA based seed sample with different cross-linking density.

2.5.4. One time light-induced bulky growth

Original HBA based seed sample was immersed in a nutrient solution containing HBA (96 wt%), HDDA (1 wt%), D1173 (1 wt%) and DBTDL (transesterification catalyst, 2 wt%) for different incubation time (5 h, 12 h, 24 h, 48 h, 72 h, and 120 h) to obtain a swollen sample. For growth, the swollen samples were subjected to UV light (intensity: 10 mW/cm^2) then heating at 150 ^{o}C for 20 min to obtain a 1st grown HBA based seed

sample.

2.5.5. Influence of heating time to the growth of seed sample

The original HBA based seed sample containing transesterification catalyst was prepared as follows: HDDA (crosslinker, 1 wt%), D1173 (photoinitiator, 1 wt%) and DBTDL (transesterification catalyst, 2 wt%) were added to HBA solution (96 wt%) to obtain the precursor. The precursor solution was coated on Teflon substrates and cured under UV light (intensity: 10 mW/cm^2) for 30 min to afford original HBA based seed sample containing transesterification catalyst, then which was baked in the oven at 150 ^{o}C with 10 min, 20 min, 30 min, 60 min, and 120 min, respectively. Then these samples were used as seed samples to study their growth capability, which were immersed in a nutrient solution containing HBA (96 wt%), HDDA (1 wt%), D1173 (1 wt%) and DBTDL (transesterification catalyst, 2 wt%) for 120 h to obtain a swollen sample. For growth, the swollen samples were subjected to UV light (intensity: 10 mW/cm^2) then heating at 150 ^{o}C for 20 min to obtain a grown HBA sample.

2.5.6. Multiply homogeneous growth of seed samples

The 1st grown HBA based seed sample was immersed in a nutrient solution containing HBA (96 wt%), HDDA (1 wt%), D1173 (1 wt%), and DBTDL (transesterification catalyst, 2 wt%) for 120 h to obtain a swollen sample. It was then subjected to UV light (intensity: 10 mW/cm^2) directly to get a 2nd grown HBA based seed sample.

The 3rd grown HBA based seed sample can be obtained by immersing the 2nd grown HBA based seed sample in a nutrient solution containing HBA (96 wt%), HDDA (1 wt%), D1173 (1 wt%) and DBTDL (transesterification catalyst, 2 wt%) for 120 h, then being subjected to UV light (intensity: 10 mW/cm^2) directly.

2.5.7. Heterogeneous growth of bulky seed with different compositions

Taking PHBA-PHEA heterogeneous grown sample as the example: the 1st grown HBA based seed sample was immersed in a nutrient solution containing HEA (96 wt%), HDDA (1 wt%), D1173 (1 wt%) and DBTDL (transesterification catalyst, 2 wt%) for 120 h to obtain a swollen sample. It was then subjected to UV light (intensity: 10 mW/cm^2) directly to fabricate PHBA-HEA seed materials.

Other kinds of one-time heterogeneous growth of materials used similar procedures, which only changing the types of nutrient solutions.

Multiply heterogeneous growth of bulk materials utilized similar methods with multiply homogeneous growth, in which the nutrient solutions can be adapted.

2.5.8. Regulating the bulk hydrophobicity of materials

The PHEA based initial seed sample was soaked in an organic nutrient containing BA/DA/THF/silicon oil (1/1/2/2, vol/vol/vol/vol) using D1173 and benzenesulfonic acid as the photoinitiator and transesterification catalyst, respectively, after growth cycle of polymerization and integration, the PHEA initial seed can be grown into organogel samples. The unpolymerized components can be washed away by THF, then which can be further immersed in aqueous nutrient containing HEA/NIPAM/water (10/10/80, wt/wt/wt) using D1173 and benzenesulfonic acid as the photoinitiator and transesterification catalyst, which can be grown into hydrophilic hydrogel samples.

Chapter 3

3 Light-regulated, site-specific growth from dynamic swollen substrates for making rough surfaces

Note: The content of this chapter has been published in: Light-regulated growth from dynamic swollen substrates for making rough surfaces. *Nature Communications* (2020). 11, 963. L. Xue, X. Xiong, B. Krishnan, F. Puza, S. Wang, Y. Zheng, and J. Cui.

This chapter describes a photoinduced strategy for regulating the localized growth of microstructures from the surface of a swollen dynamic substrate, by coupling photolysis, photopolymerization, and transesterification together. Photolysis is used to generate dissociable ionic groups to enhance the swelling ability that drives nutrient solutions containing polymerizable components into the irradiated region, photopolymerization converts polymerizable components into polymers, and transesterification incorporates newly formed polymers into the original network structure. Such light-regulated growth is spatially controllable and dose-dependent and allows fine modulation of the size, composition, and mechanical properties of the grown structures. I also demonstrate the application of this process in the preparation of microstructures on a surface and the restoration of large-scale surface damage.

3.1. Introduction

Living organisms can create various fascinating microstructures *via* a growth mode.[121] During the natural growth process, nutrient is absorbed into body, followed by being transported inside and then integrated into the organisms under the directive of

intrinsic code.[122-123] In contrast to this fully dynamic and open approach in nature, synthetic materials suffer from self-organized mechanisms to continuously incorporate external mass without compromising material's integrity. In this regard, fundamentally different ways, such as assembling,[148] molding,[149] cutting,[150] and printing,[151-152] have been utilized and applied to fabricate man-made substances. Recently, applying the concept of growth to design self-organized synthetic systems has become a powerful strategy to develop novel dynamic materials with different functions.[18, 20] For instance, Gong et al. reported a kind of self-growing hydrogels that respond to repetitive mechanical stress through mechanochemical transduction.[20] In the transduction, the supplied monomers are incorporated into the original polymer network by the mechano-generated radicals, to self-strengthen the materials. Additionally, Johnson et al. developed a class of growable polymer gels by using trithiocarbonate iniferters as a dynamic connector.[18, 101] The iniferters can incorporate monomer molecules entrapped in the gels to elongate the polymer segments between crosslinked points. By considering a similar approach, Kloxin and co-workers has developed covalently crosslinked polymer networks in which crosslinking reactions can be triggered to strengthen the material or heal damage in the material.[108] These reported studies indicate that growing strategy is promising in the post-variation of material properties. Despite these progress in this field, the growing strategy has not been applied to create microstructures on surfaces yet, e.g. to enable localized growth of a structure out from a flat substrate. To this end, a set of mechanisms for not only molecular incorporation but also mass transport and homogenization of polymer composition should be established together in a single system.

Many stimuli, such as light,[153-154] strength,[155-156] temperature,[157] and moisture,[158] have been applied to selectively trigger chemical reactions for spatial functionalization. Among them, light is environment-friendly, noncontact, and spatiotemporally

controllable, and therefore is widely used for lithography,[159] 3D printing,[160] robotic actuation,[161] cell migration,[104] self-healing,[162] switchable transitions,[163] etc. It has also been employed to initiate the incorporation of entrapped monomer molecules into polymer matrix for material growth.[18, 101, 108, 117] However, in these previous examples, photo-induced reactions were utilized to convert monomer/crosslinker to polymers, rather than to guide mass transport.

In this chapter, I report a photo-regulated strategy to control the localized growth of microstructure from the surface of swollen substrates. In my design, three kinds of reactions, including photolysis, photopolymerization, and transesterification, were coupled together to guide the transport of liquid compositions entrapped in the substrates, to convert the polymerizable compositions in the liquids to polymers, and to reconfigure new-formed and original polymers, respectively. As a result of these reactions, microstructures can grow directly from flat substrates without the requirement of any preprogramming. The developed light-induced growth approach is spatially controllable, dose-dependent, and multi-triggerable, and can be used to create various rough surfaces or restore large scale surface damage.

3.2. Results

3.2.1. Design and sample preparation

The detailed concept of light-induced growth is demonstrated in Figure 1. It starts from a swellable substrate that is made from photo-responsive polymers crosslinked by ester-based linkers (Figure 1a). The substrate can swell a solution, consisting of monomer, crosslinker, photoinitiator, and transesterification catalyst, which is defined as nutrient solution (Figure 1b). Photolabile side groups are designed as promoters that can undergo photolytic reactions to generate dissociable ionic groups to enhance

the swelling ability by the expansion of the polymer networks to drive the nutrient solution to transport into the irradiated region (Figure 1c).[164] This photo-induced mass-transport is coupled with the photopolymerization of the monomer and crosslinker in the nutrient solution, leading to a continuous swelling of irradiation region and thus the formation of protrusions on the irradiated surface (Figure 1d). During swelling, the original networks are stretched, which should prevent the nutrient solution to diffuse in. A transesterification catalyst is thus designed to trigger an exchange reaction between original and new-formed networks to release such mechanical tension, and also to reconfigure the grown structure (Figure 1e). I expect that such a coupling of three reactions could lead to an on-demand, localized growth of microstructures from material surfaces.

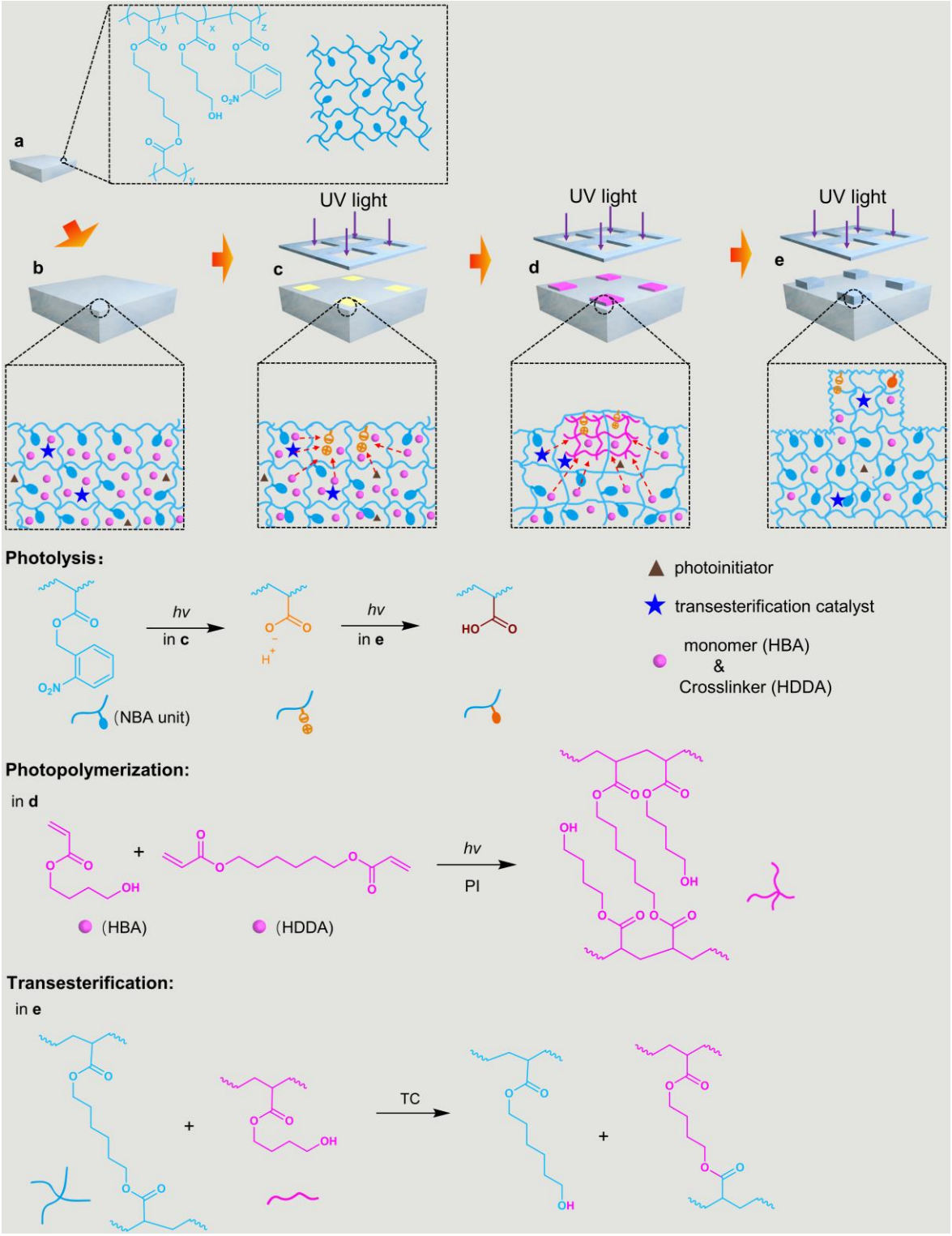

Figure 1. Schematic of light-induced growth from swollen substrates. (a) Growable seed made from 4-hydroxybutyl acrylate (HBA), *o*-nitrobenzyl acrylate (NBA, promoter), Irgacure 819 (I-819, photoinitiator) and 1,6-hexanediol diacrylate (HDDA). (b) Swollen seed. The mixture of HBA, HDDA, photoinitiator (I-819), and transesterification catalyst (benzensulfonic acid (BZSA)) were used as the nutrient solution

for swelling. (c) Swollen substrate under selective UV irradiation. Photolysis of NBA units generated dissociable ionic groups to induce liquid diffusion into the irradiated region. (d) New polymer network formed *via* photopolymerization. Liquid components diffused in, and the polymer chains in the original network were stretched. (e) The grown part was homogenized *via* transesterification reactions between the original and newly formed polymer networks.

A material system of 4-hydroxybutyl acrylate (HBA), *o*-nitrobenzyl acrylate (NBA), and 1,6-hexanediol diacrylate (HDDA) was selected to demonstrate the design. HBA is a commercially available precursor for making polymer substrates with good swelling ability to its monomer, while NBA is a photolabile monomer (promoter) that can generate dissociable ionic group of $–COO^-$ for inducing an increase in swelling ability.[165-166] The HDDA crosslinker has an ester-linkage that can undergo a transesterification reaction with the hydroxyl of HBA. The substrates of poly(HBA-*co*-NBA) with different NBA molar fraction (0%, 5%, 10%, 20%, 35% and 50%) were fabricated *via* photopolymerization under a blue LED light (460 nm, 0.6 mW/cm^2) in the presence of Irgacure 819 (I-819, initiator). Under this irradiation condition, NBA unit will not undergo photolysis since it does not have any absorption at this wavelength. This hypothesis was verified by irradiating NBA solution under the same condition (no visible change in both UV-Vis and ^1H NMR spectroscopies, Figure 2). After photopolymerization, unreacted components were washed by ethanol and the obtained specimens were denoted as seed-x where x was the feeding molar fraction of the NBA.

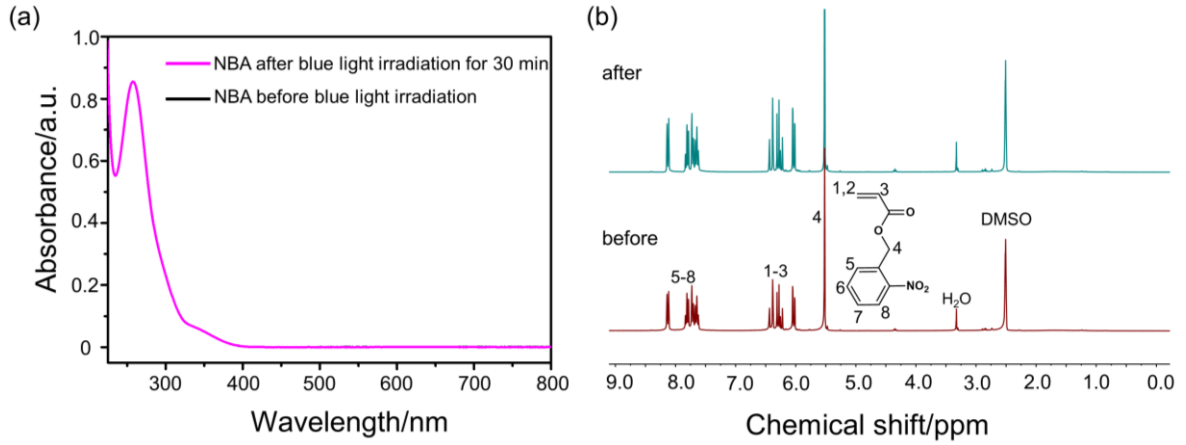

Figure 2. UV-Vis (a) and ^{1}H NMR spectroscopies (b) of NBA before and after blue light irradiation. The black and red lines are overlapped in (a). For the UV-Vis spectra, the concentration of the NBA in acetonitrile is 1.27×10^{-4} M. DMSO-$_{d6}$ was used for the NMR test.

The seeds showed an excellent swelling ability to the nutrient solution consisting of HBA (monomer), HDDA (crosslinker), I-819 (photoinitiator), and benzensulfonic acid (BZSA, transesterification catalyst). For example, an equilibrium swelling ratio of 4.6 was obtained for a seed-20% sample with a thickness of 1.4 mm. The polymerizable compositions, i.e. HBA and HDDA, entrapped in the polymer networks could undergo photopolymerization to integrate into the seeds under UV light irradiation (365 nm, 10 mW/cm^2, confirmed by the weight of the sample after removal of unreacted compositions by washing). The UV light was also expected to trigger the photolytic reaction of NBA unit (confirmed by the disappearance of -NO_2 in FTIR spectrum, Figure 3). In company with the polymerization, thermal effect generated by polymerization would trigger transesterification reactions to release any polymerization-induced mechanical tension in such dynamic networks.[4, 42, 147]

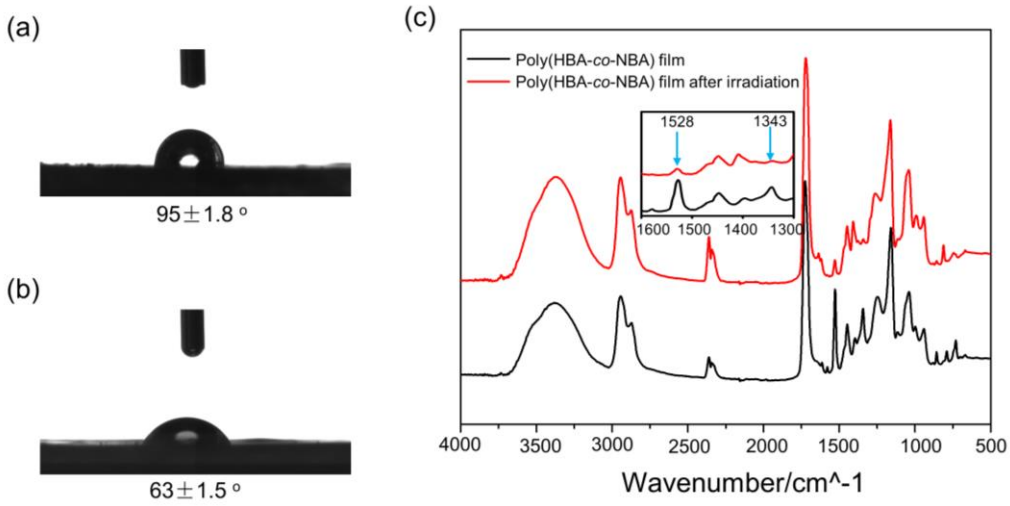

Figure 3. FTIR spectra of poly(HBA-*co*-NBA) film before and after UV irradiation for 30 min.

3.2.2. Mechanism of light-triggered localized growth

Figure 4a shows the image of light-induced growth of a pillar from the surface of a flat swollen seed-20%. During UV irradiation, a regular structure tardily grew out from the irradiated region of the material surface and the height of this grown pillar could reach up to 250 μm in the testing time.

Figure 4b shows the growing process evaluated by the height of the grown pillar. The growing process was triggered on swollen seed-20% by irradiation with either 365 nm or 460 nm light. Exposure of 365 nm light would trigger both polymerization and photolytic reaction while 460 nm light only induced polymerization. In this regard, the experiment with 460 nm light could be used as a control to evaluate the contribution of photolytic reaction. The irradiation intensity for both lights was same (10 mW/cm^2) and such design was used for getting similar photopolymerization effect (photopolymerization conversions reach their plateaus in 2 min, Figure 4c). Upon irradiation with 365 nm light, the height of the grown structure increases fast in the first 5 min (75 μm) and reaches a plateau at a value of 250 μm in 50 min. The grown sample retains its shape after being stored in dark overnight. Compared to this, growth

also occurs in the control sample but the height of the grown structure at the plateau is significantly smaller (70 μm). I attributed the growth in the absence of a photolytic reaction to the fact that photopolymerization consumed the monomer and crosslinker in the nutrient solution to form new polymer networks in the irradiated region, followed by creating a concentration gradient of monomer and crosslinker to drive these compositions to diffuse into the irradiated region to join the polymerization. Such a polymerization-diffusion cycle led to the growth of the structure. However, this photolysis-absent growth is significantly slower than the photolysis-present growth and the obtained structure is also remarkably smaller. The higher grown structure obtained in photolysis-present growth indicated that the photolytic reaction had generated an extra effect to accelerate the diffusion of nutrient solution into the irradiated region. Since the photolytic reaction of NBA units would generate carboxyl groups, I attributed the extra effect to the formation of dissociable ionic groups of -COO^- which enhanced the swelling ability of the irradiated region by the expansion of the polymer networks with electrostatic repulsion. Besides the smaller size, the grown structure seriously distorts after being stored in dark (Figure 4b).

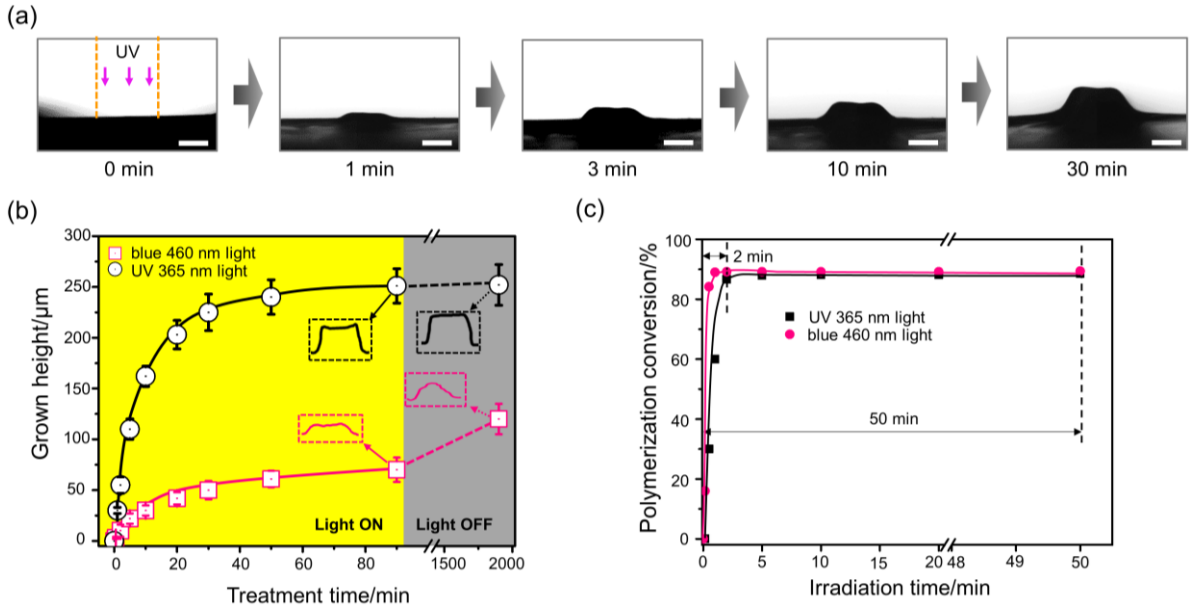

Figure 4. Light-regulated growth from HBA-based substrates. (a) Time-dependent images (side view)

of swollen substrates under UV irradiation (10 mW/cm^2). A photomask with a diameter of 500 μm was used. The scale bar is 250 μm. (b) The height of the grown microstructures (grown height) of different samples vs treatment time. The data were obtained from three independent measurements. Error bars are s.e.m. The dashed boxes show the typical profiles of the grown structures before and after being stored in the dark. (c) Polymerization conversion of HBA/NBA/HDDA/I-819 under different irradiation conditions.

A growth process based on polymerization-diffusion cycle was thus proposed: upon UV irradiation, photolysis of NBA units and polymerization of the monomer and crosslinker in the irradiated region generated the dissociable ionic group of -COO$^-$ and the concentration gradient of monomer and crosslinker, which significantly enhanced the swelling ability of the irradiated region. As a result of enhanced swelling ability and a lower concentration of monomer and crosslinker in the irradiated region, the nutrient solution diffused into the irradiated region to induce a polymerization-diffusion cycle. In this cycle, the photopolymerization was significantly faster than the diffusion process (time for photopolymerization to reach its conversion plateau: ~2 min; time for liquid molecules to diffuse into the seed to full swell it: ~4 h without irradiation and ~2 h under irradiation, Figure 4c and 5a). After the irradiation, the generated concentration gradient still existed and continued driving monomer and crosslinker (major liquid composition of the nutrient solution) to diffuse into the grown structure to swell. This swelling distorted the grown structure of the photolysis-absent sample (swollen state, Figure 5b). To confirm this, after the distorted grown structures were washed, a remarkable shrinkage was observed in the distorted sample (washed state, Figure 5b). In addition, finally obtained grown structures were stable in both swollen and dried states (Figure 5c and 5d).

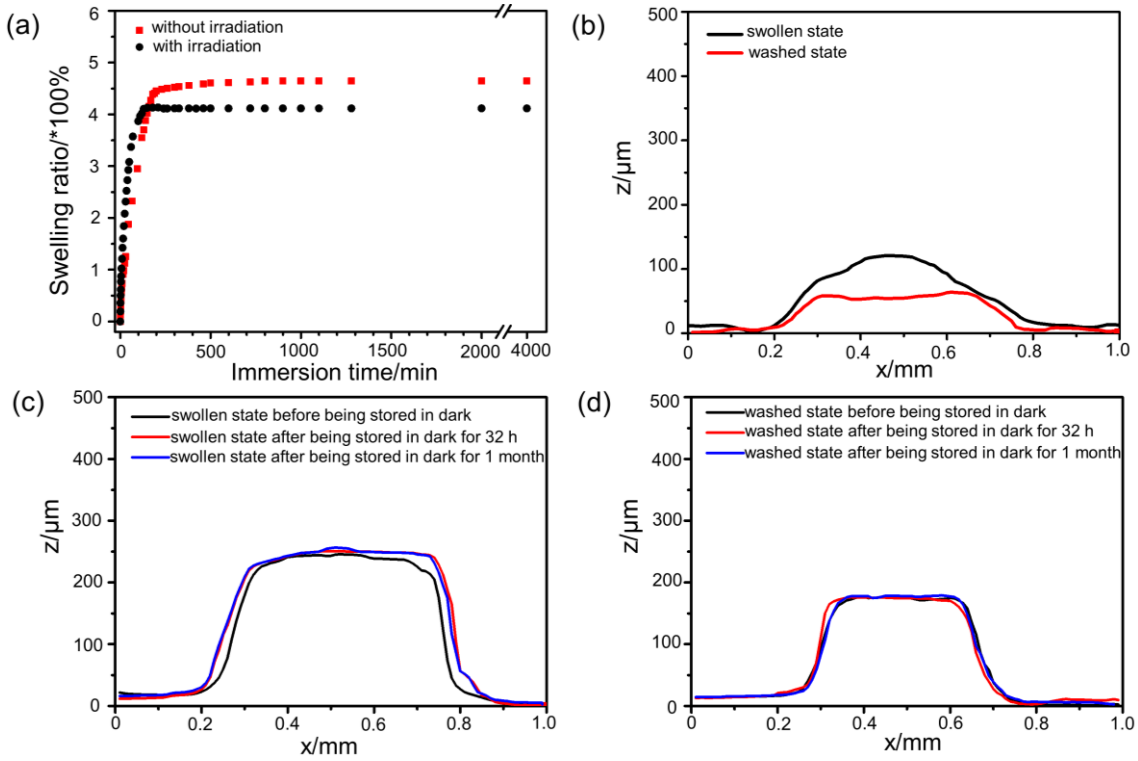

Figure 5. Swelling kinetics of seed-20% sample and its growth stability. (a) The swelling ratio of seed-20% thin film (thickness: 500 μm) in the nutrient solution containing HBA, HDDA, I-819, and BZSA with and without UV irradiation. (b) Profile of grown structures of the photolysis-absent sample under different conditions. Swollen sate: sample after being stored in dark for 32 h, washed state: sample after washing by ethanol. (c) Profile of grown structure from swollen seed-20% without washing treatment. (d) Profile of grown structure from swollen seed-20% with washing treatment.

3.2.3. Proof of promoters

I studied the formation of the dissociable ionic group of -COO^- by monitoring the Zeta potential of a linear poly(HBA-co-NBA) containing 20% NBA units (Mn = 8500, PDI = 1.16, Figure 6a and 6b) under UV illumination. The molar ratio of HBA was 22% calculated from the integration of peak c', f' and d-g, which was very accordance with the raw ratio before the polymerization. As shown in Figure 6c, the copolymer is almost neutral (-1.8 mV) before irradiation. The potential value decreases sharply to -27 mV after 2 min of UV irradiation, indicating the formation of dense negative species on the

copolymer (-COO^-). The species was assigned to the carboxyl ion, which was released from NBA unit.[166] It was highly active and would finally be neutralized into -COOH soon (thus a change from -32 mV to -2 mV in Zeta potential). To verify that the change in Zeta potential came from dissociable ionic group of -COO^- rather than the photolytic product of *o*-nitrobenzyl moiety, I selected 2-nitrobenzyl alcohol as a control, a compound that would undergo similar photolytic reaction but did not generate carboxyl group. The Zeta potential of 2-nitrobenzyl alcohol solution did not change under UV irradiation (Figure 6d), indicating that the change in Zeta potential of poly(HBA-co-NBA) should be attributed to the generation of dissociable -COO^-. The formation of -COO^- on the polymer segments would induce an increase in swelling ability[164] while the carboxyl groups reduced the swelling ability of the matrix to reduce the distortion effect. I proved this hypothesis by irradiating a control sample of seed-20% swollen by a non-polymerizable solution consisting of 4-hydroxybutyl acetate (HB acetate), I-819, and BZSA. Upon UV irradiation, a bulge forms on the irradiated region (Figure 6e), indicating a swelling process. Since the liquid compositions were non-polymerizable (thus no polymerization-diffusion cycle to drive liquid to diffuse in), the driving force for swelling was attributed to the charge-induced electrostatic repulsion. Although only a change of ~5 μm in height was observed, such a change in the polymerization-diffusion cycle could be amplified. To further confirm the contribution of photolysis to accelerate mass transport, I compared the diffusion rate of nutrient solution in seed-20% under different conditions by a swelling method (Figure 6f). It was found that the average rate of mass transport under irradiation condition was significantly higher (4.7×10^{-5} cm^2/s) than that without irradiation (4.9×10^{-6} cm^2/s). After the transition of -COO^- to -COOH, the liquid composites diffused out from the irradiated region, resulting in a cave surface. This result was consistent with the fact that irradiated seed-20% showed lower swelling ability to nutrient solution because of the formation of carboxyl

side groups (Figure 5a). The decrease in swelling ability favored the formation of non-distorted grown structures since the transport of the nutrient solution from the non-irradiated region to irradiated one during storage was reduced (Figure 4b).

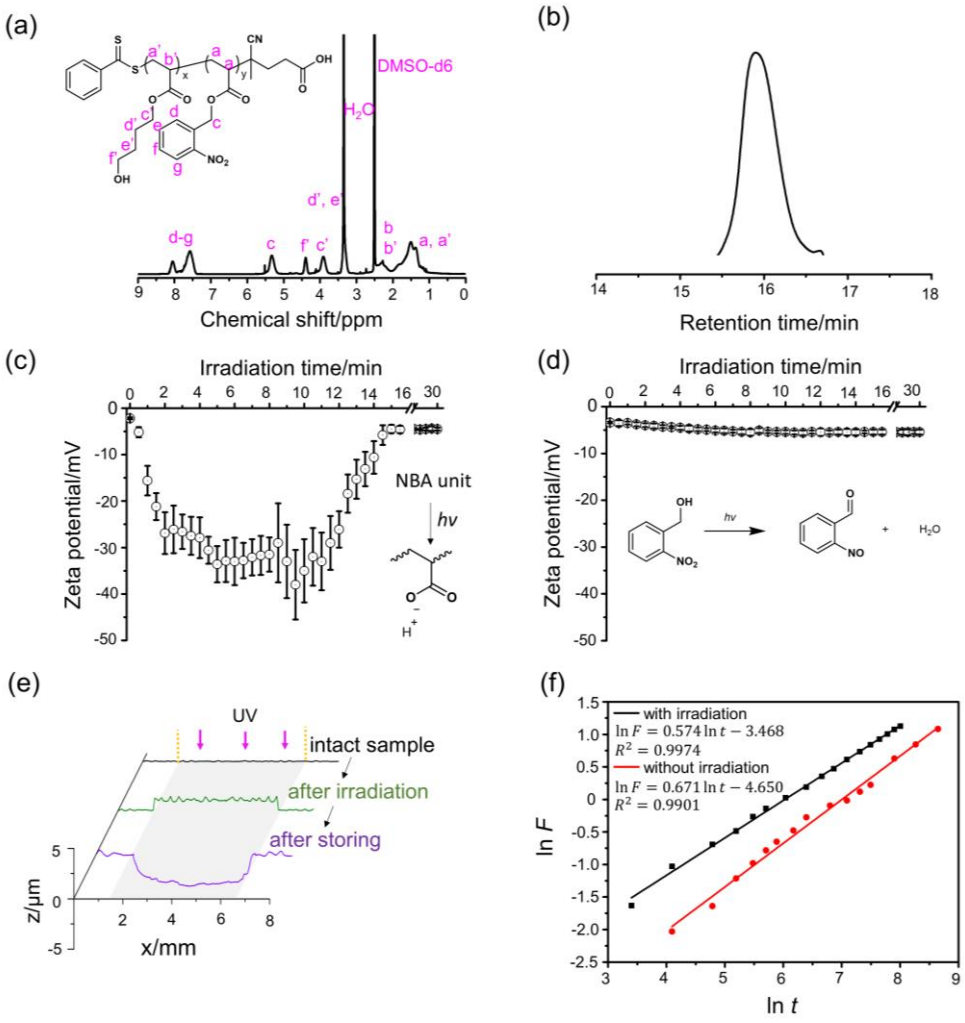

Figure 6. Demonstration of the role of promoters. ^{1}H NMR spectrum (a) and GPC traces (b) of the linear poly(HBA-*co*-NBA) obtained. (c) (d) Zeta potential of linear poly(HBA-*co*-NBA) copolymers and 2-nitrobenzyl alcohol at different irradiation times. The polymer concentration was 2 mg/mL, and an LED lamp (10 mW/cm^2) was used for irradiation. (e) Profiles of a swollen seed-20% containing HB acetate, I-819, and BZSA under different conditions. Photomasks with a diameter of 5 mm were used. (f) Swelling kinetic curve of cylindrical shaped seed-20% samples under different conditions. Samples with a diameter of 1 cm were used.

3.2.4. Integration by transesterification

Transesterification occurred during the light-induced growth. A diagram of the transesterification was shown in Figure 7a. Under this irradiation condition, the temperature of the irradiated region in a swollen seed-20% sample elevates to 62 ^{o}C in the initial 1 min (Figure 7b). At this temperature, the catalyst BZSA used in my system can induce efficient transesterification.[147] I studied the contribution of transesterification to the grown structure by a control sample without BZSA. In contrast to the flat surface of the grown structure observed in the typical sample, the surface of the grown structure obtained from the control sample is concave (Figure 7c). In the growth, since the photopolymerization of the monomer and crosslinker in nutrient solution was significantly faster than the transport of nutrient solution, the growth rate was mainly dependent on the diffusion rate of the nutrient solution. In the control sample, nutrient solution diffused into the irradiated region from outside and was integrated into the periphery *via* the rapid polymerization and thus fewer monomer and crosslinker molecules could diffuse and be integrated into the center, leading to the energy-unfavorable concave surface. In the presence of a transesterification catalyst, such energy-unfavorable concave surface could be turned into energy-favorable flat surface *via* transesterification-associated reconfiguration (Fig. 1e).[42] The transesterification was further proved by the significantly higher modulus of the grown structure of the control samples (Figure 7d). Without transesterification, a double-network structure formed to stiffen the grown structure (490 KPa) while the transesterification-induced homogenization would reduce such stiffening effect (380 KPa).[167]

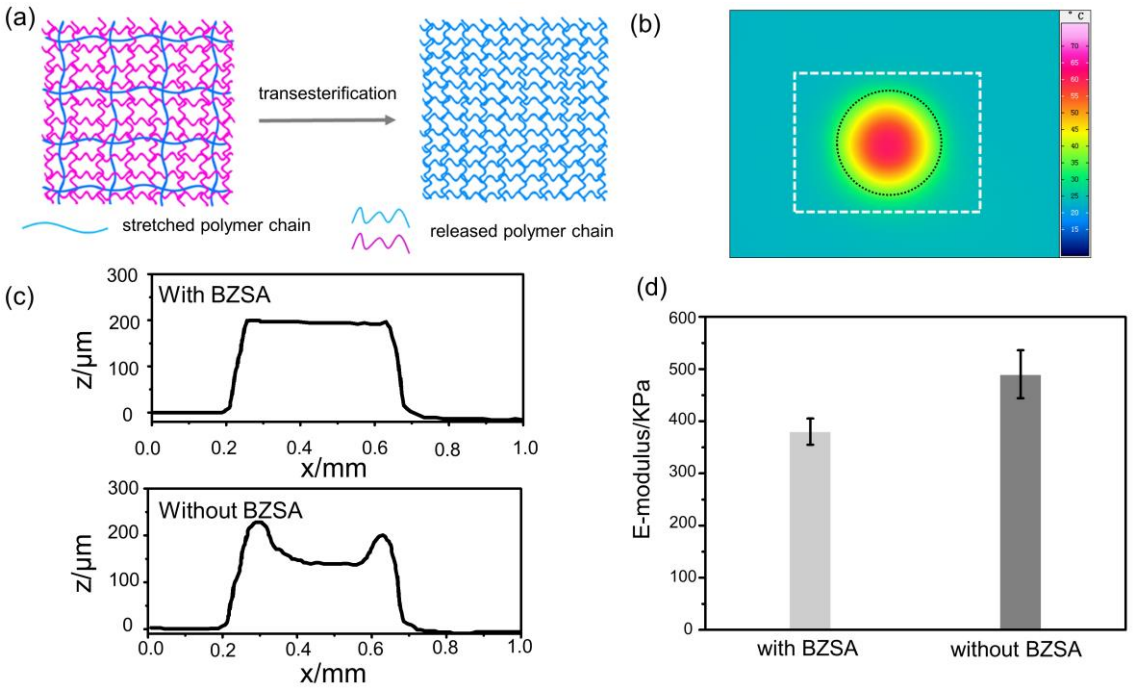

Figure 7. Transesterification to reconfigure the networks. (a) Transesterification process in the self-grown part. (b) Infrared camera image of swollen seed-20% after UV irradiation for 1 min. White dotted zone shows the position of swollen sample, while black dotted zone stands for the light irradiation area. (c) Typical profiles of the grown structures obtained from the swollen seed with (top) or without (bottom) transesterification catalyst BZSA. (d) E-moduli of the grown structures with and without BZSA as the transesterification catalyst.

3.2.5. Composition of grown structures

The composition of the grown structure was studied by confocal fluorescent spectroscopy. To enable imaging and detailed investigation in swollen substrates, the nutrient solution was labelled by a fluorescent crosslinker, bis-*N*,*N*'-6-hydroxyhexanol perylenetetracarboxylic diimide-acrylate (PDIDA). The diacrylate structure of the crosslinker was expected to significantly decrease its re-localization possibility during the transesterification-induced homogenization. A seed-20% was soaked in a nutrient solution containing 0.01 wt% PDIDA, followed by light-induced growth for 30 min. After polymerization, the unreacted compositions were washed with ethanol/$CHCl_3$

solutions, before being subjected to confocal imaging. Figure 8a shows the cross-section of grown samples. Compared to the dark surrounding, bright color was observed in the grown part, indicating that the monomer and crosslinker in the nutrient solution have been integrated into the grown structure. The bright color extends to the bottom region of the seed, suggesting that the growth started inside the sample, rather than simple polymerization from the surface of the sample. Complementary experiments were also conducted to assure the growth mechanism. The seed-20% was dyed with 0.01 wt% PDIDA and then grew from a non-dyed nutrient solution (Figure 8b). As expected, the grown region is still fluorescent but significantly diluted, indicating that the grown region was made from both original and new-formed networks. The fluorescence intensity of the surface of a newly grown structure is nearly same as that observed in the non-irradiated region (Figure 8c and 8d), indicating that nearly no growth occurred in the surface layer. It might dues to the evaporation of monomer molecules in this region or the lower swelling ability of the surface layer of the sample. In addition, the fluorescence intensity gradually increases from the top region to the bottom one. I attributed it to the gradual swollen of the networks. Based on the growth curves (Figure 4b), the growth rate decreases with time due to the consumption of the monomer. Therefore, the dilution effect in fluorescence decreases from top (early stage) to bottom (later stage) in the growth direction.

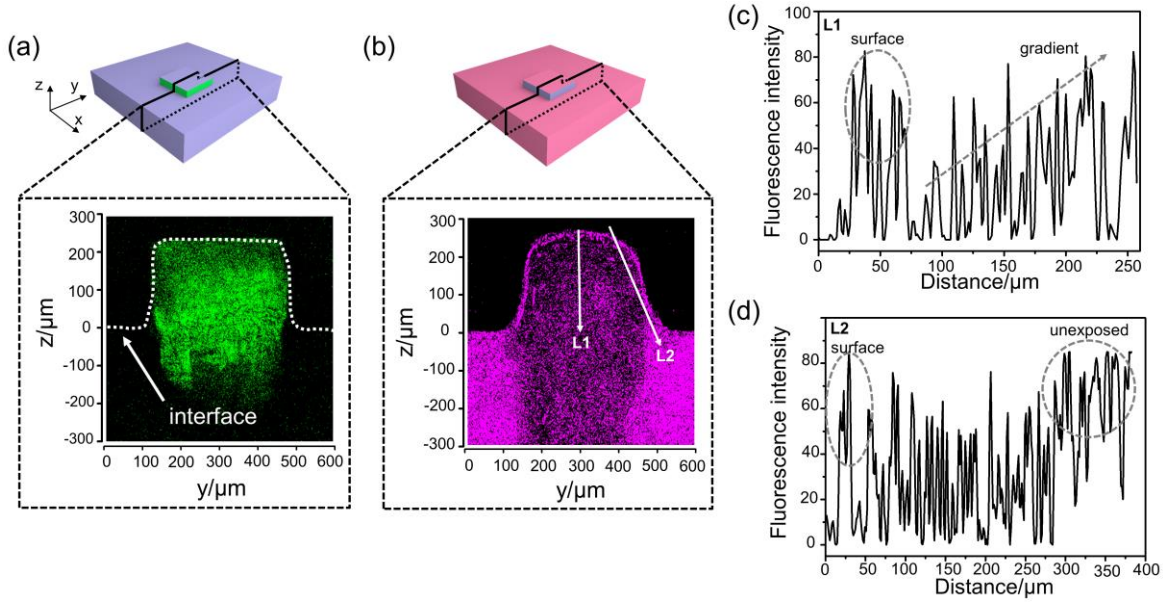

Figure 8. Composition of grown structures. Fluorescent cross-section images of the grown structure obtained from a non-dyed seed and dyed nutrient (a) and a dyed seed and non-dyed nutrient (b). PDIDA was used to dye the seed in (a) and the nutrient in (b) with a concentration of 0.01 wt%. (c) Fluorescence intensity of L1 in (b). (d)Fluorescence intensity of L2 in (b).

3.2.6. Control of growth

The light-induced growth was not only localized, but also temporally controllable. I employed seed-20% to demonstrate this capability by switching irradiation light. As shown in Figure 9a, growth was only triggered by the implementation of irradiation. For example, the height of grown structures increases to 25 μm within the first min activation and the growth stops in the case that light is turned off. The growth can be re-initiated again by turning on the light. Such on-off modulation can extend until the growth reaches its plateau. In addition, several parameters, including the crosslinking degree of the seed, the diameter of irradiation region, and the light intensity, were studied to modulate the growth. Increasing the crosslinking degree of the seed-20% decreases its swelling ability as well as the height of the grown structure at plateau state (Figure 9b). With increasing the irradiation diameter, the growth height at plateau state increases in the range from 266 μm to 600 μm but decreases in the range of >600

μm (Figure 9c). I attributed the increase to the photopolymerization-induced thermal effect (elevation in temperature would accelerate the diffusion rate of liquid molecules and thus the growth). As considering thermal dissipation, increasing irradiation diameter favored temperature elevation. On the other hand, increasing diameter also elongated the diffusion distance and thus reduced the growth. This reducing effect became more obvious in larger diameter range (>600 μm). As for light intensity, its decrease reduces the growth because of both slower photolysis and polymerization reactions (Figure 9d)

Sequential growth was also possible. Figure 9e shows a sample with a grown pillar with a height of 180 μm and a diameter of 5000 μm. This grown sample can be swelled by the nutrient solution again and activated to grow in the grown region. Under the same irradiation condition, a new pillar with a height of 110 μm forms on the previously grown pillar (Figure 9f). The lower height of second-growth was attributed to the lower concentration of the promoter in the second time photolysis.

Since the grown structure was made from feed nutrient solutions and original polymers, its composition could be easily regulated by the nutrient solutions, which provided a powerful approach to control the mechanical properties of the grown structure. I demonstrated this concept by varying crosslinker fraction in the nutrient solutions used to a seed-20% (made from 1 wt% crosslinker, modulus: 370 KPa). When a nutrient solution with a crosslinker concentration of 0.2 wt% is used, a grown structure with a modulus of 280 KPa can be obtained. On the other hand, increasing crosslinker concentration in the nutrient solutions enhanced the modulus of the grown structure. The E-moduli is even up to 1.5 MPa when a crosslinker concentration of 10 wt% is used in the nutrient solution (Figure 9g). Notably, such a growing method to spatiotemporally change the modulus of the grown structures did not induce any interface issue, since the new-formed structure was grown from inside of the original

materials.

The promoter fraction in the seed was also expected to be an important parameter to control the growth. In principle, increasing its fraction should enhance the driving force for liquid transport into the irradiation region but would also decrease the final swelling ratio of the irradiation region since both NBA unit and its photolytic product reduced material's swellability to nutrient solutions. As shown in Figure 9h, the height of the grown pillar at plateau state increases with the fraction of promoters in the range of <20 %, but decreases in the range of 35-50 %.

The concept of photo-induced growth could be applied to different material systems. I demonstrated this applicability by poly(ethylene glycol) methyl ether acrylate (PEGA), a hydrophilic monomer, and butyl acrylate (BA), a hydrophobic monomer. Figure 9i lists the grown height of different material systems under the same growth condition. The height of grown PEGA at plateau state (160 μm) is lower than that of HBA (250 μm). It was attributed to the significantly higher viscosity of PEGA (90 cSt, 20 ^{o}C)[168] than that of HBA (10.7 cSt, 20 ^{o}C). The higher viscosity led to a lower transport rate and thus less growth. The hypothesis was supported by the higher height (300 μm) of the grown pillar made from BA which has a lower viscosity (0.92 cSt, 20 ^{o}C). Moreover, a hybrid system could also be created by varying the compositions of nutrient solution. For example, I grew PEGA-based seed in HBA-based nutrient solution. The grown pillar reaches up to a height of 240 μm. Based on these results, I concluded that the light-induced growth was fully controllable and allowed for fine variation in size, strength, and compositions.

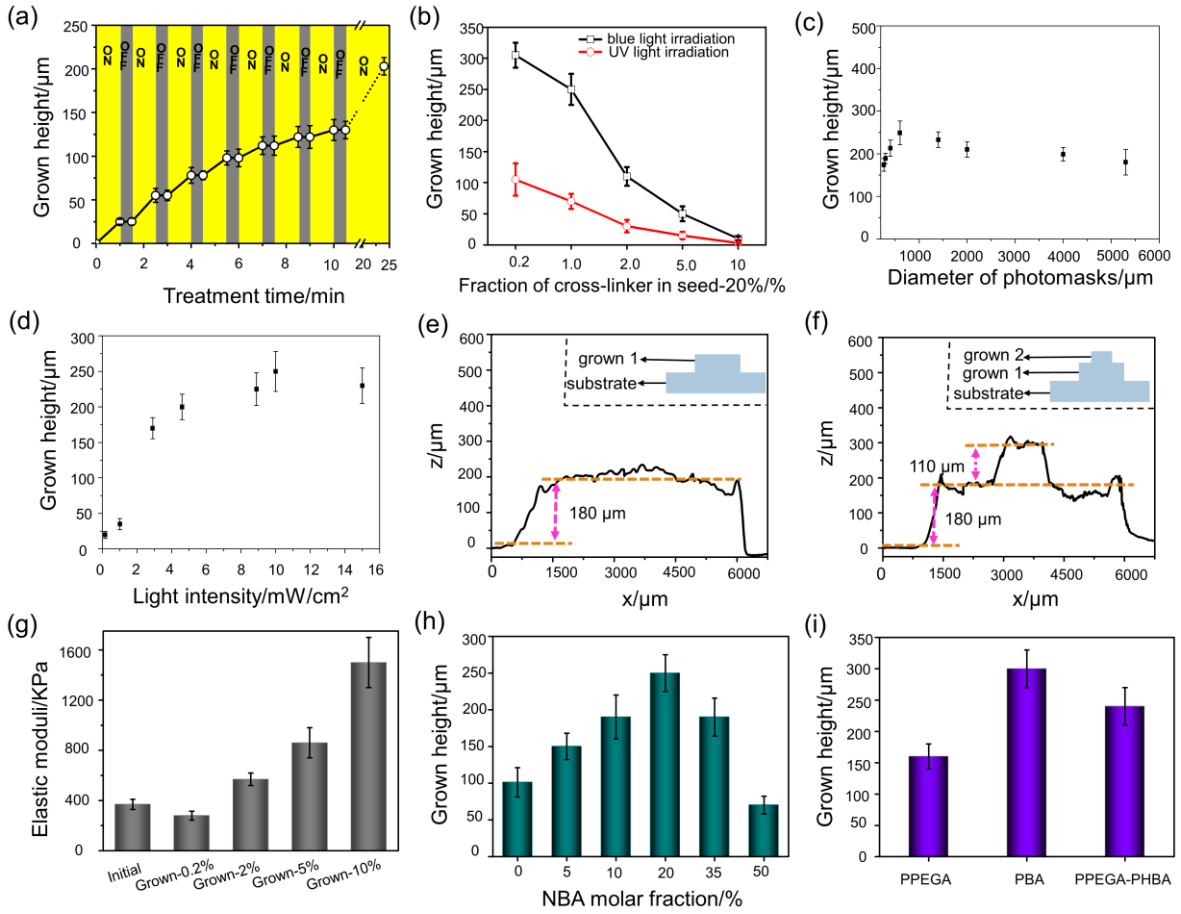

Figure 9. Control of localized growth of structures on material surface. (a) The height of the grown structures changes with irradiation conditions. The labels “ON” and “OFF” indicate the state of UV light applied to the samples. (b) The height of grown structure at plateau state *vs* different seed-20% samples with different crosslinker fractions under UV and blue light irradiation. (c) The height of grown structure at plateau state versus diameter of photomask under UV light for 30 min. (d) The height of grown structure after 30 min irradiation versus light intensity. (e) The profile of the grown structure obtained from first-cycle growth. A round photomask with a diameter of 5000 μm was used. (f) The profile of the grown structure prepared from two-cycle growth. (g) Modulus of the seed and the grown structures obtained from the nutrient solution with different crosslinker concentrations (x in Grown-x in the label). (h) The height of the grown structure obtained from the seed containing different NBA molar fractions. (i) The height of the grown structure made from different monomers. PPEGA/PBA: PEGA/BA-based seeds grew from PEGA/BA-based nutrient solution; PPEGA-PHBA: PEGA-based seeds grew from

HBA-based nutrient solution.

3.2.7. Potential application of structuring material surface

Localized growth of microstructure from a flat substrate implied a template-free method for making patterning surface. Figure 10 shows a tentative example. Upon UV illumination through a mask, a regular micropattern (diameter of 500 μm) grew out from the flat surface of the swollen sample (Figure 10a-e). The formed pillars are uniform with a height of 250 μm (Figure 10e).

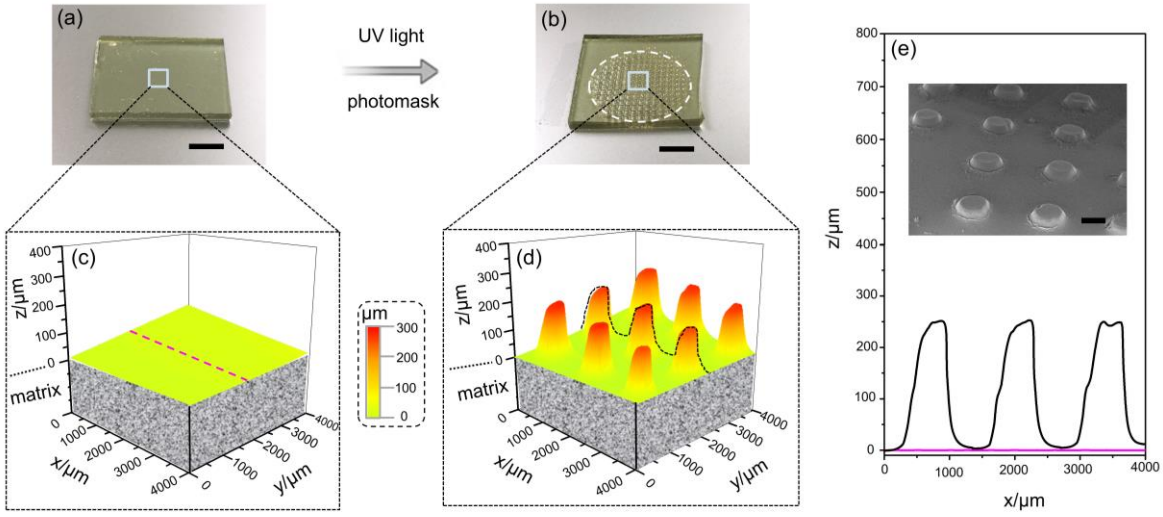

Figure 10. Structuring rough surface by light-induced growth: (a) Swollen seed-20%. (b) Formed microstructure. The dashed line highlights the irradiated zone. (Scale bar: 8 mm) 3D profiles of the surfaces of the swollen seed-20% (c) and the grown sample (d). (e) Surface profiles of the seed−20% and the formed microstructure. The regions are highlighted by dotted lines in (c) and (d). The inset in (e) shows the SEM image of the growth pattern. Scale bar: 500 μm.

3.2.8. Potential application for self-restoration of damaged materials

The growth could be used to restore large scale surface damage in millimeter level. Self-healing of large damage is extremely challenging since it not only involves molecular reconfiguration but also requires significant mass-transport.[169] Although

dynamic materials have been suggested to be self-healable, they mainly depend on the re-bonding of matrices which is normally useful in the recovery of microcracks and scratches.[33] It is difficult for them to restore large scale surface damage in millimeter level.[170] Since light-induced growth involves significant liquid transport, *in situ* polymerization, and reconfiguration, I assumed that it could be used to restore large scale surface damage by guiding the growth toward damage region. The promising demonstration of surface damage restoration by the developed strategy is detailed in Figure 11. Damage with a size of 0.60 cm (*l*) × 0.40 cm (*w*) × 0.22 mm (*h*) was tentatively created on a substrate made from seed-20%. For a better comparison, I partially irradiated the damaged region and induced the growth until it flushed with the undamaged part. It could be observed from the profile of the damaged zone that the irradiation region was regenerated, implying a powerful method to the restoration of large scale surface damage.

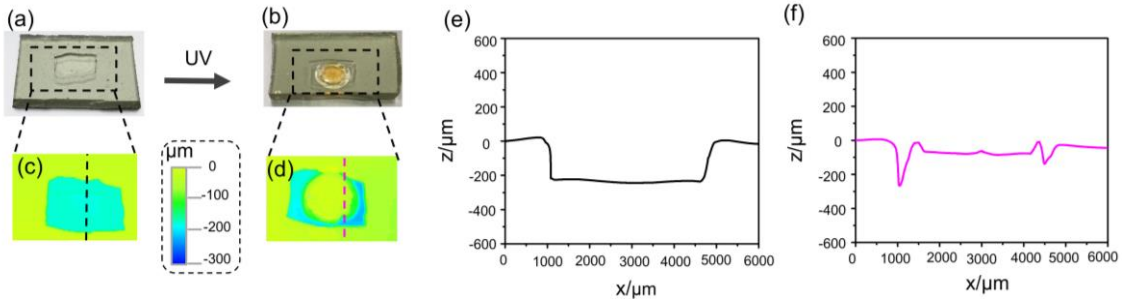

Figure 11. Restoration of large-scale surface damage by light-induced growth. (a) Images of the swollen seed-20% with damage of 0.60 cm (*l*) × 0.40 cm (*w*) × 0.22 mm (*h*) then treated with UV light (b). Top view of the 3D profile of the damaged swollen seed-20% (c) and the grown swollen seed-20% (d). Surface profiles of the damaged area before (e) and after (f) healing. A photomask was used for UV irradiation, and the irradiation time was 30 min. The scale shows the height. The dashed lines in (c) and (d) highlight the positions used for the collection of the profile data.

3.3. Discussion

In contrast to these fully dynamic, opened biological systems, synthetic materials are normally static and lack of a mechanism to spatiotemporally incorporate external "nutrition". In 2013, Zhou and Johnson firstly developed the photo-controlled growth system based on the reversible trithiocarbonates linkages.[101] Insertion of new monomer into as-prepared gels, followed by exposure to sunlight, led to an increase in the average molecular weight between crosslinks *via* direct extension of network chains. This "photo-growth" process represents a novel strategy for interconversion of sunlight energy to mass in bulk materials, demonstrating how the incorporation of iniferter units enables responsive functions in polymer networks. Later, Kloxin and co-workers introduced a photoactive monomer containing a dithiocarbamate iniferter into a polyurethane network to create a light-triggered dynamic networks that can heal and strengthen on demand in 2015.[108] On the basic of these, until 2017 Chen and co-workers developed their awesome first-generation "living additive manufacturing" to transform of parent gels into diversely functionalized daughter gels with specific size, strength and compositions.[18] Based on these photoactivation research, plenty of photo-controlled systems for post-regulating the materials' properties were developed.[116, 118-120, 164, 171] Although with these encouraged progress, all of them were only utilized to incorporate mass molecules around, rather than to drive mass transport. Another example by using the "self-growth" method to control femtosecond laser scanning on the surface of a prestretched shape memory polymer for realizing microscale localized reconfigurable architectures transformation was reported by Zhang and co-workers, in their studies there was only shape memory behaviors when the materials was heated by laser to structure material surface, no mass transport, polymerization and integration technologies were presented.[136] In my studies, I have developed a set of mechanisms in a single system for not only molecular incorporation

but also mass transport and composition rearrangement. This is the first attempt to show how light guide the mass transport within the material matrix and how light induce the growth of structures from material surface. I have regulated the controllable growth of structures by varying many parameters, and expanded its potential application in structuring material surface and restoring large-scale surface damage of materials. The main difficulty under this concept is impart this strategy to a more biocompatible hydrogel system for practical applications with precisely controlling. Another deficiency of this approach is that during consume of promoters within the material during self-growth process, the growing ability is limited. Thus there is still requirement to seek more suitable promoters which could generate *in situ* charge under light irradiation, but return its original state after removing light.

3.4. Conclusion

I have demonstrated a strategy for designing photo-induced growable materials. The strategy is based on coupling three kinds of reactions, including photolysis to generate dissociable ionic group to increase the swelling ability for driving the diffusion of nutrient solution into the irradiated region, photopolymerization to convert the monomer and crosslinker in the nutrient solution into crosslinked polymers, and transesterification to homogenize the newly formed and original polymer networks, to achieve localized growth. Such light-induced growth is spatially controllable and dose-dependent, as well as allows for fine modulation in size, composition, and mechanical properties of the grown structure. The flexible tunability enables the creation of microstructures on surfaces and the restoration of large scale surface damage. Although the methodology developed in this study was demonstrated on structuring surface, the mechanistic insights gained in governing the growth can be readily applied

to change the bulk property of materials in consideration of the capability of light to spatially trigger various reactions. I thus envision that its development will benefit areas such as self-healing materials and rough surfaces.

3.5. Materials and methods

3.5.1. Chemicals and materials

4-Hydroxybutyl acrylate (HBA) (TCI Deutschland GmbH), butyl acrylate (BA) (99%, Sigma-Aldrich) and poly(ethylene glycol) methyl ether acrylate (PEGA) (average Mn = 480 g mol^{-1}, Sigma-Aldrich) were purified by passing through a column of neutral alumina to remove the inhibitors before being used. 2-Nitrobenzyl bromide (98%, Alfa Aesar), acrylic acid (99%, Sigma-Aldrich), potassium carbonate (K_2CO_3) (99%, Alfa Aesar), 1,4-butanediol (99%, Fluka), acetic acid (99%, ABCR), bis(2,4,6-trimethylbenzoyl)-phenylphosphineoxide (I-819) (Ciba), 1,6-hexanediol diacrylate (HDDA) (99%, Alfa Aesar), sulfuric acid (H_2SO_4) (95-98%, Sigma-Aldrich), benzenesulfonic acid (BZSA) (98%, Sigma-Aldrich), 2-nitrobenzyl alcohol (97%, Sigma-Aldrich), 3,4,9,10-perylenetetracarboxylic dianhydride (98%, Alfa-Aesar), acrylic chloride (97%, Sigma-Aldrich), imidazole (ACS reagent, Sigma-Aldrich), triethylamine (TEA) (99.5%, Sigma-Aldrich), sodium chloride (NaCl) (99.9%, ABCR), sodium carbonate (Na_2CO_3) (99%, Sigma-Aldrich), sodium sulfate (Na_2SO_4) (99%, Sigma-Aldrich), 4-Cyano-4-(phenylcarbonothioylthio)pentanoic acid (CPADB, Sigma-Aldrich), and 6-aminohexanol (95%, TCI Deutschland GmbH) were used as received. *N*,*N*-dimethylformamid (DMF) (99.8%, anhydrous, Sigma-Aldrich), dichloromethane (DCM) (99.8%, anhydrous, Sigma-Aldrich) and chloroform (99.8%, anhydrous, Sigma-Aldrich) were used directly. Other solvents like petroleum ether and ethyl acetate were purchased from ABCR and used without any treatment. 2,2′-Azobisisobutyronitrile

(AIBN, 98%, Sigma-Aldrich) was purified by recrystallization from ethanol.

3.5.2. Instruments

^{1}H NMR and ^{13}C NMR spectroscopy of the products were obtained with a Bruker 200 MHz nuclear magnetic resonance equipment using chloroform-d ($CDCl_3$) and dimethyl sulfoxide-d6 (DMSO-$_{d6}$) as solvents. Mass spectra were carried out on an Agilent LC/MSD SL. The number-average molecular weight (Mn) and polydispersity index (Mw/Mn, PDI) of polymers were measured by a Agilent HPC 1100 gel permeation chromatography (GPC) system using a PSS-GRAM pre-column with a series of PMMA as standard samples. Ultraviolet-visible (UV-vis) spectroscopy were obtained from a Varian Cary 4000 UV-visible spectrophotometer. ESEM images were captured on a FEI ESEM Quanta 400 FEG. Attenuated total reflection-Fourier transform infrared (ATR-FTIR) spectroscopy were recorded with a Bruker VERTEX 70v FTIR spectrometer. Fluorescent spectroscopy were conducted with a Hitachi F-7000 fluorescence spectrophotometer. Infrared camera (InfraTec GmbH, Germany) with VarioCAM HD head was used for recording the temperatures during the polymerization. Surface profile and 3D profile of the specimens were carried out on a SURFCOM 1500SD3. Optical microscope images were acquired from a Nikon ECLIPSE LV100ND. Zeta potential of linear polymers was obtained with a Malvern Zetasizer Nano ZSP. Fluorescent images were recorded on a LSM 880 confocal, and ImageJ software was used to analyses the data. Water contact angles of materials were collected by a OCA 20 instrument. Side view of self-growing microstructures on material surfaces was recorded in the OCA 20 machine. Column chromatography was performed using silica gel (215-400 mesh). UV 365 nm and blue 460 nm collimated LED light (Olympus BX & 1X, 1700 mA) was provided by THORLABS, of which intensity was set as 10 mW/cm^2 during the experiments. Blue light LED strip lamp

(460 nm) with an intensity of 0.6 mW/cm^2 was obtained from amazon online and used to initiate the polymerizations. Elastic moduli of seed samples were measured on a universal testing machine (ZWICK 1446, Germany) with a load cell of 200 N and crosshead velocity of 10 mm/min and values were calculated in the linear elastic region of the stress-strain curves from 1 to 5%. Every measurement was conducted three times. The elastic moduli of seed-0% and seed-20% samples were measured by compression test with a load cell of 2 KN and velocity of 2 mm/min. The values were calculated in the linear elastic region of the stress-strain curves from 0.1 to 0.5%. The elastic moduli of the growing structures were obtained by indentation experiments. The ASMEC indenter type is Berkovich equipped with a diamond tip. Samples were struck on the PEEK model before measurements. Indentations were carried out in the load-controlled mode, with an initial quadratic up to 20 mN within 10 s, a creep period of 5 s, and a quadratic decrease of the force to 0.08 mN within 5 s. The results were collected by eight different areas for each sample and analyzed according to the Fast hardness and modulus measurements (ISO 14557). The fit range of the unloading curve is from 98 to 40%.

3.5.3. Synthesis

3.5.3.1. *o*-Nitrobenzyl acrylate (NBA)

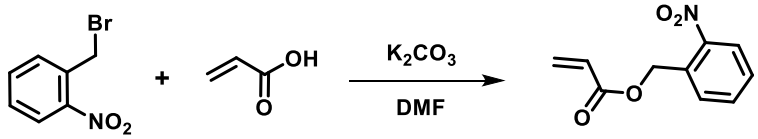

Scheme 1. Synthetic route for *o*-nitrobutyl acrylate (promoters)

It was synthesized according to a reported procedure.[172] To a mixture of 2-nitrobenzyl bromide (5.4 g, 25 mmol) and potassium carbonate (6.9 g, 50 mmol) in DMF (60 mL), acrylic acid (8.575 mL, 125 mmol) was added dropwise. The mixture was stirred at

room temperature overnight. 40 mL water was added to dissolve the insoluble salts, and the mixture was extracted with 100 mL ethyl acetate. The organic layer was washed with brine and dried over anhydrous Na_2SO_4. After column chromatographic separation (silica gel, dichloromethane), a yellow liquid product was obtained (yield: 82%).

^{1}H NMR (200 MHz, $CDCl_3$) δ: 7.96-8.03 (d, 1H), 7.50-7.60 (t, 2H), 7.35-7.45 (d, 1H), 6.35-6.48 (d, 1H), 6.10-6.25 (t, 1H), 5.80-5.90 (d, 1H), 5.55 (s, 2H) ppm. ^{13}C NMR (200 MHz, $CDCl_3$) δ: 165.4, 147.5, 133.7, 132.1, 131.9, 128.9, 127.7, 125.0, 62.9 ppm. LC MS (m/z): Calcd for $[M+NH_4]^+$: 255.0, Found: 255.0.

3.5.3.2. Linear poly(HBA-*co*-NBA)

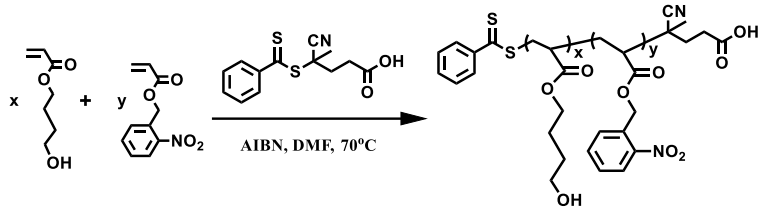

Scheme 2. Synthesis of the poly(HBA-*co*-NBA) *via* RAFT polymerization.

Poly(HBA-*co*-NBA) was synthesized by reversible addition-fragmentation chain-transfer (RAFT) polymerization. Briefly, the mixture of 397.6 mg of HBA, 134.6 mg of NBA, 0.964 mg CPADB, and 2.83 mg AIBN in 2 mL of anhydrous dimethylformamide (DMF) was purged with Argon for 30 min. The initial molar ratio of HBA, NBA, CPADB and AIBN was 160: 40: 1: 0.2. Then the mixture was sealed and heated up to 70 °C for 24 h for polymerization. The polymers were obtained by precipitating the solutions in cold diethyl ether, then dissolved in 1 mL DMF and precipitating in cold diethyl ether (three cycles), followed by drying in a vacuum.

3.5.3.3. 4-Hydroxybutyl acetate (HB acetate)

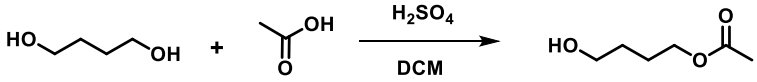

Scheme 3. Synthetic scheme for 4-hydroxybutyl acetate (HB acetate)

It was synthesized *via* a protocol previously reported.[173] An oven-dried round bottom flask was charged with a magnetic stir bar. To this flask, 1,4-butanediol (8.8 mL, 98 mmol), acetate acid (5.6 mL, 98 mmol) and DCM (60 mL) were added. Then 2 drops of H_2SO_4 was added into the above solution. The mixture was stirred for 18 h and then water was added. After that, the mixture was extracted with DCM and the organic layer was washed with a saturated solution of Na_2CO_3 and brine, dried over Na_2SO_4. After column chromatographic separation (silica gel, dichloromethane: ethyl acetate=10: 1, *v*: *v*), the final product was given as a colorless oil (yield: 56%).

^{1}H NMR (200 MHz, $CDCl_3$) δ: 4.10-4.20 (t, 2H), 3.63-3.72 (t, 2H), 2.05 (s, 3H), 1.50-1.74 (m, 4H) ppm. ^{13}C NMR (200 MHz, $CDCl_3$) δ: 171.3, 64.3, 62.1, 29.0, 25.0, 20.9 ppm. LC MS (m/z): Calcd for $[M+NH_4]^+$: 150.0, Found: 150.1.

3.5.3.4. Bis-*N*, *N*'-6-hydroxyhexanol perylenetetracarboxylic diimide-acrylate (PDIDA)

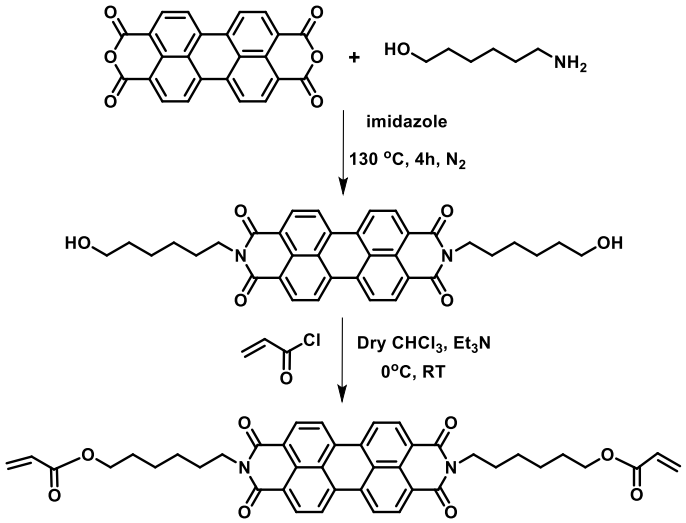

Scheme 4. Synthetic process of PDIDA.

Bis-*N*, *N*'-6-hydroxyhexanol perylenetetracarboxylic diimide-acrylate (PDIDA) was synthesized *via* a previously reported method.[174] Briefly, 3,4,9,10-perylenetetracarboxylic dianhydride (0.5 g, 1.295 mmol), 6-aminohexanol (0.47 g, 4.014 mmol) and imidazole (3 g) were placed in a round bottom flask and heated at 130 ºC for 4 h under N_2 atmosphere. The reaction mixture was diluted with ethanol and the resulting dark red solution was filtered to remove the undissolved substance. The filtrate was acidified with 2 M HCl aqueous solution to generate red precipitate. The precipitate (bis-*N*, *N*'-6-hydroxyhexanol perylenetetracarboxylic diimide, OHPDI) was collected by vacuum filtration, washed with water until the filtrate was neutral and dried at 75 ºC overnight in a vacuum oven (yield: 61%).

^{1}H NMR (200 MHz, $CDCl_3$) δ: 8.35-8.65 (d, 8H), 3.75-4.46 (m, 8H), 1.50-1.90 (m, 16H) ppm. ^{13}C NMR (200 MHz, $CDCl_3$) δ: 165.2, 135.5, 132.9, 129.1, 126.1, 124.1, 68.8, 40.4, 30.8, 27.7, 26.2, 25.0 ppm. LC MS (m/z): Calcd for $[M+NH_4]^+$: 608.1, Found: 608.2.

OHPDI (60.8 mg, 0.1 mmol), triethylamine (72 μL, 0.5 mmol) and dry $CHCl_3$ (20 mL) were added in a round bottom flask under N_2 atmosphere. Acrylyl chloride (52 μL, 0. 5 mmol) was dissolved in 10 mL $CHCl_3$ and added dropwise into the above solution. After stirred at room temperature for 24 h, the mixture was washed with water and brine. After column chromatographic separation (silica gel, dichloromethane: methanol=20: 1, *v*:*v*), the product (PDIDA) was obtained as a red solid (yield: 30%).

^{1}H NMR (200 MHz, $CDCl_3$) δ: 8.35-8.68 (d, 8H), 6.36-6.48 (d, 1H), 6.07-6.15 (t, 1H), 5.71-5.85 (d, 1H), 3.83-4.40 (m, 8H), 1.49-1.90 (m, 16H) ppm. ^{13}C NMR (200 MHz, $CDCl_3$) 165.3, 159.1, 134.1, 131.3, 130.2, 129.5, 127.5, 125.8, 123.9, 63.5, 44.7, 31.2, 30.9, 28.6, 25.3 ppm. LC MS (m/z): Calcd for $[M+NH_4]$+: 716.2, Found: 716.1.

3.5.4. Fabrication of seeds

Taking seed-20% as an example: to a mixture of HBA (80 mol%) and NBA (20 mol%) were added HDDA (crosslinker, 1 wt%) and I-819 (photoinitiator, 1 wt%) to obtain the precursor. The precursor solution was coated on Teflon substrates and cured under blue light (intensity: 0.6 mW/cm^2) for 20 min. The obtained substrate was immersed in ethanol, and the solution was changed every 8 h (3 times) to remove unreacted specimens. Then, it was dried to afford seed-20%.

3.5.5. Light-induced growth

Seed-20% was immersed in a nutrient solution containing HBA (96 wt%), HDDA

(1 wt%), I-819 (1 wt%) and BZSA (2 wt%) for 12 h to obtain swollen samples. For growth, the swollen samples were subjected to UV light (intensity: 10 mW/cm^2) with a suitable photomask.

3.5.6. Polymerization kinetic of HBA/NBA/HDDA/I-819 under lights

The precursor solution used for preparing seed-20% was mixed and purged with Argon for 20 min. 50 μL of the mixture (weighted as M_0) was taken for each polymerization with different exposure times (10 s, 30 s, 1 min, 2 min, 5 min, 10 min, 20 min, 30 min, 40 min, 50 min) under 460 nm or 365 nm light irradiation (intensity: 10 mW/cm^2). After polymerization, the unreacted components were removed by ethanol rinsing (3 times), followed by drying to obtain the crosslinked polymers (weighted as M_t). The polymerization conversion was defined as M_t/M_0. The polymerization reaches its plateau in 2 min under UV or blue light irradiation.

3.5.7. Calculation of mass transport rate

A fresh seed-20% sample with a thickness of 500 μm was immersed into 4-hydroxylbutyl acetate and its weight was recorded at different times.

The diffusion rate can be determined using the following supplementary equation (1):[175-176]

$$F = \frac{M_t - M_0}{M_0} = Kt^n \qquad (1)$$

where *F* is the rate of diffusion per area; *K* is a swelling constant, *t* is the time (s), *n* is a swelling exponent; M_t and M_0 are the weight of the swollen and dry sample at time *t*, respectively. From supplementary equation (2), it is known that

$$ln\, F = \ln K + n \ln t \qquad (2)$$

ln *F* versus ln *t* was plotted by using the kinetic of swelling yields straight lines up to almost 60% increase in the mass of the swollen sample.[177-178] The swelling exponents *n* and the swelling constant *K* were calculated from the slopes and intercept of the

lines. The intercept *K* value was used for determination of the diffusion coefficient *D*:

$$K = 4\sqrt[2]{D/\pi r^2} \qquad (3)$$

where *D* is the diffusion coefficient (cm^2/s), *r* is the radius of the cylindrical seed-20% sample (cm).

3.5.8. Restoration of large damage

An unregular damaged region was created on HBA-based seed-20% by adding a piece of unregular glass slide in the seed solution before photopolymerization. The obtained seed-20% with the damaged region was immersed in a nutrient solution containing HBA, HDDA, I-819, and BZSA to afford swollen seed-20%. A photomask with a diameter of 3.6 mm was put above the material surface, and 365 nm UV light was used to trigger the growth to self-restore the materials. The pictures were recorded by a camera. The 3D profiles and surface profile were collected by a profilometer.

Chapter 4

4. Evaporation-induced entropy replenishment for preparation of self-growable polycatenane networks with interlocked topology

Currently, only several growing materials, including the systems discussed in previous Chapters, have been developed, and they display significantly different properties from each other. Developing new growing material systems can not only enrich this field but also provide more examples for studying their unique properties and capabilities. Note that the growing materials currently available are all made from crosslinked linear polymers. In this Chapter, the attempt of exploiting a new growing material system made from different network topology, i.e. polycatenanes, was described. The interlocked structure of polycatenanes is entropy-unfavorable and currently, no reliable method has been proposed to synthesize high-molecular-weight polycatenanes to get a fully interlocked material. To address this issue, an evaporation-induced entropy replenishment strategy was developed to fabricate polycatenane-based networks. The strategy was demonstrated in a class of poly(disulfide)s made from DL-thiotic hydroxyethyl. In the presence of a liquid base, the DL-thiotic hydroxyethyl monomer would undergo polymerization to form both linear and cyclic polymers/oligomers. Solvent evaporation compensates the entropy loss todrive the cyclization, leading to the formation of high-molecular-weight polycatenanes. The obtained interlocked poly(disulfide)s based polycatenane networks not only display dynamic functions under stimuli, but also show excellent growth ability with self-strengthening properties through entropy replenishment

strategy.

4.1. Introduction

Polymer network topology defines how the polymer chain segments (strands) and connecting points (junctions) are connected, including branch functionality, cyclic defects, entanglements, and density fluctuations. It plays a critical role in dictating material properties, ranging from elasticity, the gel point, network dynamics to the degree of defect tolerance.[179-183] In principle, two possible strategies can be used to control polymer network topology: programming topological information directly into network precursors, or biasing the polymerization kinetics. Many efforts have been devoted to controlling topological features in polymer networks, including polymer network branch functionality, chain topology, and loops.[184-187] Introducing polymer chain topology such as cyclic polymers, polyrotaxanes, and polycatenanes into functional soft materials not only features them novel topologically macromolecular architectures comparing with crosslinked linear analogues, but also endows them with unique rheological, mechanical, and dynamic properties.[188-191] For instance, cyclic gels exhibit greater swelling ability and maximum strain at break, while slide-ring gel (a subset of polyrotaxanes) shows anti-scratch and healing characteristics because of the sliding of the ring along a thread or rotation of rings.[192-193]

Polycatenanes, composed entirely of mechanically interlocked rings, have attracted increasing attention and been shown to participate in a wide range of applications in molecular switches and machines, as careers for drug delivery and molecular electronic devices.[190, 194-195] Polycatenanes are linked solely by “topological bonds” (regarded as a “soft but strong bond” in comparison with covalent bonds) and allow full rotational mobility of every ring (with sufficient ring size) and exhibit more

conformational flexibility. Recently, Endo and co-workers reported a plausible polycatenane network made from the bulk polymerization of 1,2-dithiane. This elastomer formed by the entanglement of polycatenanes swells at first, but finally dissolve in its good solvent, indicating an unstable character of the chain.[196-198] The molecular mechanism behind this property is that these reported polycatenane networks don't possess fully interlocked structures to crosslink the polymers within the dynamic network. Moreover, dynamic rings potentially play multiple roles from reinitiating polymerization (latent initiating sites) to incorporating polymer chains (bonding and debonding of rings) in a single system. Considering this in mind, the attempt of exploiting new growing material systems made from interlocked topology not only provides novel growth strategy for materials' growth, but also enriches the diversity of dynamic soft materials.

In addition, an interlocked ring architecture is unfavorable from an energy point of view, which makes difficult to synthesize polymeric topologies with high molar mass.[199-200] Previous studies only reported limited linear polycatenane with 7-26 consecutively interlocking rings or cyclic polycatenanes with 4-7 interlocking rings.[199] This fact limits the formation of fully interlocked material, as well as the mechanical performance of polycatenane based bulk materials. Up to now, a stable polycatenane network with interlocked topology has not been achieved, and its potential capability in growing material still needs exploration.

In this chapter, a solvent evaporation-based approach to synthesize interlocked poly(disulfide)s-based polycatenanes with elastomeric properties is described. In my design, the DL-thioctic hydroxyethyl monomer undergoes base-catalyzed ring-opening polymerization in weak base solution (e.g., DMF) to form a viscous mixture consisting of cyclic and linear polymers/oligomers under a sealed condition. The system is in an equilibration state of free rings and interlocking rings due to reversible

S-S exchange. In this state, the evaporation of solvent from the mixture compensates for the entropy loss of the closure of linear polymers to interlock cyclic polymers/oligomers together and finally form bulk elastomers. The obtained fully interlocked poly(disulfide)s-based elastomer shows dynamic features under stimuli. This evaporation-induced entropy replenishment method is applied to develop self-growing and self-strengthening polycatenane based materials.

4.2. Results

4.2.1. Fabrication of soft elastomer crosslinked by polycatenanes

When macrocycles undergo ring-opening polymerization, it is nearly impossible for the propagating chains to close to form ring structures, since ring-closure is entropy-unfavorable. Thus, it is necessary to replenish the entropy loss for the synthesis of polycatenanes with high molecular weight. One plausible strategy to compensate the entropy loss of ring closure could be the entropy contribution from solvent evaporation. Such an evaporation-induced entropy replenishment strategy could lead to the formation of interlocked network structures. Figure 1a shows the proposed gelling process. Under a base condition, monomer molecules undergo ring-opening polymerization and the system reaches equilibrium in which cyclic polymer/oligomer, linear polymer/oligomer and monomers coexist. Allowing the solvent molecules to evaporate could offer adequate entropic energy to drive the system towards the formation of interlocking structures.

DL-Thioctic hydroxyethyl (THE) was used as a model to investigate the formation of polycatenane networks with interlocked structure due to its easy synthesis procedure and high yielding. Note that other thioctic derivatives such as DL-thioctic ethylene

glycol and propane dithioctic can also form this structure. THE was mixed with a weak base (i.e., DMF, 30 %, molar fraction) and sealed in an Argon atmosphere to prepare the viscous precursor. During the mixing period, DMF is expected to catalyze and trigger the ring-opening polymerization of disulfide group. This was confirmed by the formation of viscous liquid. MALDI-TOF and GPC analysis confirmed the presence of monomer, linear polymer/oligomer, and cyclic polymers/oligomers (Figure 1b).

When the system equilibrates, the mixture of linear and cyclic oligomers is expected to form interlocked structures. The ratio of the formation of interlocked structures in the mixture as the function of the evaporation of DMF was then investigated. With DMF evaporation, the viscosity of this mixture increases, as followed by gelation and finally the formation of an elastomer. For a certain evaporation degree of DMF, the unlinked components were washed away by THF to evaluate the interlocking structure formation efficiency. When DMF evaporated 48%, only 3% interlocked structures formed. However, after DMF removed completely, interlocked structures reached nearly 100% (Figure 2). This may due to that (1) at the initial stage, a portion of formed cyclic polymers/oligomers may undergo debonding under base surroundings, leading to lower interlocking efficiency in this period; (2) after complete evaporation of DMF, no external stimuli exist within interlocked elastomer to destruct its structure.

The increased entropy during DMF evaporation at room temperature can be calculated as $\Delta S_{vap} = \Delta H_{vap}/T_{vap}$, where ΔS_{vap} is the entropy of vaporization of DMF, ΔH_{vap} is the enthalpy of vaporization of DMF (47.6 KJ/mol), and T_{vap} is the boiling point of DMF (426.16 K).[201] Accordingly, the entropy of vaporization of DMF is about 111.7 J/mol·K.

Macrocyclic alkanes are essentially strainless if the ring is made from >14 atoms, and thus the enthalpy in my system can be considered negligible.[202-203] The activation entropy of ring closure reactions is in the range of -3.7~-4.9 e.u., i.e. cyclization

involves an entropy loss. In the following I take -4.5 e.u. as a representative value for entropy loss during ring closure.[204-206] Although the conformational entropy of polymers/oligomers decreases in the interlocking process, the evaporation of DMF molecules is an entropy-increasing process and the sum of the whole system entropy is still positive. As a result, fully interlocked structures can form. In detail, when 4 mmol DMF is evaporated at room temperature, the increased energy would be 190.4 J. The energy loss for the formation of cyclic polymers/oligomers (9.3 mmol) would be 74.5 J. Thus, the lost entropy of inter/intramolecular cyclization can be compensated by the vaporization.

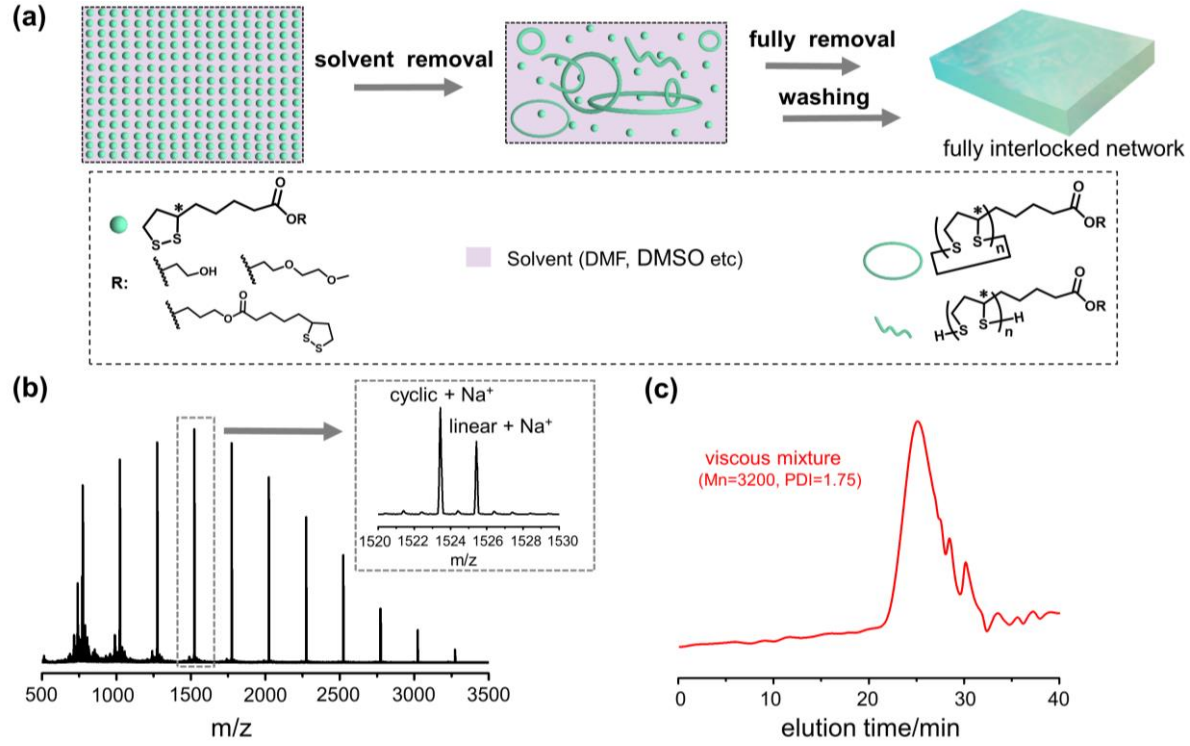

Figure 1. Formation of fully interlocked material. (a) Schematic image of fabrication of fully interlocked elastomer. (b) MALDI-TOF spectrum of sealed viscous precursor. (c) GPC spectroscopy of sealed viscous precursor. The concentration of polymers used in (b) and (c) is 2 mg/mL in THF.

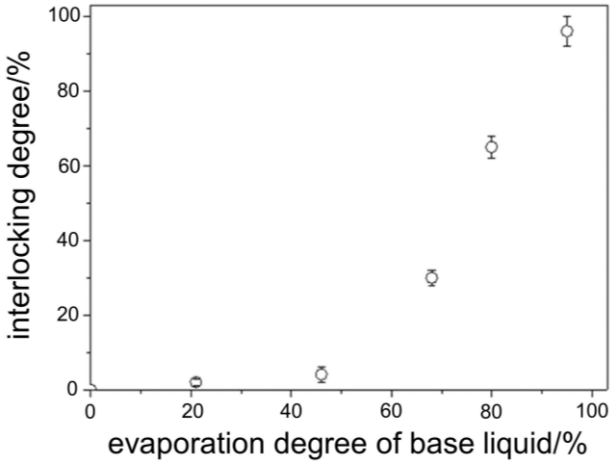

Figure 2. The relationship between interlocking structure formation efficiency and volatile degree of DMF.

To probe the evaporation-induced entropy replenishment mechanism for the formation of fully interlocked network structures, I several control experiments were designed. I first replace DMF by THF and prepared a mixture of THE molecule and THF solvent. After the evaporation of THF, I did not detect any polymer/oligomer or elastomer from the precursors, which indicates that solvent evaporation alone could not trigger the formation of interlocked structures of THE monomers. Then I tested if the formation of interlocked structures required both solvent evaporation and base atmosphere, I added a base catalyst, 1,8-diazabicyclo[5.4.0]undec-7-ene (DBU), into the mixture of THE/THF. An interlocked elastomer was generated after the evaporation of THF. Note that DBU only catalyzes the polymerization, but did not evaporate in my experiment conditions. These results proved that the evaporation-induced entropy replenishment approach could be used to obtain interlocked elastomer from THE based mixtures when the catalyst was incorporated.

I hypothesize that the entropy replenishment approach is a generic methodology to prepare interlocked materials. To prove this hypothesis, interlocked PDMS was prepared through this strategy.

4.2.2. Characterization of fully interlocked polycatenanes structures

Different methods are utilized to prove the formation of fully interlocked polycatenane structures. Firstly, I used a swelling method to prove the crosslinked network structure. Figure 3a demonstrates the swelling kinetics of the interlocked elastomer. At the beginning of three hours, the weight of the gel material increased as a consequence of solvent uptake. Some small cyclic oligomer or monomers which cannot be incorporated into the interlocked gel diffuse out to the solution, therefore a slight drop in weight was observed before swelling equilibrium is achieved. The swelling ratio reaches 8.1 after 8h swelling in tetrahydrofuran (THF). Several previous studies have claimed the formation of polycatenane network structures but the structures are dissolved by the solvents used for soaking.196-198 It indicates that they do not have fully interlocked structures. Other crosslinkers are required to connect the polycatenane clusters for the formation of 3D network structures. Here, for the first time, I have prepared the stable and indissoluble fully interlocked materials without introducing external linkages.

I then analyzed the unlocked residual molecules collected from the elastomer for a better understanding of the interlocking process. The remaining solvent after swelling was collected and removed and analyzed by liquid chromatography–mass spectrometry (LC-MS). A mixture of monomer, dimer, trimer, tetramer and pentamer could be found in the residue (Figure 3b), which means that during the formation of interlocking structure, some monomers and small cyclic oligomers are not incorporated into the elastomers. These cyclic oligomers also indicated that polycatenane structure formed in the networks.

Finally, I synthesized a cyclic dye and used it to demonstrate the formation of the 3D interlocked network structures. Since this cyclic fluorescent molecule could not react

with any composition in the solution, the integration of the dye would indicate the crosslinking mechanism of interlocking. The cyclic dye was added into the curing solution and the obtained samples were washed by THF to remove any unclocked composition. As expected, the washed elastomer shows strong fluorescence. Figure 3c shows the fluorescent interlocking elastomer. From the 3D confocal fluorescence image, it can be found that the dye molecules were homogeneously integrated in the sample. Meanwhile, it also possesses strong fluorescence emission under UV light illumination comparing with that under visible light (Figure 3d), implying that the integrated fluorescent molecule still possesses its emission activity under excitation. These results adequately certify the interlocked structures of the poly(disulfide)s elastomers.

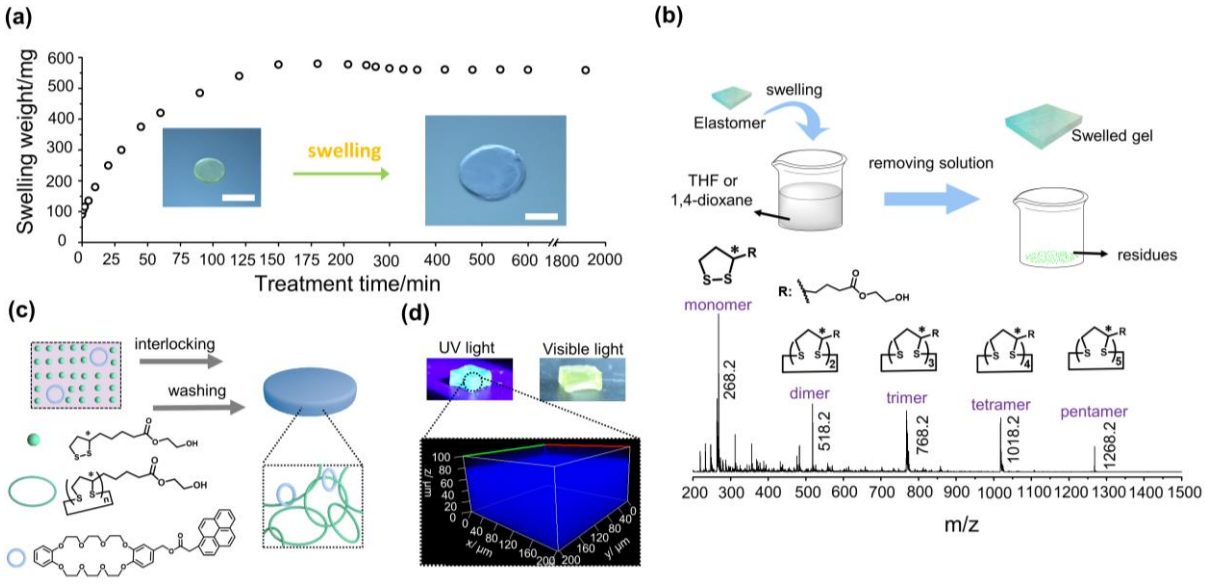

Figure 3. Certification of interlocking structures. (a) Swelling weight *vs* incubation time. The as-prepared elastomer was immersed in THF solution to swell. The insert images are the photographs of this elastomer before and after totally swelling. (b) LC-MS analysis of the residual molecules of the solution in (a). The cartoon images show this process. (c) Fluorescent labelling of interlocking structure by confocal microscopy. The cartoon picture shows this tracing program. (d) Visualized emission of fluorescent network under UV light, while no emission with visible light. Dashed box

involves the fluorescent 3D image of this network.

4.2.3. Stimuli-responsiveness of fully interlocked poly(disulfide)s

Disulfide group is unstable under base environment, and can be cleaved under base stimuli.[207-208] In fact, the fully interlocked poly(disulfide)s network could be dissolved by base solution treatment, e.g., soaking in DMF, DMSO and N-Methyl-2-pyrrolidon (NMP) for 7 days (Figure 4a, insert images). I used ^{1}H NMR spectroscopy to trace the chemical reactions during the solvent evaporation and base treatment processes. DMSO-$_{d6}$ was chosen as both deuterated reagents and base catalyst. I mixed THE monomer and DMSO-$_{d6}$. The partial evaporation of DMSO-$_{d6}$ can trigger the formation of interlocked poly(disulfide)s (gel state), while the re-adding of DMSO-$_{d6}$ induce depolymerization of poly(disulfide)s to the sol state. As shown in Figure 4a (red line), THE monomers could be easily detected from ^{1}H NMR spectrum before the evaporation, which was demonstrated by the signals at 3.12 (-S-C$\underline{H}_2$-) and 3.55 (-S-C$\underline{H}$-) ppm. Note that there is still some small peak [2.70 (-N-C$\underline{H}_3$), 2.85 (-N-C$\underline{H}_3$) and 8.12 (-C$\underline{H}$O) ppm) assigned to DMF solvent because it is nearly impossible to remove DMF totally during the synthesis of THE. During the soaking and evaporation of DMSO-$_{d6}$, polymer/oligomers generated (Figure 4a, green line) and the gel formed (Figure 4a). New peaks around 2.80 (-S-C$\underline{H}_2$- and -S-C$\underline{H}$-) ppm belonged to their polymer/oligomer state appear, while peaks at 3.12 (-S-C$\underline{H}_2$-) and 3.55 (-S-C$\underline{H}$-) ppm decrease. Re-adding DMSO-$_{d6}$ to the gel lead to dissolution to generate the monomer again (Figure 4a, blue line). In this process, signals assigned to polymer/oligomer [2.80 (-S-C$\underline{H}_2$- and -S-C$\underline{H}$-) ppm] disappeared and signals at 3.12 (-S-C$\underline{H}_2$-) and 3.55 (-S-C$\underline{H}$-) ppm return to their monomer state. DMSO-$_{d6}$ is the solvent and also the catalyst for ring-opening polymerization/depolymerization.

The disulfide group is widely used to construct photo-responsive and self-healing materials.[24-25] Since the fully interlocked elastomer contains numerous disulfide groups in the main chain, I then study its photoresponsiveness under UV 365 nm light irradiation by rheology. Without UV irradiation, the as-prepared elastomer showed stable storage modulus (12 KPa) and loss modulus (2.6 KPa). When exposed to UV light, the elasticity (G') decreased and the plasticity (G'') increased. The G'' can even overpass G' and the solid material became liquids (Figure 4b). With UV illumination, poly(disulfide)s debond to break the interlocked structures. As interlocked structures are energy-unfavorable, this reaction would lead to the formation of free cyclic polymers/oligomers. After this elastomer became liquid, without external treatment, it could not turn to an elastomer. The light-induced transition from elastomer to liquid is irreversible since the unlocked state is energy-favorable.

The fully interlocked elastomer shows a glass transition at 101.6 ^{o}C. When annealed at 110 ^{o}C, the elastomer softens and turns into viscous liquid in 15 min, which allowed for molding the material into different shapes. As shown in Figure 4c, I can easily break the shaped elastomer into pieces by manpower, then remold them into quadrate shape upon heating and cooling. This process is highly reversible and effective. Circular and pentagonal shaped materials are fabricated by simply heating/cooling circle to demonstrate this property. Figure 4d shows the elastic modulus of reprocessed elastomers. The Young's modulus of the reshaped elastomers slightly increased after the heating/cooling circle (Figure 4d), which may due to the recombination and further polymerization upon heating. Therefore, poly(disulfide)s-based interlocked elastomer shows multiple dynamic functions under stimuli, from base sensitive, light responsiveness, to temperature dependence.

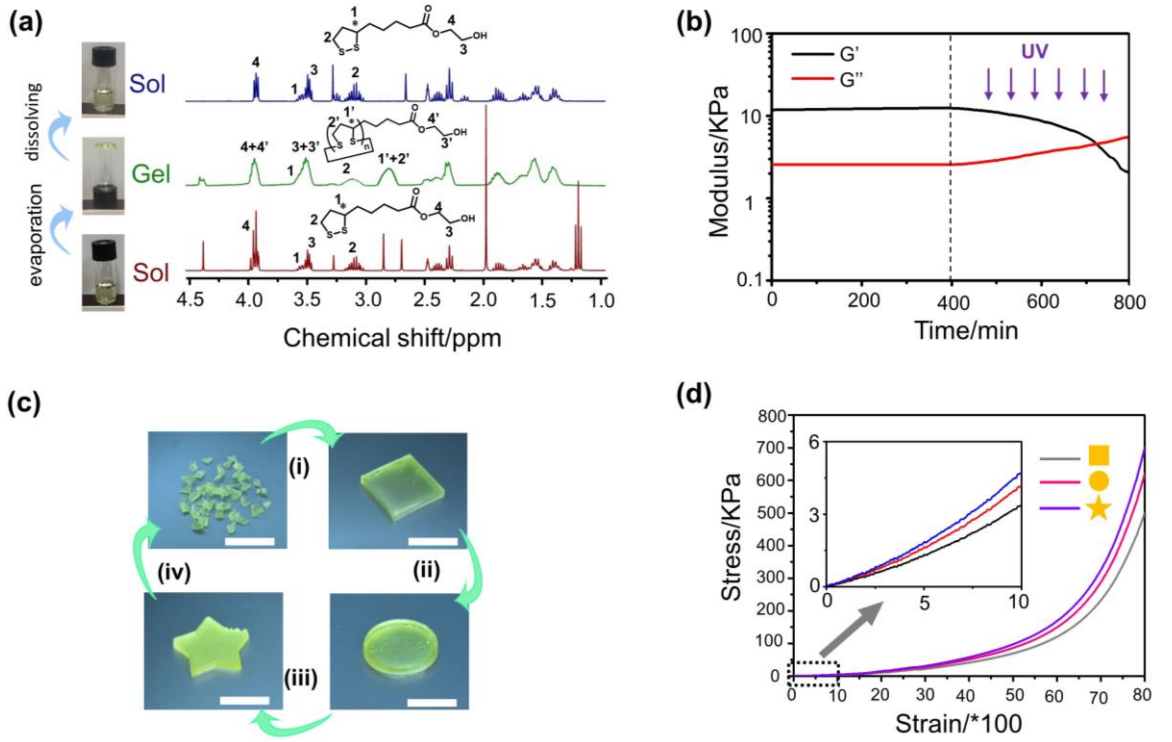

Figure 4. Dynamic functions of interlocking poly(disulfides). (a) Base-responsive opening/closing behavior between THE monomers and polymers/oligomers. After removing portion of DMSO-$_{d6}$, polymers/oligomers formed. When adding DMSO-$_{d6}$ again, polymers/oligomers transfer to monomers. (b) UV responsive of poly(disulfides) based interlocking elastomer. During irradiation, interlocked structure was destructed. (c) Reprocessable treating into different shaped elastomers by heating. This fully dynamic interlocked elastomer was cut into pieces and heated in the mold to achieve different morphology. (d) Elastic modulus of the different shaped elastomers in (c).

4.2.4. Self-growth and self-strengthening of interlocked elastomer through evaporation-induced entropy replenishment

THE based poly(disulfide)s elastomer shows fast and well swelling ability in its monomer solution, and the evaporation-induced entropy replenishment approach can trigger the formation of interlocked elastomers. These features make this kind of interlocked elastomers appropriate for investigating self-growth behavior. Although

THE based interlocked elastomer is unstable and can be dissolved in the solvents with weak basic character upon long-term swelling (over 7 days), short-time soaking (i.e., 12 h) in THE/DMF mixture (70/30, mol/mol) could not break its interlocking structures. Figure 5a demonstrates a potential self-growing mechanism of interlocked poly(disulfide)s. At first, the obtained original interlocked elastomer (denoted as original seed sample) can swell the nutrient solution consisting of THE/DMF (70/30, mol/mol) and its weight increases up to 8 times of its original weight in 12 h. It was noted that 9% of interlocked structures were lost in this process based on the evaluation by weighting the sample after removing all the diffused-in liquids because of partial debonding of poly(disulfide)s in a base environment. Thus, some interlocked poly(disulfide)s released from the bulk elastomer during the short time mixing process of the original seed sample in THE/DMF solution. When the DMF entrapped in the gel was allowed to evaporate under Argon atmosphere, the polymerization equilibration was driven toward the formation of new interlocked poly(disulfide)s ring. During the evaporation of DMF, the newly formed cyclic polymers/oligomers were incorporated into the original ones to generate fully interlocked polycatenane structures. After removing the unlocked ring poly(disulfide)s, fully interlocked grown elastomers were obtained (denoted as grown samples). This swelling/evaporation process can be performed multiple times to achieve step-grown of the interlocked elastomers.

Cartoon images in Figure 5b show the growing abilities of fully interlocked elastomers. After the first swelling-evaporating cycle, the original seed sample grew into 1st grown sample, and the size of materials increased during this process (Figure 5b). It was also expected that the interlocked materials could become bigger and bigger after multiple growth cycle. Figure 5c shows the grown index and elastic modulus of the interlocked seed and grown elastomers. After three self-growing cycles, the 3rd grown elastomer is nearly 24 times larger than the seed. Interestingly, the grown elastomers

self-strengthen by this evaporation-induced entropy replenishment strategy. The Young's moduli increased twice after three growing cycles of interlocked elastomer, which was attributed to the increased interlocking ratio (Figure 5a and 5c). I can also substantially regulate this self-strengthened property by adding a crosslinker (propane dithioctic, PDT) bearing bifunctionalized disulfide group in the nutrient solution (Figure 5d). The interlocked seed samples were immersed in nutrient solution containing different PDT fractions (from 0.1 wt% to 10 wt%) for 12 h to get the swollen interlocked seeds, then which were put under Argon atmosphere for evaporation. The obtained grown interlocked elastomer became stiffer (Figure 5d). When the fraction of PDT was 10 wt%, the Young's moduli of the grown sample was over 12 times stiffer than the original seed. More importantly, as this robust swelling-evaporating approach, the interlocked seed can grow infinitely. In this work, I only show the properties of the samples after three growing cycles. The grown interlocked elastomer became thicker, larger, and stiffer.

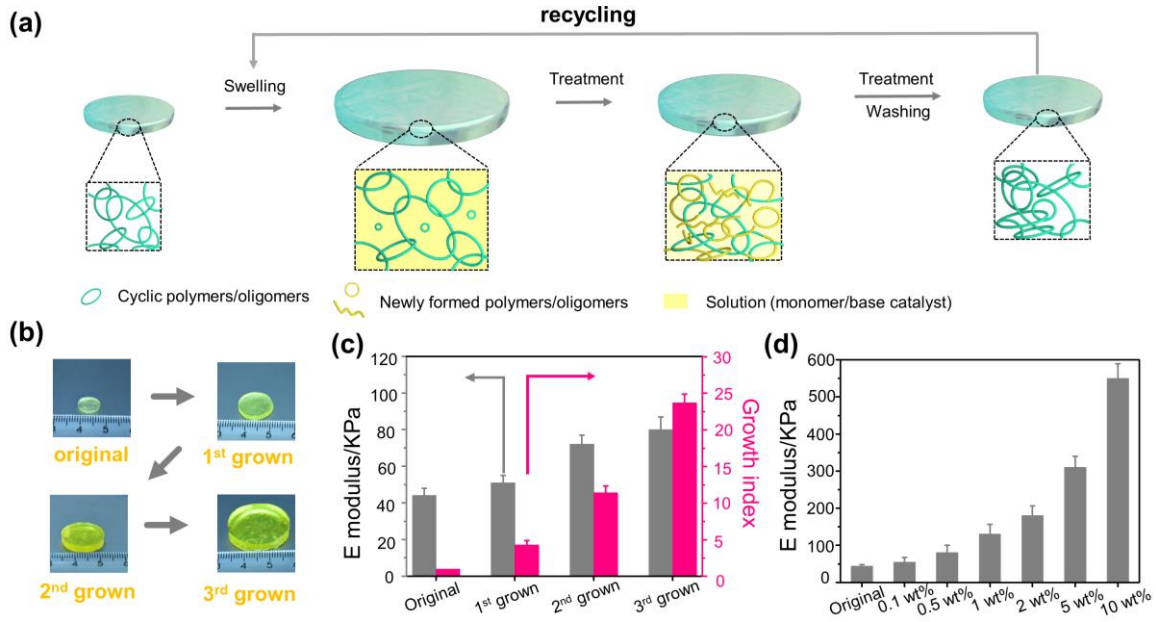

Figure 5. Self-growing and self-strengthening of interlocked poly(disulfide)s elastomers. (a) Potential mechanism of self-growing interlocked elastomers. The treatment here is evaporation. (b) Optical images of interlocked seed before and after multi-time growth. (c) Grown index and Young's moduli of

seed samples swelling in THE/DMF nutrients before and after multi-time growth. (d) Young's moduli of seed samples swelling in THE/PDT/DMF nutrients before and after growth.

4.3. Discussion

Polycatenanes are composed entirely of mechanically interlocked rings, which allow full rotational mobility of every ring (with sufficient ring size) and exhibit more conformational flexibility. Up to date, little attention has been focused on exploiting these molecular characteristics to create polycatenanes based materials. This is due to the following reasons: (1) it is challenging to prepare crosslinked 3D networks without chains ends, (2) it is difficult to prepare polycatenanes with high molecular weight, and (3) polycatenates possess energy-unfavorable conformations.

Endo and co-workers firstly reported the bulky materials consisting of polycatenane structures.[196-198] In their systems, they prepared a series of poly(disulfide)s based polycatenane materials by heating, which swelled in a good solvent like THF at first but dissolved finally. These kinds of materials are only crosslinked by entanglements of polycatenanes thus lacking stabilities and limiting their applications. Zhang and co-workers reported polymer network blends to "interlock" material functions. In this process, these two revisable covalent networks dissociated after heating, then which were mixed and cured under lower temperature for the re-formation of covalent bonds to generate "interlocked" topology.[209-210] In these examples, they had successfully fabricated polycatenane segments or "theoretically" interlocked networks, but none of them were crosslinked stably without introducing external crosslinking agent. Considering the energy-unfavorable property of polycatenane topology, I develop the evaporation-induced entropy replenishment approach to prepare fully interlocked poly(disulfide)s elastomers. This is the first example of stably polycatenanes material

with fully interlocked crosslinking structures, which shows well swelling ability in its good solvent and keeps stable both under inert atmosphere and in solutions (good solvents) for over half a year. The approach is simple and robust for fabricating interlocked elastomer both in air and Argon atmosphere, and it is a supplementary technology for the generation of self-growing materials. There are still some disadvantages for this system, such as toxic and low stability in base environments. In the future, it is possible to exploit other polymer systems based on the interlocking of polycatenanes with more stable property and biocompatibility.

4.4. Conclusion

In this chapter, I have introduced an evaporation-induced entropy replenishment approach to synthesize fully interlocked poly(disulfide)s based networks and gels for the first time. The material is crosslinked by the interlocking of energy-unfavorable polycatenanes. I have calculated the entropy increasing during the evaporation of the solvent molecules in the system, which provides extra entropy energy to compensate for entropy loss after cyclization for the generation of interlocked structures. MALDI-TOF and LC-MS spectra show the formation of cyclic structures while GPC results indicate the appearance of polymers/oligomers. Swelling capability in good solvents and the integration of dye molecules have proved the interlocked structures. Fully interlocked poly(disulfide)s based materials not only show responsiveness to different stimuli (base atmosphere, light, and temperature), but also possess self-growing and self-strengthening properties. With soaking the original interlocked seed in different nutrient solutions for self-growth, the samples can be 24 times heavier and 12 times stiffer. Expanding the scope of polymer network topologies to include fully interlocked architectures creates new opportunities at the intersection of chemistry, materials

science, and engineering.

4.5. Materials and methods

4.5.1. Chemicals and materials

DL-Thioctic acid (98%, Alfa aesar), 2-bromoethanol (95%, Sigma-Aldrich), diethylene glycol monomethyl ether (Sigma-Aldrich), 1,3-dibromopropane (98%, Alfa aesar), , catechol (99%, Sigma-Aldrich), 2-[2-(2-chloroethoxy)ethoxy]ethanol (96%, Sigma-Aldrich), potassium iodide (KI) (99%, Alfa Asear), 4-toluenesulfonyl chloride (Sigma-Aldrich), 3,4-dihydroxybenzaldehyde (97%, Sigma-Aldrich), sodium borohydride (NaBH4) (99%, Sigma-Aldrich), 1,3,5,7-tetramethyltetracyclosiloxane (Gelest), ferric chloride (Alfa aesar), 1-pyrenecarboxylic acid (97%, Sigma-Aldrich), oxalyl chloride (99%, Sigma-Aldrich), 1,8-Diazabicyclo[5.4.0]undec-7-ene (DBU) (99%, Sigma-Aldrich), trimethylamine (TEA) (99%, Sigma-Aldrich), cesium carbonate (Cs_2CO_3) (99%, Sigma-Aldrich), 4-(dimethylamino)pyridine (DMAP) (99%, Sigma-Aldrich), 1-(3-dimethylaminopropyl)-3-ethylcarbodiimide hydrochloride (EDC·HCl) (98%, TCI Deutschland GmbH), potassium carbonate (K_2CO_3) (99%, Alfa Aesar), 2-hydroxy-2-methylpropiophenonel (97%, Sigma-Aldrich), sodium chloride (99.9%, ABCR), sodium bicarbonate (NaHCO3) (99%, Sigma-Aldrich) and sodium sulfate (Na_2SO_4) (99%, Sigma-Aldrich) were used as received. *N*, *N*-dimethylformamid (DMF) (99.8%, anhydrous, Sigma-Aldrich) and dichloromethane (DCM) (99.8%, anhydrous, Sigma-Aldrich) were used directly. Solvents for column chromatography like petroleum ether, dichloromethane and ethyl acetate were purchased from ABCR and used without any treatment.

4.5.2. Instruments

^{1}H NMR and ^{13}C NMR spectra of the products were obtained with a Bruker 200 MHz nuclear magnetic resonance equipment using $CDCl_3$ and DMSO-$_{d6}$ as solvents. The number-average molecular weight (Mn) and polydispersity index (Mw/Mn, PDI) of polymers were measured by Agilent HPC 1100 Serie gel permeation chromatography (GPC) system using a PSS-GRAM pre-column with a series of polystyrene (PS) as standard samples. The concentration of polymers for GPC is 2 mg/mL in THF. Mass spectrum was carried out on an Agilent LC/MSD SL. Matrix-assisted laser desorption/ionization-time of flight (MALDI-TOF) mass spectrometry were performed on a 4800 MALDI-TOF Analyzer mass spectrometer in reflection mode with 2,5-dihydroxybenzoic acid (DHB) as matrix. Differential scanning calorimetry (DSC) analysis was conducted with DSC 1 STAR System (METTLER TOLEDO). Fluorescent images were recorded on a LSM 880 confocal. Column chromatography was performed using silica gel (215-400 mesh). UV 365 nm collimated LED light (Olympus BX & 1X, 1700 mA) was provided by THORLABS, of which intensity was set as 10 mW/cm^2 during the experiments.

Elastic modulus of fully interlocked poly(disulfide)s elastomers were carried out by a universal testing machine (ZWICK 1446, Germany) with a load cell of 200 N and crosshead velocity of 20 mm/min, which was calculated in the linear elastic region of the stress-strain curves from 2-5 %. Every measurements were conducted at least three times.

Metathesis of fully interlocked poly(disulfide)s elastomers was performed on a Gemini 200 Rheometer with a UV source (intensity: 10 mW/cm^2). The diameter of samples was fitted on an 8 mm plate (Malvern). The storage (G′) and loss (G″) modulus of samples was measured with frequency sweep of 1Hz and strain of 0.1% at 25 ℃.

4.5.3. Synthesis

4.5.3.1. DL-Thioctic hydroxyethyl (THE)

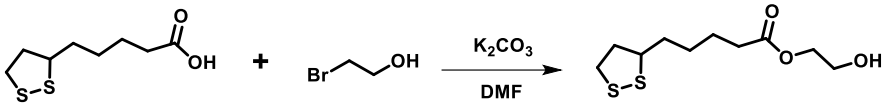

Scheme 1. Synthetic route for DL-thioctic hydroxyethyl.

It was synthesized according to a reported procedure.[172] To a mixture of DL-thiocric acid (2.06 g, 10 mmol) and potassium carbonate (2.74 g, 20 mmol) in DMF (20 mL), 2-bromoethanol (1.87 g, 15 mmol) was added dropwise. The mixture was stirred at room temperature in dark overnight. Afterwards, 20 mL water was added to dissolve the insoluble salts, and the mixture was extracted with 40 mL dichloromethane. The organic layer was washed with saturated sodium chloride, 1 M hydrochloric acid, and saturated sodium bicarbonate, then dried over anhydrous Na_2SO_4. After concentrated with rotary vapor and column chromatographic separation (silica gel, dichloromethane), a yellow liquid product was obtained (yield: 80%).

^{1}H NMR (200 MHz, $CDCl_3$) δ: 4.09-4.18 (t, 2H), 3.70-3.79 (t, 2H), 3.43-3.56 (m, 1H), 2.99-3.17 (t, 2H), 2.34-2.46 (m, 1H), 2.25-2.33 (t, 2H), 1.77-1.91 (m, 1H), 1.51-1.71 (m, 4H), 1.30-1.50 (m, 2H) ppm. ^{13}C NMR (200 MHz, $CDCl_3$) δ: 173.5, 65.9, 60.4, 56.2, 40.2, 38.3, 34.3, 33.6, 28.5, 24.4 ppm. LC-MS (m/z): Calcd for $[M+NH_4]^+$: 268.2, Found: 268.1.

4.5.3.2. DL-Thioctic ethylene glycol (TEG)

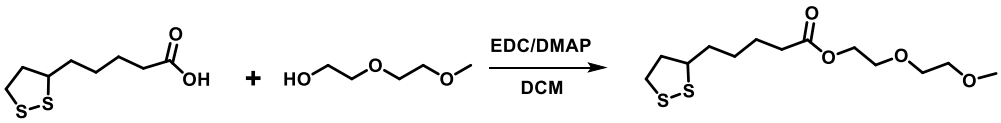

Scheme 2. Synthesis of DL-thioctic ethylene glycol.

TEG was synthesized by a previous study.[211] DL-Thiocric acid (824 mg, 4 mmol),

diethylene glycol monomethyl ether (570 mg, 4.8 mmol) and 4-(dimethylamino)pyridine (DMAP) (154.6 mg, 1.2 mmol) were added into the oven-dried round flask with a stirring bar, then anhydrous dichloromethane (20 mL) was added to dissolve them. After totally dissolving, 1-(3-dDimethylaminopropyl)-3-ethylcarbodiimide hydrochloride (EDC·HCl) (2.3 g, 12 mmol) was dissolved in 10 mL dichloromethane and added in the as-prepared solution under nitrogen atmosphere. The reaction was conducted at room temperature in dark overnight. Then, the solution was washed with saturated sodium chloride, 1 M hydrochloric acid and saturated sodium bicarbonate, and dried over anhydrous Na_2SO_4. The crude product was obtained by rotary vapor. Finally, after the separation by column chromatographic (silica gel, petroleum ether to petroleum ether/ethyl acetate=3/1), the pure product was received as a light yellow liquid (yield: 65%).

^{1}H NMR (200 MHz, $CDCl_3$) δ: 4.13-4.21 (t, 2H), 3.61-3.66 (t, 2H), 3.53-3.60 (t, 2H), 3.51 (m, 1H), 3.43-3.49 (t, 2H), 3.29-3.32 (m, 3H), 2.99-3.17 (t, 2H), 2.32-2.45 (m, 1H), 2.24-2.33 (t, 2H), 1.75-1.90 (m, 1H), 1.50-1.69 (m, 4H), 1.30-1.48 (m, 2H) ppm. ^{13}C NMR (200 MHz, $CDCl_3$) δ: 173.2, 71.7, 70.5, 69.2, 58.9, 56.1, 40.1, 38.3, 34.4, 33.8, 28.4, 24.5 ppm. LC-MS (m/z): Calcd for $[M+NH_4]^+$: 326.1, Found: 326.2.

4.5.3.3. Propane dithioctic (PDT)

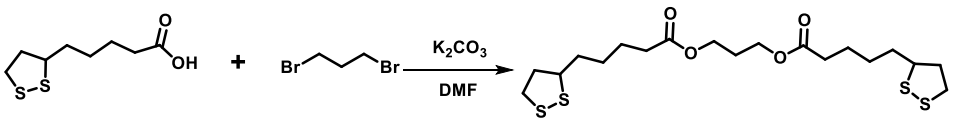

Scheme 3. Synthesis of propane dithioctic.

Propane dithioctic was synthesized by same protocol of DL-thioctic hydroxyethyl (THE) above. Typically, 1,3-dibromopropane (460 μL, 4.5 mmol) was added dropwise into a mixture of DL-thiocric acid (2.06 g, 10 mmol), potassium carbonate (2.74 g, 20 mmol)

and DMF (20 mL). The reaction was performed at room temperature in dark overnight. Then, 20 mL water was added to dissolve the solid salt. This as-prepared mixture was exacted with 40 mL ethyl acetate. And the organic layer was washed by saturated sodium chloride, 1 M hydrochloric acid and saturated sodium bicarbonate, then dried over anhydrous Na_2SO_4. After concentrated by vacuum and column chromatographic separation (silica gel, dichloromethane), the final product was gained as a light yellow liquid (yield: 40%).

^{1}H NMR (200 MHz, $CDCl_3$) δ: 3.99-4.13 (t, 4H), 3.43-3.57 (m, 2H), 2.99-3.17 (t, 4H), 2.33-2.47 (m, 2H), 2.20-2.30 (t, 4H), 1.77-1.94 (m, 4H), 1.53-1.69 (m, 8H), 1.31-1.47 (m, 4H) ppm. ^{13}C NMR (200 MHz, $CDCl_3$) δ: 173.1, 60.8, 56.3, 40.1, 38.3, 34.6, 33.8, 28.6, 24.5, 20.9 ppm. LC-MS (m/z): Calcd for $[M+NH_4]^+$: 470.1, Found: 470.2.

4.5.3.4. Pyrene-terminated dibenzo 24 crown 8 (DB24C8)

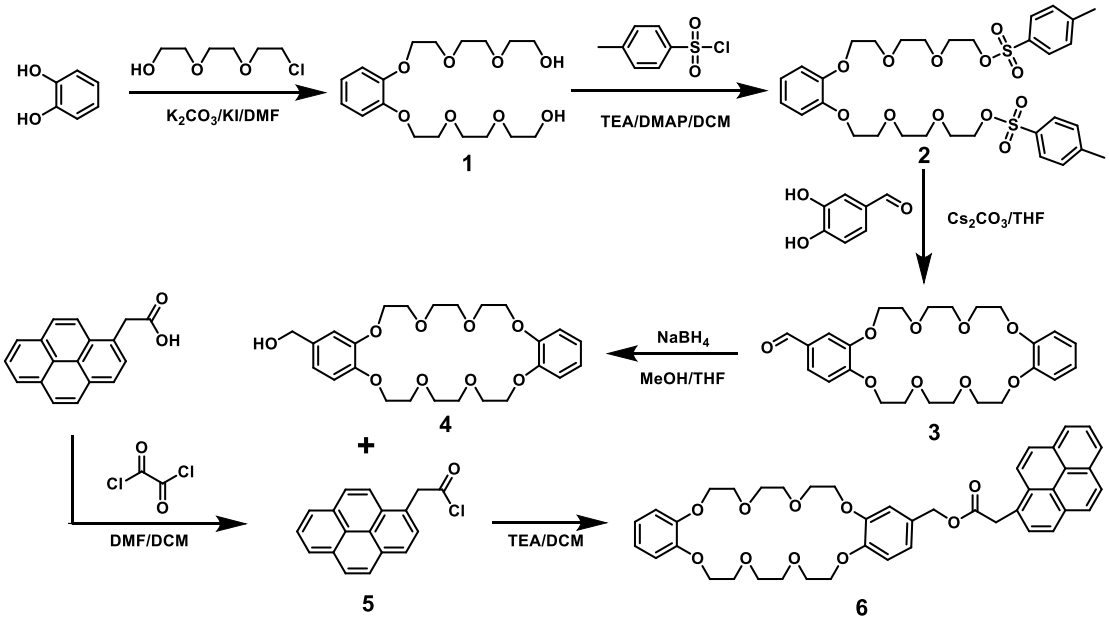

Scheme S4. Synthesis of pyrene-terminated DB24C8

Pyrene-terminated DB24C8 was synthesized according to a previous study.[212]

Compound 1: Catechol (1.1 g, 10 mmol), 2-[2-(2-chloroethoxy)ethoxy]ethanol (3.05 ml, 21 mmol), K_2CO_3 (4.15 g, 30 mmol), KI (.05 g, 3.0 mmol) and DMF (60 ml) were

mixed in an oven-dried round flask. The mixture was heated at 100 ^{o}C for 24 h. Then 60 mL water added to dissolve the unsolvable solid and the solution was exacted by 120 mL DCM. The organic layer was washed by saturated sodium chloride, saturated sodium bicarbonate, and saturated sodium chloride, then dried over anhydrous Na_2SO_4. After concentrated by evaporation, the final product was obtained as a brown oil (yield: 80%).

^{1}H NMR (200 MHz, $CDCl_3$) δ: 6.88 (s, 4H), 4.11-4.21 (t, 4H), 3.81-3.91 (t, 4H), 3.65-3.79 (m, 12H), 3.56-3.62 (q, 4H), 3.08 (s, 2H) ppm. ^{13}C NMR (200 MHz, $CDCl_3$) δ: 148.9, 121.7, 114.7, 72.7, 70.9, 70.4, 69.8, 68.8, 61.7 ppm. LC-MS (m/z): Calcd for $[M+NH_4]^+$: 392.2, Found: 392.2.

Compound 2: Compound 1 (2.8 g, 7.5 mmol), triethylamine (TEA) (4.35 ml, 31 mmol) and 4-dimethylamino pyridine (DMAP) (5 mg, 0.075 mmol) were mixed in DCM (30 ml). 4-Toluenesulfonyl chloride (3.6 g, 19 mmol) dissolved in DCM (70 mL) and added dropwise to the reaction mixture with vigorously stirring. The reaction was stirred at room temperature overnight. After that, the solution was washed by 1 M hydrochloric acid, saturated sodium bicarbonate and saturated chloride, then dried over anhydrous Na_2SO_4. The crude product was purified by column chromatography (silica gel, DCM to DCM/MeOH=20/1) to give a brown colored oil (yield: 55%).

^{1}H NMR (200 MHz, $CDCl_3$) δ: 7.71-7.82 (d, 4H), 7.27-7.35 (d, 4H), 6.89 (s, 4H), 4.08-4.19 (m, 8H), 3.75-3.84 (t, 4H), 3.54-3.72 (m, 12H), 2.41 (s, 6H) ppm. ^{13}C NMR (200 MHz, $CDCl_3$) δ: 149.0, 144.8, 133.0, 129.9, 128.0, 121.7, 114.9, 70.8, 70.7, 69.8, 69.3, 68.8, 68.7, 21.6 ppm. LC-MS (m/z): Calcd for $[M+NH_4]^+$: 700.2, Found: 700.2.

Compound 3: 3,4-Dihydroxybenzaldehyde (0.345 g, 2.5 mmol) and Cs_2CO_3 (4.075 g, 12.5 mmol) were mixed in THF (70 ml), then heated under reflux for 1h. After that, compound 2 (1.71 g, 2.5 mmol) in THF (20 ml) was added and heated under reflux for 24 h. After cooling down to the room temperature, the solvent was removed under

vacuum. The residue was dissolved in 40 mL DCM, and washed by 1 M hydrochloric acid and saturated chloride, then dried over anhydrous Na_2SO_4. After column chromatography separation (silica gel, DCM to ethyl acetate/MeOH=10/1), the final product was received as a yellowish solid (yield: 70%).

^{1}H NMR (200 MHz, $CDCl_3$) δ: 9.79 (s, 1H), 7.33-7.43 (m, 2H), 6.77-3.96 (m, 5H), 4.04-4.22 (m, 8H), 3.78-3.97 (m, 16H) ppm. ^{13}C NMR (200 MHz, $CDCl_3$) δ: 190.9, 154.3, 149.2, 148.9, 130.2, 126.9, 121.4, 113.9, 111.9, 111.0, 71.6, 71.5, 71.3, 70.0, 69.8, 69.7, 69.5, 69.4, 69.4, 69.3 ppm. LC-MS (m/z): Calcd for $[M+NH_4]^+$: 494.4, Found: 494.4.

Compound 4: Compound 3 (0.6 g, 1.25 mmol) was dissolved in a mixture of MeOH/THF (5 mL/5 mL) and the solution was cooled to 0 ºC for 30 min. $NaBH_4$ (0.1425 g, 3.75 mmol) was added into the solution with vigorously stirring. Then the mixture was stirred at room temperature overnight. After quenching by adding 5 mL water, the solution was exacted by DCM. The organic layer was washed by saturated sodium chloride twice and dried by Na_2SO_4. After removing the solvent, the final product was got as white solid (quantitative yielding).

^{1}H NMR (200 MHz, $CDCl_3$) δ: 6.80-6.94 (m, 7H), 4.55-4.61 (s, 2H), 4.09-4.18 (m, 8H), 3.79-3.95 (m, 16H) ppm. ^{13}C NMR (200 MHz, $CDCl_3$) δ: 149.0, 148.9, 148.4, 134.3, 121.4, 119.9, 114.1, 113.9, 71.3, 70.9, 69.9, 69.8, 69.6, 69.4, 65.1 ppm. LC-MS (m/z): Calcd for $[M+NH_4]^+$: 496.2, Found: 496.2.

Compound 5: 1-Pyrenecarboxylic acid (78.1 mg, 0.3 mmol) and oxalyl chloride (76.2 mg, 0.6 mmol) were mixed with DCM (15 mL). A drop of DMF was added in the mixture and the reaction was performed at room temperature for 2 h. Then the solvent was removed under vacuum to get yellowish solid (quantitative yielding), which was used directly without further processing.

Compound 6: Compound 4 (120 mg, 0.25 mmol) and trimethylamine (50 mg, 0.5 mmol) were mixed in DCM (15 mL), then stirring for 1 h under nitrogen atmosphere.

After adding the fresh prepared compound 5 (quantitative yielding) in DCM (5 mL), the reaction was kept at room temperature overnight under nitrogen atmosphere. After concentrating by vacuum, the crude product was purified by column chromatography (silica gel, ethyl acetate/petroleum ether=4/1). The final product (pyrene-terminated DB24C8) was obtained as a yellowish solid (yield: 40%).

^{1}H NMR (200 MHz, $CDCl_3$) δ: 7.80-8.16 (d, 9H), 6.60-6.82 (m, 6H), 6.45 (d, 1H), 4.95 (s, 2H), 4.26 (s, 2H), 3.96-4.09 (m, 8H), 3.46-3.84 (m, 16H) ppm. ^{13}C NMR (200 MHz, $CDCl_3$) δ: 149.0, 148.9, 148.4, 134.3, 121.4, 119.9, 114.1, 113.9, 71.3, 70.9, 69.9, 69.8, 69.6, 69.4, 65.1 ppm. LC-MS (m/z): Calcd for $[M+NH_4]^+$: 738.2, Found: 738.2.

4.5.4. Synthesis of fully interlocked elastomers and gels

Taking DL-thioctic hydroxyethyl (THE) based fully interlocked elastomers and gels as example:

The mixture of DL-thioctic hydroxyethyl (70 %, molar fraction) and DMF (30 %, molar fraction) was added on a PTFE based rectangular mold, which was put in a glove box purged with Argon. After DMF was totally evaporated, the obtained elastomers was immersed in THF for 1 day with changing it every 8 hours to remove the unreacted components. Then the fully interlocked THE based elastomers formed after drying.

The fully interlocked THE based gels were prepared by swelling the THE elastomers in THF or 1,4-diaxone solvents.

The DL-thioctic ethylene glycol (TEG) and propane dithioctic (PDT) based fully interlocked elastomers and gels were prepared by the same method.

4.5.5. Synthesis of fluorescent fully interlocked elastomers

The mixture of DL-thioctic hydroxyethyl (69.99 %, molar fraction), pyrene-terminated DB24C8 (0.01 %, molar fraction) and DMF (30 %, molar fraction) was added on a PTFE based rectangular mold, which was put in a glove box purged with Argon. After

DMF was totally evaporated, the obtained elastomers were immersed in THF/$CHCl_3$ solution for 1 day with changing it every 8 hours to remove the unreacted and unlocked components. Then the fluorescent interlocked THE based elastomers was formed after drying.

4.5.6. Self-growing interlocked elastomers

Firstly, THE based interlocked elastomer was swelled in a nutrient solution of THE/DMF (70/30, mol/mol) for 12 h to obtain the swollen THE based interlocked seed. Then, the swollen seed sample was put under Argon atmosphere to let DMF fully evaporate. Then, the sample was immersed in THF solution for 1 day with changing it every 8 hours to remove the unreacted components. Finally, the grown interlocked THE based elastomer was obtained after drying.

The multi-time growth of interlocked elastomer was processed with similar above procedure.

The mechanical properties of the obtained seed materials were measured by the tensile test.

4.5.7. Enhanced self-strengthening of interlocked elastomers

Firstly, THE based interlocked elastomer was swelled in a nutrient solution of THE/PDT/DMF with various PDT molar fractions (0.1 %, 1 %, 2 %, 5 % and 10 %) while the ratio of DMF is kept at 30 % (molar fraction) for 12 h to obtain the swollen THE based interlocked seed. Then, the swollen seed sample was put under Argon atmosphere to let DMF fully evaporate. Then, the sample was immersed in THF solution for 1 day with changing it every 8 hours to remove the unreacted components. Finally, the enhanced self-strengthened interlocked THE based elastomer was obtained after drying. The mechanical properties of the obtained seed materials were measured by the tensile test.

Chapter 5

5. Conclusions and outlook

In this thesis, I have developed several approaches for the fabrication of self-growing elastomer materials that can be used to mimic the apparent growing feature of living organisms fundamentally. I have carried out light-activated strategies for regulating the growth of dynamic materials, both surface structures and bulky substrates. Employing light-induced growth, the pristine soft materials can be grown with modulation in size, composition and mechanical properties. Moreover, I have proposed a novel evaporation-induced entropy replenishment approach to fabricate fully interlocked poly(disulfide)s material with interlocking network topology. Self-growing and self-strengthening of interlocked material owing to the facile evaporation approach were evaluated. Finally, I have demonstrated the potential application of self-growing polymeric materials in making rough surfaces, self-restoration of materials, and self-stiffening of soft elastomers.

The following are the major conclusions and outlook of this work:

- Photo-activation of dynamic polyHBA elastomers allows easily materials growth by the swelling-polymerization-homogenization approach. Multiple treatments allow a grown index up to 19. By varying nutrient solutions, both the composition of grown material can be modulated. Homogeneous and heterogeneous growth of bulk materials can be achieved and easily

combined in multiple steps. The bulk hydrophobicity of the material can be modulated through growth cycle treatment without any preprogramming. Further studies can extend this system into self-growing biocompatible hydrogels by featuring mild chain exchanging reactions.

- Photoinduced site-specifically self-growable materials can be designed based on coupling three kinds of reactions: photolysis, photopolymerization, and transesterification in a single system. The size, shape and composition of such materials can be regulated by changing the hydrophilicity of the grown monomers. The mechanical properties of the grown microstructures can also be adjusted. The materials can also be restored after irregular damage at the surface. Although the methodology was demonstrated on structured surfaces, the mechanistic insights can be readily applied to change the bulk properties within materials in consideration of the capability of two-photon polymerization.
- Evaporation-induced entropy replenishment is a new and interesting methodology to synthesize fully interlocked polycatenanes elastomers. The increase of entropy during evaporation of base catalyst can compensate for the entropy loss of cyclization of polymers/oligomers within the precursor to form fully interlocked polycatenannes. The obtained crosslinked materials possess a unique interlocking network topology, which is an excellent expansion in the field of polymer topologies and creates a new opportunity in chemistry and material science. This work can be further extended in other polymeric materials accordingly, like the preparation of interlocked PDMS and hydrogels.

This Thesis presented a variety of strategies to guide the growth of synthetic dynamic

soft materials in a bioinspired manner. Although this Thesis only focuses on growable polymer material systems using organic solvents, this principle could be extended to other elastic materials and biocompatible hydrogels. Moreover, other approaches involving pH and temperature can also be used as candidates for the investigation of novel dynamic soft and self-growing materials.

List of scientific contributions

Articles

1. **L. Xue**, X. Xiong, B. Krishnan, F. Puza, S. Wang, Y. Zheng and J. Cui. Light-regulated growth from dynamic swollen substrates for making rough surfaces. *Nature Communications*, **2020**, *11*, 963.
2. B. Krishnan, L. Prieto-López, S. Hoefgen, **L. Xue**, S. Wang, V. Valiante and J. Cui. Thermomagneto-responsive smart biocatalysts for Malonyl-Coenzyme A synthesis. *ACS Appl. Mater. Interfaces*, **2020**, *12*, 20982.
3. F. Puza, Y. Zheng, L. Han, **L. Xue** and J. Cui. Physical entanglement hydrogels: ultrahigh water content but good toughness and stretchability. *Polym. Chem.*, **2020**, *11*, 2339.
4. L. Han, Y. Zheng, H. Luo, J. Feng, R. Engstler, **L. Xue**, G. Jing, X. Deng, A. del Campo and J. Cui. Macroscopic self-evolution of dynamic hydrogels to create hollow interiors. *Angew. Chem. Int. Ed.* **2020**, *59*, 5611.
5. B. Krishnan, **L. Xue**, X. Xiong and J. Cui. Photoinduced strain-assisted synthesis of a stiff-stilbene polymer by ring-opening metathesis polymerization. *Chem. Eur. J.*, 2020, DOI: 10.1002/chem.202002418.
6. S. Wang, L. Yang, H. Wang, **L. Xue**, J. Chen and J. Cui. Nonequilibrium transesterification for programming a material's stiffening. *ACS Appl. Polym. Mater.* **2019**, *1*, 3227.
7. X. Xiong, **L. Xue** and J. Cui. Phototriggered growth and detachment of polymer brushes with wavelength selectivity. *ACS Macro Lett.* **2018**, 7, 239.
8. S. Wang, H. Wang, P. Zhang, L. Xue, J. Chen and J. Cui. Folding fluorescent probes for self-reporting transesterification in dynamic polymer networks. 2020, **Submitted**.

Curriculum Vitae

Lulu Xue, Male

Date of Brith: 05. 03. 1989

Nationality: P. R. China

Affiliation: INM-Leibniz Institute for New Materials,

Campus D22, 66123, Saarbrücken, Germany

Tel: +49(0)17628616443

E-mail: luluxue0426@gmail.com

EDUCATION

PhD 2016-2020

- Doctorate studies at Leibniz Institute for New Materials and Saarland University, Saarbrücken, Germany
- Tentative title of the Thesis: Guiding synthetic dynamic soft materials to grow like living organisms
- Supervisor: Prof. Dr. Aránzazu del Campo, second supervisor: Prof. Dr. Tobias Kraus, adviser: Dr. Jiaxi Cui
- Major: Chemistry

Master of Science 2013-2016

- Master studies at Soochow University, Suzhou, P. R. China
- Supervisor: Prof. Dr. Hong Chen
- Major: Polymer Chemistry and Physics

Bachelor of Engineering 2009-2013

- Bachelor studies at Qingdao University of Science and Technology, Qingdao, P. R. China
- Major: Polymer Materials and Engineering

HONORS

- The scholarship of China Scholarship Council (2016-2020)
- Excellent Student Award by Soochow University, Jiangsu, China (2016)
- National Scholarship, China (Autumn, 2015)
- Excellent Student Award by Qingdao University of Science and Technology, Shandong, China (2013)
- Shandong Provincial Government Scholarship (Spring, 2011)

INTERESTS

- Listening music
- Doing sports (e.g., playing basketball, running)
- Writing proses

References

1. Hamley, I. W.; Castelletto, V., Biological soft materials. *Angew. Chem. Int. Ed.,* **2007,** *46*, 4442-4455.

2. de Gennes, P. G., Soft matter. *Angew. Chem. Int. Ed.,* **1992**, *31,* 842-845.

3. Hassan, P. A.; Verma, G.; Ganguly, R., Soft materials-properties and applications. *Functional Materials*., **2012**, 1-59.

4. Zou, W.; Dong, J.; Luo, Y.; Zhao, Q.; Xie, T., Dynamic covalent polymer networks: from old chemistry to modern day innovations. *Adv. Mater.,* **2017,** *29,* 1606100.

5. Chakma, P.; Konkolewicz, D., Dynamic covalent bonds in polymeric materials. *Angew. Chem. Int. Ed.,* **2019,** *58*, 9682-9695.

6. Winne, J. M.; Leibler, L.; Du Prez, F. E., Dynamic covalent chemistry in polymer networks: a mechanistic perspective. *Polym. Chem.,* **2019,** *10*, 6091-6108.

7. Mohammed, J. S.; Murphy, W. L., Bioinspired design of dynamic materials. *Adv. Mater.,* **2009,** *21*, 2361-2374.

8. Podgorski, M.; Fairbanks, B. D.; Kirkpatrick, B. E.; McBride, M.; Martinez, A.; Dobson, A.; Bongiardina, N. J.; Bowman, C. N., Toward stimuli-responsive dynamic thermosets through continuous development and improvements in covalent adaptable networks (CANs). *Adv. Mater.,* **2020**, 1906876.

9. Roy, D.; Cambre, J. N.; Sumerlin, B. S., Future perspectives and recent advances in stimuli-responsive materials. *Prog. Polym. Sci.,* **2010,** *35*, 278-301.

10. Hines, L.; Petersen, K.; Lum, G. Z.; Sitti, M., Soft actuators for small-scale robotics. *Adv. Mater.,* **2017,** *29*, 1603483.

11. Gupta, P.; Vermani, K.; Garg, S., Hydrogels: from controlled release to pH-responsive drug delivery. *Drug. Discov. Today.,* **2002,** *7*, 569-579.

12. Taylor, D. L.; In Het Panhuis, M., Self-healing hydrogels. *Adv. Mater.,* **2016,** *28*, 9060-9093.

13. Huynh, T. P.; Sonar, P.; Haick, H., Advanced materials for use in soft self-healing devices. *Adv. Mater.,* **2017,** *29*, 1604973.

14. Chen, Y.; Kushner, A. M.; Williams, G. A.; Guan, Z., Multiphase design of autonomic self-healing thermoplastic elastomers. *Nat. Chem.,* **2012,** *4*, 467-472.

15. Pei, Z.; Yang, Y.; Chen, Q.; Terentjev, E. M.; Wei, Y.; Ji, Y., Mouldable liquid-crystalline elastomer actuators with exchangeable covalent bonds. *Nat. Mater.,* **2014,** *13*, 36-41.

16. Li, T.; Hu, K.; Ma, X.; Zhang, W.; Yin, J.; Jiang, X., Hierarchical 3D patterns with dynamic wrinkles produced by a photocontrolled Diels-Alder reaction on the surface. *Adv. Mater.,* **2020,** *32*, 1906712.

17. Cui, J.; Daniel, D.; Grinthal, A.; Lin, K.; Aizenberg, J., Dynamic polymer systems with self-regulated secretion for the control of surface properties and material healing. *Nat. Mater.,* **2015,** *14*, 790-795.

18. Chen, M.; Gu, Y.; Singh, A.; Zhong, M.; Jordan, A. M.; Biswas, S.; Korley, L. T.; Balazs, A. C.; Johnson, J. A., Living additive manufacturing: transformation of parent gels into diversely functionalized daughter gels made possible by visible light photoredox catalysis. *ACS Cent. Sci.,* **2017,** *3*, 124-134.

19. Cuthbert, J.; Balazs, A. C.; Kowalewski, T.; Matyjaszewski, K., STEM gels by controlled radical polymerization. *Trends in Chemistry* **2020,** *2*, 341-353.

20. Matsuda, T.; Kawakami, R.; Namba, R.; Nakajima, T.; Gong, J. P., Mechanoresponsive self-growing hydrogels inspired by muscle training. *Science* **2019,** *363*, 504-508.

21. Martin, R.; Rekondo, A.; de Luzuriaga, A. R.; Casuso, P.; Dupin, D.; Cabañero, G.; Grande, H. J.; Odriozola, I., Dynamic sulfur chemistry as a key tool in the design of self-healing polymers. *Smart. Mater. Struct.,* **2016,** *25*, 084017.

22. Sastri, V. R.; Tesoro, G. C., Reversible crosslinking in epoxy resins. II. new appraches *J. Appl. Polym. Sci.,* **1990,** *39*, 1439-1457.

23. Zhang, Z. P.; Rong, M. Z.; Zhang, M. Q., Polymer engineering based on reversible covalent chemistry: A promising innovative pathway towards new materials and new functionalities. *Prog. Polym. Sci.,* **2018,** *80*, 39-93.

24. Canadell, J.; Goossens, H.; Klumperman, B., Self-healing materials based on disulfide links. *Macromolecules* **2011,** *44*, 2536-2541.

25. Michal, B. T.; Jaye, C. A.; Spencer, E. J.; Rowan, S. J., Inherently photohealable and thermal shape-memory polydisulfide networks. *ACS Macro. Lett,* **2013,** *2*, 694-699.

26. Scott, T. F.; Schneider, A. D.; Cook, W. D.; Bowman, C. N., Photoinduced plasticity in cross-linked polymers. *Science* **2005,** *308*, 1615-1617.

27. Amamoto, Y.; Otsuka, H.; Takahara, A.; Matyjaszewski, K., Self-healing of covalently cross-linked polymers by reshuffling thiuram disulfide moieties in air under visible light. *Adv. Mater.,* **2012,** *24*, 3975-3980.

28. Amamoto, Y.; Kamada, J.; Otsuka, H.; Takahara, A.; Matyjaszewski, K., Repeatable photoinduced self-healing of covalently cross-linked polymers through reshuffling of trithiocarbonate units. *Angew. Chem. Int. Ed.,* **2011,** *50*, 1660-1663.

29. Worrell, B. T.; Mavila, S.; Wang, C.; Kontour, T. M.; Lim, C.-H.; McBride, M. K.; Musgrave, C. B.; Shoemaker, R.; Bowman, C. N., A user's guide to the thiol-thioester exchange in organic media: scope, limitations, and applications in material science. *Polym. Chem.,* **2018,** *9*, 4523-4534.

30. Worrell, B. T.; McBride, M. K.; Lyon, G. B.; Cox, L. M.; Wang, C.; Mavila, S.; Lim, C. H.; Coley, H. M.; Musgrave, C. B.; Ding, Y.; Bowman, C. N., Bistable and photoswitchable states of matter. *Nat. Commun.,* **2018,** *9*, 2804.

31. Fan, F.; Ji, S.; Sun, C.; Liu, C.; Yu, Y.; Fu, Y.; Xu, H., Wavelength-controlled dynamic metathesis: a light-driven exchange reaction between disulfide and diselenide bonds. *Angew. Chem. Int. Ed.,* **2018,** *57*, 16426-16430.

32. Nicolaou, K. C.; Snyder, S. A.; Montagnon, T.; Vassilikogiannakis, G., The Diels-Alder reaction in total synthesis. *Angew. Chem. Int. Ed.*. **2002,** *41*, 1668-1698.

33. Chen, X.; Dam, M. A.; Ono, K.; Mal, A.; Shen, H.; Nutt, S. R.; Sheran, K.; Wudl, F., A thermally re-mendable cross-linked polymeric material. *Science* **2002,** *295*, 1698-1702.

34. Liu, Y. L.; Chen, Y. W., Thermally Reversible cross-linked polyamides with high toughness and self-repairing ability from maleimide- and furan-functionalized aromatic polyamides. *Macromol. Chem. Phys.,* **2007,** *208*, 224-232.

35. Inoue, K.; Yamashiro, M.; Iji, M., Recyclable shape-memory polymer: Poly(lactic acid) crosslinked by a thermoreversible Diels-Alder reaction. *J. Appl. Polym. Sci.,* **2009,** *112*, 876-885.

36. Defize, T.; Riva, R.; Raquez, J. M.; Dubois, P.; Jerome, C.; Alexandre, M., Thermoreversibly crosslinked poly(epsilon-caprolactone) as recyclable shape-memory polymer network. *Macromol. Rapid. Commun.,* **2011,** *32*, 1264-1269.

37. Yu, S.; Zhang, R.; Wu, Q.; Chen, T.; Sun, P., Bio-inspired high-performance and recyclable cross-linked polymers. *Adv. Mater.,* **2013,** *25*, 4912-4917.

38. Tian, Q.; Yuan, Y. C.; Rong, M. Z.; Zhang, M. Q., A thermally remendable epoxy resin. *J. Mater. Chem.,* **2009,** *19*, 1289-1296.

39. Zhang, Y.; Broekhuis, A. A.; Picchioni, F., Thermally self-healing polymeric materials: the next step to recycling thermoset polymers? *Macromolecules* **2009,** *42*,. 1906-1912.

40. Polgar, L. M.; van Duin, M.; Broekhuis, A. A.; Picchioni, F., Use of Diels–Alder chemistry for thermoreversible cross-linking of rubbers: the next step toward recycling of rubber products? *Macromolecules* **2015,** *48*, 7096-7105.

41. Roling, O.; De Bruycker, K.; Vonhoren, B.; Stricker, L.; Korsgen, M.; Arlinghaus, H. F.; Ravoo, B. J.; Du Prez, F. E., Rewritable polymer brush micropatterns grafted by Triazolinedione click chemistry. *Angew. Chem. Int. Ed.,* **2015,** *54*, 13126-13129.

42. Montarnal, D.; Capelot, M.; Tournilhac, F.; Leibler, L., Silica-like malleable materials from permanent organic networks. *Science* **2011,** *334*, 965-968.

43. Otera, J., Transesterification. *Chem. Rev.* **1993**, *93*, 1449-1470.

44. Zhang, H.; Cai, C.; Liu, W.; Li, D.; Zhang, J.; Zhao, N.; Xu, J., Recyclable polydimethylsiloxane network crosslinked by dynamic transesterification reaction. *Sci. Rep.,* **2017,** *7*, 11833.

45. Zhang, B.; Kowsari, K.; Serjouei, A.; Dunn, M. L.; Ge, Q., Reprocessable thermosets for sustainable three-dimensional printing. *Nat. Commun.,* **2018,** *9*, 1831.

46. Ciaccia, M.; Di Stefano, S., Mechanisms of imine exchange reactions in organic solvents. *Org. Biomol. Chem.,* **2015,** *13*, 646-654.

47. Belowich, M. E.; Stoddart, J. F., Dynamic imine chemistry. *Chem. Soc. Rev.,* **2012,** *41*, 2003-2024.

48. Zhang, Y.; Tao, L.; Li, S.; Wei, Y., Synthesis of multiresponsive and dynamic chitosan-based hydrogels for controlled release of bioactive molecules. *Biomacromolecules* **2011,** *12*, 2894-2901.

49. Kathan, M.; Kovaricek, P.; Jurissek, C.; Senf, A.; Dallmann, A.; Thunemann, A. F.; Hecht, S., Control of imine exchangek inetics with photoswitches to modulate self-healing in polysiloxane networks by light illumination. *Angew. Chem. Int. Ed.*, **2016**, *55*, 13882-13886.

50. Deng, G.; Tang, C.; Li, F.; Jiang, H.; Chen, Y., Covalent cross-linked polymer gels with reversible sol−gel transition and self-healing properties. *Macromolecules* **2010**, *43*, 1191-1194.

51. Lu, Y. X.; Guan, Z., Olefin metathesis for effective polymer healing *via* dynamic exchange of strong carbon-carbon double bonds. *J. Am. Chem. Soc.,* **2012,** *134*, 14226-14231.

52. Lu, Y. X.; Tournilhac, F.; Leibler, L.; Guan, Z., Making insoluble polymer networks malleable *via* olefin metathesis. *J. Am. Chem. Soc.,* **2012,** *134*, 8424-8427.

53. Brooks, W. L.; Sumerlin, B. S., Synthesis and applications of boronic acid-containing polymers: from materials to medicine. *Chem. Rev.,* **2016,** *116*, 1375-1397.

54. Smithmyer, M. E.; Deng, C. C.; Cassel, S. E.; LeValley, P. J.; Sumerlin, B. S.; Kloxin, A. M., Self-healing boronic acid-based hydrogels for 3D co-cultures. *ACS Macro. Letters.,* **2018,** *7*, 1105-1110.

55. Bapat, A. P.; Sumerlin, B. S.; Sutti, A., Bulk network polymers with dynamic B–O bonds: healable and reprocessable materials. *Mater. Horiz.,* **2020,** *7*, 694-714.

56. Osthoff, R. C.; Bueche, A. M.; Grubb, W. T., Chemical stress-relaxation of polydimethylsiloxane elastomers1. *J. Am. Chem. Soc.*, **1954,** *76***,** 4659-4663.

57. Zheng, P.; McCarthy, T. J., A surprise from 1954: siloxane equilibration is a simple, robust, and obvious polymer self-healing mechanism. *J. Am. Chem. Soc.,* **2012,** *134*, 2024-2027.

58. Schmolke, W.; Perner, N.; Seiffert, S., Dynamically cross-linked polydimethylsiloxane networks with ambient-temperature self-healing. *Macromolecules* **2015,** *48*, 8781-8788.

59. Nishimura, Y.; Chung, J.; Muradyan, H.; Guan, Z., Silyl ether as a robust and thermally stable dynamic covalent motif for malleable polymer design. *J. Am. Chem. Soc.,* **2017,** *139*, 14881-14884.

60. Muller-Dethlefs, K.; Hobza, P., Noncovalent interactions: a challenge for experiment and theory. *Chem. Rev.,* **2000,** *100*, 143-168.

61. Cerny, J.; Hobza, P., Non-covalent interactions in biomacromolecules. *Phys. Chem. Chem. Phys.,* **2007,** *9*, 5291-5303.

62. Otero-de-la-Roza, A.; Johnson, E. R., A benchmark for non-covalent interactions in solids. *J. Chem. Phys.,* **2012,** *137*, 054103.

63. Kunzle, M.; Lach, M.; Budiarta, M.; Beck, T., Higher-order structures based on molecular interactions for the formation of natural and artificial biomaterials. *Chembiochem* **2019**, *20*, 1637-1641.

64. Hu, X.; Vatankhah-Varnoosfaderani, M.; Zhou, J.; Li, Q.; Sheiko, S. S., Weak hydrogen bonding enables hard, strong, tough, and elastic hydrogels. *Adv. Mater.,* **2015,** *27*, 6899-6905.

65. Huang, S.; Liu, Y.; Zhao, Y.; Ren, Z.; Guo, C. F., Flexible electronics: stretchable electrodes and their future. *Adv. Funct. Mater.,* **2018,** *29*, 1805924.

66. Zhang, Q.; Liu, L.; Pan, C.; Li, D., Review of recent achievements in self-healing conductive materials and their applications. *J. Mater. Sci.,* **2017,** *53*, 27-46.

67. Hohl, D. K.; Weder, C., (De)bonding on demand with optically switchable adhesives. *Adv. Optical. Mater.,* **2019,** *7*, 1900230.

68. Savjani, J. Co-crystallization: An approach to improve the performance characteristics of active pharmaceutical ingredients. *Asian J. Pharm.* **2015**, 147-151.

69. Zhang, H.; Xia, H.; Zhao, Y., Poly(vinyl alcohol) hydrogel can autonomously self-heal. *ACS Macro. Lett.,* **2012,** *1*, 1233-1236.

70. Hunt, J. N.; Feldman, K. E.; Lynd, N. A.; Deek, J.; Campos, L. M.; Spruell, J. M.; Hernandez, B. M.; Kramer, E. J.; Hawker, C. J., Tunable, high modulus hydrogels driven by ionic coacervation. *Adv. Mater.,* **2011,** *23*, 2327-2331.

71. Sun, T. L.; Kurokawa, T.; Kuroda, S.; Ihsan, A. B.; Akasaki, T.; Sato, K.; Haque, M. A.; Nakajima, T.; Gong, J. P., Physical hydrogels composed of polyampholytes demonstrate high toughness and viscoelasticity. *Nat. Mater.,* **2013,** *12*, 932-937.

72. Okay, O., Self-healing hydrogels formed *via* hydrophobic interactions . *S. Seiffert (ed.), Supramolecular Polymer Networks and Gels*, **2015,** *268*, 101-142.

73. Tuncaboylu, D. C.; Sari, M.; Oppermann, W.; Okay, O., Tough and self-healing hydrogels formed *via* hydrophobicinteractions. *Macromolecules* **2011,** *44*, 4997-5005.

74. Tuncaboylu, D. C.; Argun, A.; Sahin, M.; Sari, M.; Okay, O., Structure optimization of self-healing hydrogels formed via hydrophobic interactions. *Polymer* **2012,** *53*, 5513-5522.

75. Jiang, G.; Liu, C.; Liu, X.; Zhang, G.; Yang, M.; Chen, Q.; Liu, F., Self-healing Mechanism and Mechanical Behavior of Hydrophobic Association Hydrogels with High Mechanical Strength. *J. Macromol. Sci. A.,* **2010,** *47*, 335-342.

76. Tuncaboylu, D. C.; Sahin, M.; Argun, A.; Oppermann, W.; Okay, O., Dynamics and Large Strain Behavior of Self-Healing Hydrogels with and without Surfactants. *Macromolecules* **2012**, *45*, 1991-2000.

77. Akay, G.; Hassan-Raeisi, A.; Tuncaboylu, D. C.; Orakdogen, N.; Abdurrahmanoglu, S.; Oppermann, W.; Okay, O., Self-healing hydrogels formed in catanionic surfactant solutions. *Soft Matter* **2013,** *9*, 2254-2261.

78. Appel, E. A.; Tibbitt, M. W.; Webber, M. J.; Mattix, B. A.; Veiseh, O.; Langer, R., Self-assembled hydrogels utilizing polymer-nanoparticle interactions. *Nat. Commun.,* **2015,** *6*, 6295.

79. Puza, F.; Zheng, Y.; Han, L.; Xue, L.; Cui, J., Physical entanglement hydrogels: ultrahigh water content but good toughness and stretchability. *Polym. Chem.,* **2020,** *11*, 2339-2345.

80. Kakuta, T.; Takashima, Y.; Nakahata, M.; Otsubo, M.; Yamaguchi, H.; Harada, A., Preorganized hydrogel: self-healing properties of supramolecular hydrogels formed by polymerization of host-guest-monomers that contain cyclodextrins and hydrophobic guest groups. *Adv. Mater.,* **2013,** *25*, 2849-2853.

81. Liao, X.; Chen, G.; Liu, X.; Chen, W.; Chen, F.; Jiang, M., Photoresponsive pseudopolyrotaxane hydrogels based on competition of host-guest interactions. *Angew. Chem. Int. Ed.,* **2010,** *49*, 4409-4413.

82. Liu, G.; Yuan, Q.; Hollett, G.; Zhao, W.; Kang, Y.; Wu, J., Cyclodextrin-based host–guest supramolecular hydrogel and its application in biomedical fields. *Polym. Chem.,* **2018,** *9*, 3436-3449.

83. Tan, S.; Ladewig, K.; Fu, Q.; Blencowe, A.; Qiao, G. G., Cyclodextrin-based supramolecular assemblies and hydrogels: recent advances and future perspectives. *Macromol. Rapid. Commun.,* **2014,** *35*, 1166-1184.

84. Li, J.; Harada, A.; Kamachi, M., Sol-gel transition during inclusion complex-formation between alpha-cyclodextrin and high-molecular-weight poly(ethylene glycol)S in aqueous-solution. *Polym. J.,* **1994,** *26*, 1019-1026.

85. Shi, L.; Ding, P.; Wang, Y.; Zhang, Y.; Ossipov, D.; Hilborn, J., Self-healing polymeric hydrogel formed by metal-ligand coordination assembly: design, fabrication, and biomedical applications. *Macromol. Rapid. Commun.,* **2019,** *40*, 1800837.

86. Talebian, S; Mehrali, M; Taebnia, N; Pennisi, C; Kadumudi, F; Foroughi, J; Hasany, M; Nikkhah, M; Akbari, M; Orive, G; Dolatshahi-Pirouz, A. Self-healing hydrogels: the next paradigm shift in tissue engineering*? Adv. Sci.* **2019**, *6*, 1801664.

87. Li, H.; Yang, P.; Pageni, P.; Tang, C., Recent advances in metal-containing polymer hydrogels. *Macromol. Rapid. Commun.,* **2017,** *38*, 1700109.

88. Yang, J.; Bai, R.; Chen, B.; Suo, Z., Hydrogel adhesion: a supramolecular synergy of chemistry, topology, and mechanics. *Adv. Funct. Mater.,* **2019,** *30*, 1901693.

89. Sun, J. Y.; Zhao, X.; Illeperuma, W. R.; Chaudhuri, O.; Oh, K. H.; Mooney, D. J.; Vlassak, J. J.; Suo, Z., Highly stretchable and tough hydrogels. *Nature* **2012,** *489*, 133-136.

90. Banavar, J. R.; Cooke, T. J.; Rinaldo, A.; Maritan, A., Form, function, and evolution of living organisms. *Proc. Natl. Acad. Sci.,* **2014,** *111*, 3332-3337.

91. Rochon, P.; Batalla, E.; Natansohn, A., Optically induced surface gratings on azoaromatic polymer films. *Appl. Phys. Lett.,* **1995,** *66*, 136-138.

92. Hou, H.; Yin, J.; Jiang, X., Smart patterned surface with dynamic wrinkles. *Acc. Chem. Res.,* **2019,** *52*, 1025-1035.

93. Hou, H.; Hu, K.; Lin, H.; Forth, J.; Zhang, W.; Russell, T. P.; Yin, J.; Jiang, X., Reversible surface patterning by dynamic crosslink gradients: controlling buckling in 2D. *Adv. Mater.,* **2018**, *30*, 1803463.

94. Zhao, H.; Xu, J.; Jing, G.; Prieto-Lopez, L. O.; Deng, X.; Cui, J., Controlling the localization of liquid droplets in polymer matrices by evaporative lithography. *Angew. Chem. Int. Ed.,* **2016,** *55*, 10681-10685.

95. Zhao, H.; Sun, Q.; Deng, X.; Cui, J., Earthworm-inspired rough polymer coatings with self-replenishing lubrication for adaptive friction-reduction and antifouling surfaces. *Adv. Mater.,* **2018**, *30*, 1802141.

96. Chen, G.; Liu, S.; Sun, Z.; Wen, S.; Feng, T.; Yue, Z., Intrinsic self-healing organogels based on dynamic polymer network with self-regulated secretion of liquid for anti-icing. *Prog. Org.Coat.,* **2020,** *144*, 105641.

97. Yan, M.; Zhang, C.; Chen, R.; Liu, Q.; Liu, J.; Yu, J.; Gao, L.; Sun, G.; Wang, J., Fast self-replenishing slippery surfaces with a 3D fibrous porous network for the healing of surface properties. *J. Mater. Chem. A.,* **2019,** *7*, 24900-24907.

98. Rao, Q.; Zhang, J.; Zhan, X.; Chen, F.; Zhang, Q., UV-driven self-replenishing slippery surfaces with programmable droplet-guiding pathways. *J. Mater. Chem. A.,* **2020,** *8*, 2481-2489.

99. Gelebart, A. H.; Liu, D.; Mulder, D. J.; Leunissen, K. H. J.; van Gerven, J.; Schenning, A. P. H. J.; Broer, D. J., Photoresponsive sponge-like coating for on-demand liquid release. *Adv. Funct. Mater.,* **2018,** *28*, 1705942.

100. Spradling, A.; Drummond-Barbosa, D.; Kai, T., Stem cells find their niche. *Nature* **2001,** *414*, 98-104.

101. Zhou, H.; Johnson, J. A., Photo-controlled growth of telechelic polymers and end-linked polymer gels. *Angew. Chem. Int. Ed.,* **2013,** *52*, 2235-2238

102. Stuart, M. A.; Huck, W. T.; Genzer, J.; Muller, M.; Ober, C.; Stamm, M.; Sukhorukov, G. B.; Szleifer, I.; Tsukruk, V. V.; Urban, M.; Winnik, F.; Zauscher, S.; Luzinov, I.; Minko, S., Emerging applications of stimuli-responsive polymer materials. *Nat. Mater.,* **2010,** *9*, 101-113.

103. Yamada, M.; Kondo, M.; Mamiya, J.; Yu, Y.; Kinoshita, M.; Barrett, C. J.; Ikeda, T., Photomobile polymer materials: towards light-driven plastic motors. *Angew. Chem. Int. Ed.,* **2008,** *47*, 4986-4988.

104. Kloxin, A. M.; Kasko, A. M.; Salinas, C. N.; Anseth, K. S., Photodegradable hydrogels for dynamic tuning of physical and chemical properties. *Science* **2009,** *324*, 59-63.

105. Zhang, K.; Lackey, M. A.; Cui, J.; Tew, G. N., Gels based on cyclic polymers. *J. Am. Chem. Soc.,* **2011,** *133*, 4140-4148.

106. Otsu, T., Iniferter concept and living radical polymerization. *J. Polym. Sci. Pol. Chem.,* **2000,** *38*, 2121-2136.

107. Otsu, T.; Yoshida, M.; Tazaki, T., A model for living radical polymerization. *Makromol. Chem. Rapid. Commun.,* **1982,** *3*, 133-140.

108. Gordon, M. B.; French, J. M.; Wagner, N. J.; Kloxin, C. J., Dynamic bonds in covalently crosslinked polymer networks for photoactivated strengthening and healing. *Adv. Mater.,* **2015,** *27*, 8007-8010.

109. Singh, A.; Kuksenok, O.; Johnson, J. A.; Balazs, A. C., Tailoring the structure of polymer networks with iniferter-mediated photo-growth. *Polym. Chem.,* **2016,** *7*, 2955-2964.

110. Singh, A.; Kuksenok, O.; Johnson, J. A.; Balazs, A. C., Photo-regeneration of severed gel with iniferter-mediated photo-growth. *Soft Matter* **2017,** *13*, 1978-1987.

111. Lampley, M. W.; Harth, E., Photocontrolled growth of cross-linked Nanonetworks. *ACS Macro Lett.* **2018,** *7*, 745-750.

112. Angier, D. J.; Watson, W. F., Mastication of rubber. II. interpolymerization of natural rubber and neoprene on cold milling. *J. Polym. Sci.,* **1955**, *XVIII*, 129-140

113. Sohma, J., Mechanochemistry of Polymers. *Prog. Polym. Sci.,* **1989,** *14*, 451-596.

114. Baytekin, H. T.; Baytekin, B.; Grzybowski, B. A., Mechanoradicals created in "polymeric sponges" drive reactions in aqueous media. *Angew. Chem. Int. Ed.,* **2012,** *51*, 3596-3600.

115. Gordon, M. B.; Wang, S.; Knappe, G. A.; Wagner, N. J.; Epps, T. H.; Kloxin, C. J., Force-induced cleavage of a labile bond for enhanced mechanochemical crosslinking. *Polym. Chem.,* **2017,** *8*, 6485-6489.

116. Beziau, A.; Fortney, A.; Fu, L.; Nishiura, C.; Wang, H.; Cuthbert, J.; Gottlieb, E.; Balazs, A. C.; Kowalewski, T.; Matyjaszewski, K., Photoactivated structurally tailored and engineered macromolecular (STEM) gels as precursors for materials with spatially differentiated mechanical properties. *Polymer* **2017,** *126*, 224-230.

117. Cuthbert, J.; Beziau, A.; Gottlieb, E.; Fu, L. Y.; Yuan, R.; Balazs, A. C.; Kowalewski, T.; Matyjaszewski, K., Transformable materials: structurally tailored and engineered macromolecular (STEM) gels by controlled radical polymerization. *Macromolecules* **2018,** *51*, 3808-3817.

118. Cuthbert, J.; Zhang, T.; Biswas, S.; Olszewski, M.; Shanmugam, S.; Fu, T.; Gottlieb, E.; Kowalewski, T.; Balazs, A. C.; Matyjaszewski, K., Structurally tailored and engineered macromolecular (STEM) gels as soft elastomers and hard/soft interfaces. *Macromolecules* **2018,** *51*, 9184-9191.

119. Shanmugam, S.; Cuthbert, J.; Flum, J.; Fantin, M.; Boyer, C.; Kowalewski, T.; Matyjaszewski, K., Transformation of gels *via* catalyst-free selective RAFT photoactivation. *Polym. Chem.,* **2019,** *10*, 2477-2483.

120. Zhang, Z.; Corrigan, N.; Bagheri, A.; Jin, J.; Boyer, C., A versatile 3D and 4D printing system through photocontrolled RAFT polymerization. *Angew. Chem. Int. Ed.,* **2019,** *131*, 18122-18131.

121. Friml, J., Auxin transport - shaping the plant. *Curr. Opin. Plant. Biol.,* **2003,** *6*, 7-12.

122. Trewavas, A., Green plants as intelligent organisms. *Trends. Plant. Sci.,* **2005,** *10*, 413-419.

123. Mann, S., Life as a nanoscale phenomenon. *Angew. Chem. Int. Ed.* **2008,** *47*, 5306-5320.

124. Gates, B. D.; Xu, Q.; Stewart, M.; Ryan, D.; Willson, C. G.; Whitesides, G. M., New approaches to nanofabrication: molding, printing, and other techniques. *Chem. Rev.,* **2005,** *105*, 1171-1196.

125. Whitesides, G. M.; Grzybowski, B., Self-assembly at all scales. *Science* **2002,** *295*, 2418-2421.

126. Gross, B. C.; Erkal, J. L.; Lockwood, S. Y.; Chen, C.; Spence, D. M., Evaluation of 3D printing and its potential impact on biotechnology and the chemical sciences. *Anal. Chem.,* **2014,** *86*, 3240-3253.

127. Tapaszto, L.; Dobrik, G.; Lambin, P.; Biro, L. P., Tailoring the atomic structure of graphene nanoribbons by scanning tunnelling microscope lithography. *Nat. Nanotechnol.,* **2008,** *3*, 397-401.

128. Chaterji, S.; Kwon, I. K.; Park, K., Smart polymeric gels: redefining the limits of biomedical devices. *Prog. Polym. Sci.,* **2007,** *32*, 1083-1122.

129. Cangialosi, A.; Yoon, C.; Liu, J.; Huang, Q.; Guo, J.; Nguyen, T. D.; Gracias, D. H.; Schulman, R., DNA sequence-directed shape change of photopatterned hydrogels via high-degree swelling. *Science* **2017,** *357*, 1126-1130.

130. Behl, M.; Razzaq, M. Y.; Lendlein, A., Multifunctional shape-memory polymers. *Adv. Mater.,* **2010,** *22*, 3388-3410.

131. Kuksenok, O.; Dayal, P.; Bhattacharya, A.; Yashin, V. V.; Deb, D.; Chen, I. C.; Van Vliet, K. J.; Balazs, A. C., Chemo-responsive, self-oscillating gels that undergo biomimetic communication. *Chem. Soc. Rev.,* **2013,** *42*, 7257-7277.

132. Ikeda, T.; Mamiya, J.; Yu, Y., Photomechanics of liquid-crystalline elastomers and other polymers. *Angew. Chem. Int. Ed.,* **2007,** *46*, 506-528.

133. Koh, S. J. A.; Keplinger, C.; Li, T.; Bauer, S.; Suo, Z., Dielectric elastomer generators: how much energy can be converted? *IEEE-ASME T Mech.* **2011,** *16*, 33-41.

134. Lendlein, A.; Jiang, H.; Junger, O.; Langer, R., Light-induced shape-memory polymers. *Nature* **2005,** *434*, 879-882.

135. Xue, L.; Xiong, X.; Krishnan, B. P.; Puza, F.; Wang, S.; Zheng, Y.; Cui, J., Light-regulated growth from dynamic swollen substrates for making rough surfaces. *Nat. Commun.,* **2020,** *11*, 963.

136. Zhang, Y.; Li, Y.; Hu, Y.; Zhu, X.; Huang, Y.; Zhang, Z.; Rao, S.; Hu, Z.; Qiu, W.; Wang, Y.; Li, G.; Yang, L.; Li, J.; Wu, D.; Huang, W.; Qiu, C.; Chu, J., Localized self-growth of reconfigurable architectures induced by a femtosecond laser on a shape-memory polymer. *Adv. Mater.,* **2018,** *30*, 1803072.

137. Blaiszik, B. J.; Kramer, S. L. B.; Olugebefola, S. C.; Moore, J. S.; Sottos, N. R.; White, S. R., Self-healing polymers and composites. *Annu. Rev. Mater. Res.* **2010,** *40*, 179-211.

138. Wojtecki, R. J.; Meador, M. A.; Rowan, S. J., Using the dynamic bond to access macroscopically responsive structurally dynamic polymers. *Nat. Mater.,* **2011,** *10*, 14-27.

139. Aida, T.; Meijer, E. W.; Stupp, S. I., Functional supramolecular polymers. *Science* **2012,** *335*, 813-817.

140. Browne, W. R.; Feringa, B. L., Making molecular machines work. *Nat. Nanotechnol.,* **2006,** *1*, 25-35.

141. Peppas, N. A.; Hilt, J. Z.; Khademhosseini, A.; Langer, R., Hydrogels in biology and medicine: from molecular principles to bionanotechnology. *Adv. Mater.,* **2006,** *18*, 1345-1360.

142. Cordier, P.; Tournilhac, F.; Soulie-Ziakovic, C.; Leibler, L., Self-healing and thermoreversible rubber from supramolecular assembly. *Nature* **2008,** *451*, 977-980.

143. Braunecker, W. A.; Matyjaszewski, K., Controlled/living radical polymerization: Features, developments, and perspectives. *Prog. Polym. Sci.,* **2007,** *32*, 93-146.

144. Andrzejewska, E., Photopolymerization kinetics of multifunctional monomers. *Prog. Polym. Sci.,***2001,** *26*, 605-665.

145. Wang, S.; Yang, L.; Wang, H.; Xue, L.; Chen, J.; Cui, J., Nonequilibrium transesterification for programming a material's stiffening. *ACS Applied Polym. Mater.,* **2019,** *1*, 3227-3232.

146. Capelot, M.; Montarnal, D.; Tournilhac, F.; Leibler, L., Metal-catalyzed transesterification for healing and assembling of thermosets. *J. Am. Chem. Soc.,* **2012,** *134*, 7664-7667.

147. Self, J. L.; Dolinski, N. D.; Zayas, M. S.; de Alaniz, J. R.; Bates, C. M., Bronsted-acid-catalyzed exchange in polyester dynamic covalent networks. *Acs Macro Lett.,* **2018,** *7*, 817-821.

148. Glotzer, S. C.; Solomon, M. J., Anisotropy of building blocks and their assembly into complex structures. *Nat. Mater.,* **2007,** *6*, 557-562.

149. Zhao, X. M.; Xia, Y.; Whiteside, G. M., Fabrication of three-dimensional micro-structures: microtransfer molding. *Adv. Mater.,* **1996**, *8*, 837-840.

150. Bartholomeusz, D. A.; Boutte, R. W.; Andrade, J. D., Xurography: Rapid prototyping of microstructures using a cutting plotter. *J. Microelectromech. Syst.,* **2005,** *14*, 1364-1374.

151. Hong, S.; Sycks, D.; Chan, H. F.; Lin, S.; Lopez, G. P.; Guilak, F.; Leong, K. W.; Zhao, X., 3D printing of highly stretchable and tough hydrogels into complex, cellularized structures. *Adv. Mater.,* **2015,** *27*, 4035-4040.

152. Gladman, A. S.; Matsumoto, E. A.; Nuzzo, R. G.; Mahadevan, L.; Lewis, J. A., Biomimetic 4D printing. *Nat. Mater.,* **2016,** *15*, 413-418.

153. Zhao, H.; Sterner, E. S.; Coughlin, E. B.; Theato, P., *o*-Nitrobenzyl alcohol derivatives: opportunities in polymer and materials science. *Macromolecules* **2012,** *45*, 1723-1736.

154. Maruo, S.; Nakamura, O.; Kawata, S., Three-dimensional microfabrication with two-photon-absorbed photopolymerization. *Opt. Lett.,* **1997,** *22*, 132-134.

155. Chen, Y.; Spiering, A. J.; Karthikeyan, S.; Peters, G. W.; Meijer, E. W.; Sijbesma, R. P., Mechanically induced chemiluminescence from polymers incorporating a 1,2-dioxetane unit in the main chain. *Nat. Chem.,* **2012,** *4*, 559-562.

156. Ramirez, A. L.; Kean, Z. S.; Orlicki, J. A.; Champhekar, M.; Elsakr, S. M.; Krause, W. E.; Craig, S. L., Mechanochemical strengthening of a synthetic polymer in response to typically destructive shear forces. *Nat. Chem.,* **2013,** *5*, 757-761.

157. Jin, C. Y.; Li, Z.; Williams, R. S.; Lee, K. C.; Park, I., Localized temperature and chemical reaction control in nanoscale space by nanowire array. *Nano Lett* **2011,** *11*, 4818-4825.

158. Liu, Y.; Xu, B.; Sun, S.; Wei, J.; Wu, L.; Yu, Y., Humidity- and photo-induced mechanical actuation of cross-linked liquid crystal polymers. *Adv. Mater.,* **2017,** *29*, 1604792.

159. Du, X.; Li, L.; Li, J.; Yang, C.; Frenkel, N.; Welle, A.; Heissler, S.; Nefedov, A.; Grunze, M.; Levkin, P. A., UV-triggered dopamine polymerization: control of polymerization, surface coating, and photopatterning. *Adv. Mater.,* **2014,** *26*, 8029-8033.

160. Truby, R. L.; Lewis, J. A., Printing soft matter in three dimensions. *Nature* **2016,** *540*, 371-378.

161. Yu, H.; Ikeda, T., Photocontrollable liquid-crystalline actuators. *Adv. Mater.,* **2011,** *23*, 2149-2180.

162. Habault, D.; Zhang, H.; Zhao, Y., Light-triggered self-healing and shape-memory polymers. *Chem. So.c Rev.,* **2013,** *42*, 7244-7256.

163. Zhou, H.; Xue, C.; Weis, P.; Suzuki, Y.; Huang, S.; Koynov, K.; Auernhammer, G. K.; Berger, R.; Butt, H. J.; Wu, S., Photoswitching of glass transition temperatures of azobenzene-containing polymers induces reversible solid-to-liquid transitions. *Nat. Chem.,* **2017,** *9*, 145-151.

164. Ono, T.; Sugimoto, T.; Shinkai, S.; Sada, K., Lipophilic polyelectrolyte gels as super-absorbent polymers for nonpolar organic solvents. *Nat. Mater.,* **2007,** *6*, 429-433.

165. Pelliccioli, A. P.; Wirz, J., Photoremovable protecting groups: reaction mechanisms and applications. *Photochem. Photobiol. Sci.,* **2002,** *1*, 441-458.

166. Cui, J.; Miguel, V. S.; del Campo, A., Light-triggered multifunctionality at surfaces mediated by photolabile protecting groups. *Macromol. Rapid. Commun.,* **2013,** *34*, 310-329.

167. Ducrot, E.; Chen, Y.; Bulters, M.; Sijbesma, R. P.; Creton, C., Toughening elastomers with sacrificial bonds and watching them break. *Science* **2014,** *344*, 186-189.

168. Jerome, F. S.; Tseng, J. T.; Fan, L. T., Viscosities of Aqueous Glycol Solutions. *J. Chem. Eng. Data* **1968***, 13,* 496.

169. Hager, M. D.;, Greil, P.; Leyens, C.; van der Zwaag, S.; Schubert, U. S.; Self-Healing Materials. *Adv. Mater.,* **2010,** *22*, 5420-5430.

170. White, S. R.; Moore, J. S.; Sottos, N. R.; Krull, B. P.; Santa Cruz, W. A.; Gergely, R. C., Restoration of large damage volumes in polymers. *Science* **2014,** *344*, 620-623.

171. Bagheri, A.; Bainbridge, C.; Jin, J., Visible Light-induced transformation of polymer networks. *ACS Appl. Polym. Mater.,* **2019,** *1*, 1896-1904.

172. Lai, J.; Mu, X.; Xu, Y.; Wu, X.; Wu, C.; Li, C.; Chen, J.; Zhao, Y., Light-responsive nanogated ensemble based on polymer grafted mesoporous silica hybrid nanoparticles. *Chem. Commun.,* **2010,** *46*, 7370-7372.

173. Desrat, S.; Remeur, C.; Roussi, F., Development of an efficient route toward meiogynin A-inspired dual inhibitors of Bcl-xL and Mcl-1 anti-apoptotic proteins. *Org. Biomol. Chem.,* **2015,** *13*, 5520-5531.

174. Zhu, L.; Wu, W.; Zhu, M. Q.; Han, J. J.; Hurst, J. K.; Li, A. D., Reversibly photoswitchable dual-color fluorescent nanoparticles as new tools for live-cell imaging. *J. Am. Chem. Soc.,* **2007,** *129*, 3524-3526.

175. Saraydin, E. K. O. B. U. D., Swelling equilibria and dye adsorption studies of chemically crosslinked superabsorbent acrylamide/maleic acid hydrogels. *Eur. Polym. J.,* **2002,** *38*, 2133-2141.

176. Yiamsawas, D.; Kangwansupamonkon, W.; Chailapakul, O.; Kiatkamjornwong, S., Synthesis and swelling properties of poly[acrylamide-co-(crotonic acid)] superabsorbents. *React. Funct. Polym.* **2007,** *67*, 865-882.

177. Peppas, N. A.; Franson, N. M., The swelling interface number as a criterion for prediction of diffusional solute release mechanisms in swellable polymers. *J. Polym. Sci. Polym. Phys. Ed.,* **1983**, *21*, 983-997.

178. Esmaiel Jabbari, S. N., Swelling behavior of acrylic acid hydrogels prepared by irradiation crosslinking of polyacrylic acid in aqueous solution . *Eur. Polym. J.,* **2000,** *36*, 2685-2692.

179. Ahn, S.-k.; Kasi, R. M.; Kim, S.-C.; Sharma, N.; Zhou, Y., Stimuli-responsive polymer gels. *Soft Matter* **2008,** *4*, 1151.

180. Osada, Y; Gong, J. Soft and wet materials: polymer gels. *Adv. Mater.,* **1998,** *10*, 827-837.

181. Kloxin, C. J.; Bowman, C. N., Covalent adaptable networks: smart, reconfigurable and responsive network systems. *Chem. Soc. Rev.,* **2013,** *42*, 7161-7173.

182. Yang, Y.; Urban, M. W., Self-healing polymeric materials. *Chem. Soc. Rev.,* **2013,** *42*, 7446-7467.

183. Denissen, W.; Winne, J. M.; Du Prez, F. E., Vitrimers: permanent organic networks with glass-like fluidity. *Chem. Sci.,* **2016,** *7*, 30-38.

184. Gu, Y.; Zhao, J.; Johnson, J. A., A (Macro)Molecular-Level Understanding of Polymer Network Topology. *Trends in Chemistry* **2019,** *1*, 318-334.

185. Gao, H.; Matyjaszewski, K., Synthesis of functional polymers with controlled architecture by CRP of monomers in the presence of cross-linkers: From stars to gels. *Prog. Polym. Sci.,* **2009,** *34*, 317-350.

186. Gu, Y.; Zhao, J.; Johnson, J. A., Polymer Networks: From Plastics and Gels to Porous Frameworks. *Angew. Chem. Int. Ed., 2***020,** *59*, 5022-5049.

187. Zhou, H.; Woo, J.; Cok, A. M.; Wang, M.; Olsen, B. D.; Johnson, J. A., Counting primary loops in polymer gels. *Proc. Natl. Acad. Sci.,* **2012,** *109*, 19119-19124.

188. Tu, X.-Y.; Liu, M.-Z.; Wei, H., Recent progress on cyclic polymers: Synthesis, bioproperties, and biomedical applications. *J. Polym. Sci. A. Polym. Chem.,* **2016,** *54*, 1447-1458.

189. Wenz, G.; Han, B. H.; Muller, A., Cyclodextrin rotaxanes and polyrotaxanes. *Chem. Rev.,* **2006,** *106*, 782-817.

190. Haque, F. M.; Grayson, S. M., The synthesis, properties and potential applications of cyclic polymers. *Nat. Chem.,* **2020,** *12*, 433-444.

191. Niu, Z.; Gibson, H. W., Polycatenanes. *Chem. Rev.,* **2009,** *109*, 6024-6046.

192. Zhang, K.; Tew, G. N., Cyclic polymers as a building block for cyclic brush polymers and gels. *React. Funct. Polym.,* **2014,** *80*, 40-47.

193. Ito, K., Novel Cross-linking concept of polymer network: synthesis, structure, and properties of slide-ring gels with freely movable junctions. *Polym. J.,* **2007,** *39*, 489-499.

194. Takata, T.; Kihara, N.; Furusho, Y., Polyrotaxanes and polycatenanes: recent advances in syntheses and applications of polymers comprising of interlocked structures. *Adv. Polym. Sci.,* **2004,** *171*, 1-76.

195. Harry W. Gibson, M. C. B. a. P. T. E., Rotaxanes, catenanes, polyrotaxanes, polycatenanes and related materials. *Prog. Polym. Sci* **1994,** *19*, 843-945.

196. Endo, K.; Shiroi, T.; Murata, N.; Kojima, G.; Yamanaka, T., Synthesis and characterization of poly(1,2-dithiane). *Macromolecules* **2004,** *37*, 3143-3150.

197. Endo, K.; Yamanaka, T., Copolymerization of lipoic acid with 1,2-dithiane and characterization of the copolymer as an interlocked cyclic polymer. *Macromolecules* **2006,** *39*, 4038-4043.

198. Yamanaka, T.; Endo, K., Network formation of interlocked copolymer obtained from copolymerization of 1,2-dithiane and lipoic acid by metal salt. *Polym. J.,* **2007,** *39*, 1360-1364.

199. Wu, Q.; Rauscher, P. M.; Lang, X.; Wojtecki, R. J.; de Pablo, J. J.; Hore, M. J. A.; Rowan, S. J., Poly[n]catenanes: Synthesis of molecular interlocked chains. *Science* **2017,** *358*, 1434-1439.

200. Gil-Ramirez, G.; Leigh, D. A.; Stephens, A. J., Catenanes: fifty years of molecular links. *Angew. Chem. Int. Ed.,* **2015,** *54*, 6110-6150.

201. Demirel, Y., Fundamentals of nonequilibrium thermodynamics. *Nonequilibrium Thermodynamics.*, **2014**, 119-176.

202. Strandman, S.; Gautrot, J. E.; Zhu, X. X., Recent advances in entropy-driven ring-opening polymerizations. *Polym. Chem.* **2011,** *2*, 791-799.

203. Hodge, P., Entropically driven ring-opening polymerization of strainless organic macrocycles. *Chem. Rev.,* **2014,** *114*, 2278-2312.

204. Page, M. I.; Jencks, W. P., Entropic contributions to rate accelerations in enzymic and intramolecular reactions and the chelate effect. *Proc. Natl. Acad. Sci.,* **1971,** *68*, 1678-1683.

205. Mandolini, G. l. a. L., Ring closure reactions of bifunctional chain molecules. *Acc. Chem. Res.,* **1981,** *14*, 95-102.

206. Zhou, H. X., Loops, linkages, rings, catenanes, cages, and crowders: entropy-based strategies for stabilizing proteins. *Acc. Chem. Res.,* **2004,** *37*, 123-130.

207. Bang, E.-K.; Lista, M.; Sforazzini, G.; Sakai, N.; Matile, S., Poly(disulfide)s. *Chem. Sci.,* **2012,** *3*, 1752-1763.

208. Black, S. P.; Sanders, J. K.; Stefankiewicz, A. R., Disulfide exchange: exposing supramolecular reactivity through dynamic covalent chemistry. *Chem. Soc. Rev.,* **2014,** *43*, 1861-1872.

209. You, Y.; Peng, W. L.; Xie, P.; Rong, M. Z.; Zhang, M. Q.; Liu, D., Topological rearrangement-derived homogeneous polymer networks capable of reversibly interlocking: From phantom to reality and beyond. *Mater. Today.,* **2020,** *33*, 45-55.

210. Peng, W. L.; You, Y.; Xie, P.; Rong, M. Z.; Zhang, M. Q., Adaptable interlocking macromolecular networks with homogeneous architecture made from immiscible single networks. *Macromolecules* **2020,** *53*, 584-593.

211. Zhang, X.; Waymouth, R. M., 1,2-dithiolane-derived dynamic, covalent materials: cooperative self-assembly and reversible cross-linking. *J. Am. Chem. Soc.,* **2017,** *139*, 3822-3833.

212. Liu, D.; Wang, D.; Wang, M.; Zheng, Y.; Koynov, K.; Auernhammer, G. K.; Butt, H.-J.; Ikeda, T., Supramolecular organogel based on crown ether and secondary ammoniumion functionalized glycidyl triazole polymers. *Macromolecules* **2013,** *46*, 4617-4625.